

Frequency-based Substructuring (and more)

Daniel J. Rixen

Technical University of Munich - TUM



Course outline

0. Introduction

- Some history
- Basic notations

1. Frequency-based Substructuring for starters

- Assembly of admittances (2 subdomains)
- Example of a guitar
- Generalization to more subdomains

2. Some important tricks to make FBS work

- Weakening of compatibility: the virtual point transformation
- Example of the AM-structure in PyFBS
- Decoupling
- Example of a rubber mount

3. Blocked forces and transfer path analysis

- The concept of blocked forces
- In-situ measurements of blocked forces
- example

4. Some other tastes of experimental substructuring

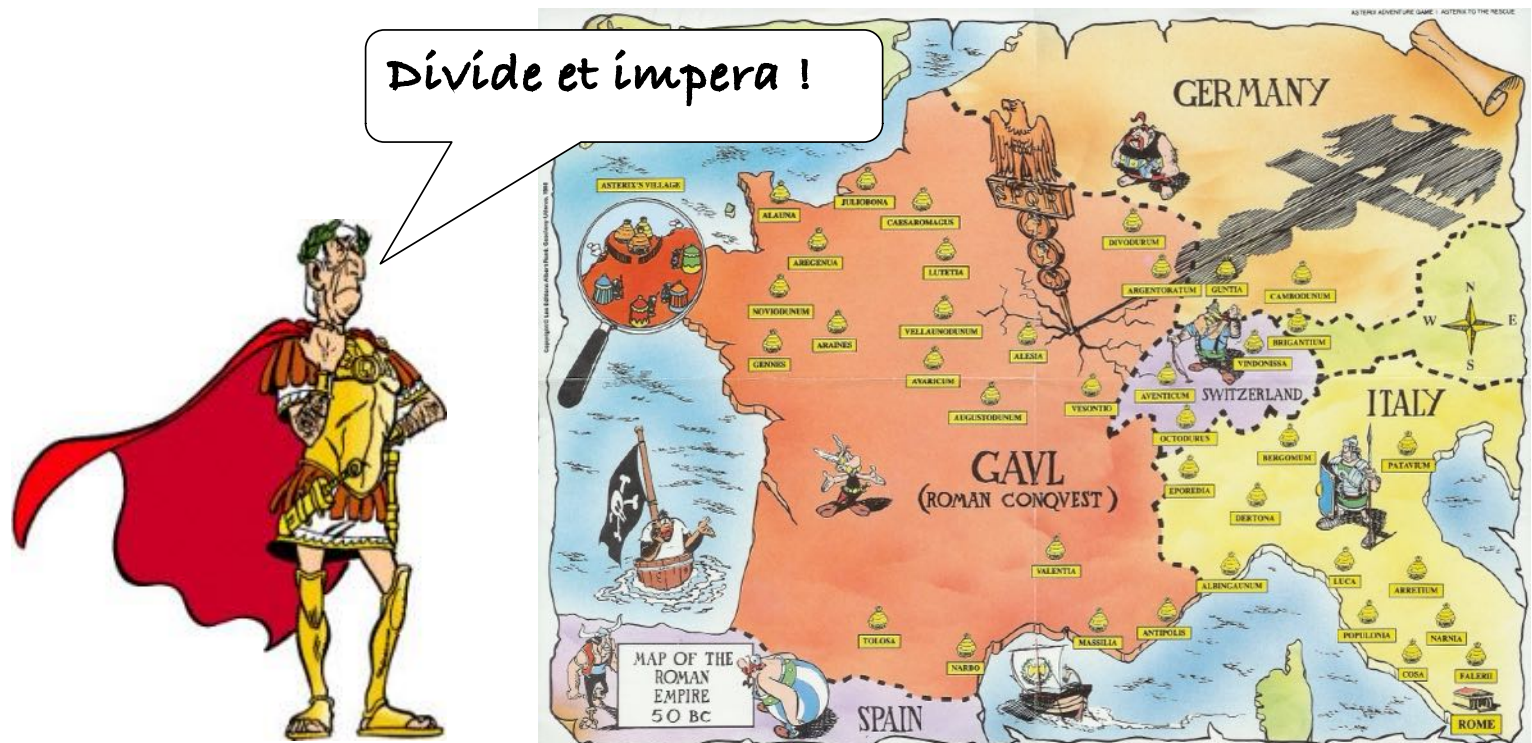
- Numerical substructures – model reduction
- Impulse-Based Substructuring

0. Introduction and motivation



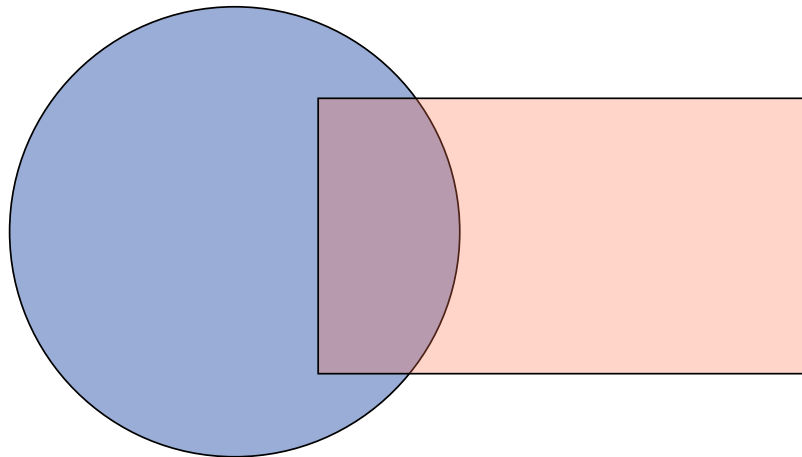
The paradigm of “*Divide and Conquer*”

.... already promoted by Julius Caesar himself ...



The paradigm of “*Divide and Conquer*”

But the first mathematical application of it was by H. Schwarz, in 1890, who wanted to prove the existence and uniqueness of the solution to the Laplace equation in a complex domain:



The paradigm of “*Divide and Conquer*”

- Later, with the work of Courant (1943), the idea of subdivision was used to define Ritz approximation per elements.
Finite Elements were born ...
- In the 60's the idea of partitioning a finite element model in substructures was proposed to reduce the complexity of the models
- In the 80's, in order to speed-up the solution of linear algebraic system, like in $Ku=F$, the computational domain was cut in sub-domains in order to share work amongst several CPUs. That was the start of *Domain Decomposition*.
- End of the 60's, but especially in the 80's, decomposing a structure in experimental mechanics was applied in order to simplify the testing



Often, in operating machines or in vibrating structures, engineers are confronted with the task to predict the level of vibration (or of sound) at certain locations as a consequence of a badly known vibration source or an unwanted transfer path of the excitation source across the structure.



An engineer would be interested to understand what sources create the excitation and how those sources propagate through the structure (“*transfer path*”) to create the vibration/noise at the receiver.

Knowing how the vibration is transmitted through different components and how they “shape” the frequency response of the assembly is also important when designing a machine or a product.

For instance, in a string instrument, the specific sound (timber) of that instrument is defined by the way the vibration of strings is transmitted to the body of the instrument, and how the body amplifies some frequencies and attenuates others.

To summarize, an engineer (designing a new system or troubleshooting an existing one) often has to answer the following questions:

- How can the dynamic characteristics of components be defined and how can they be combined to build a dynamic description of the assembled system?
- What is the contribution of each component to the transfer of a vibration source across the system?
- How can the excitation source be described in an operating machine or structure?
- How can the response to sources be computed and the most important transfer paths be identified?



Typically, the response of a linear time-invariant system to an excitation can be described in the frequency domain by the dynamic equation (discretized system)

$$(\mathbf{K} - \Omega^2 \mathbf{M}) \mathbf{X} = \mathbf{F}$$

*dynamic stiffness
"Impedance"*

Example:

$$\mathbf{K} = \begin{bmatrix} c_1 + c_2 & -c_2 \\ -c_2 & c_2 \end{bmatrix} \quad \mathbf{x}(t) = \begin{bmatrix} X_1 \\ X_2 \end{bmatrix} \cos \Omega t = \mathbf{X} \cos \Omega t$$

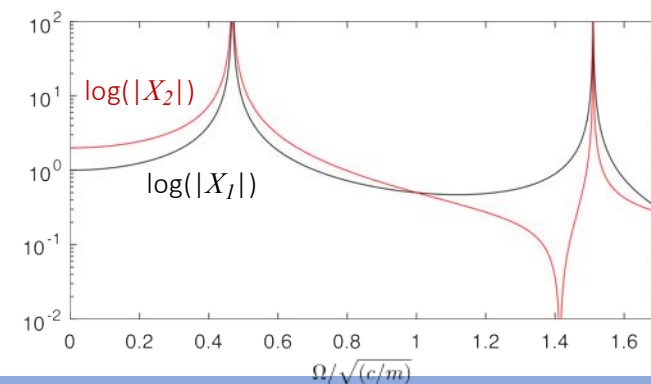
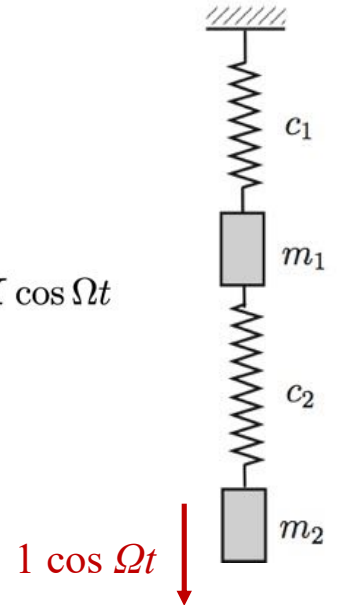
$$\mathbf{M} = \begin{bmatrix} m_1 & 0 \\ 0 & m_2 \end{bmatrix} \quad \mathbf{f}(t) = \begin{bmatrix} F_1 \\ F_2 \end{bmatrix} \cos \Omega t$$

This algebraic equation can be solved for the response:

$$\mathbf{X} = (\mathbf{K} - \Omega^2 \mathbf{M})^{-1} \mathbf{F} = \mathbf{Y} \mathbf{F}$$

*dynamic flexibility
"Admittance"*

(also called Frequency Response Function, FRF
or "compliance", "mobility", "accelerance")



$$\mathbf{X} = (\mathbf{K} - \Omega^2 \mathbf{M})^{-1} \mathbf{F} = \mathbf{Y} \mathbf{F}$$

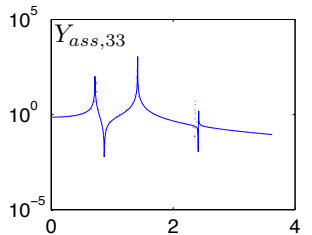
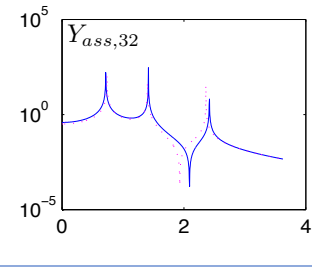
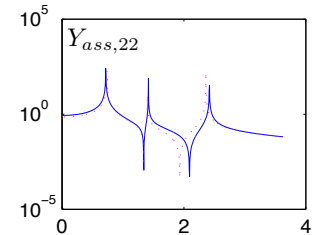
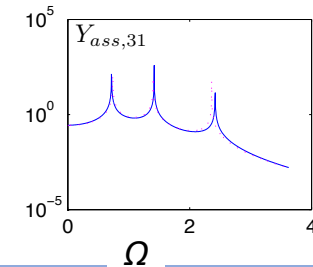
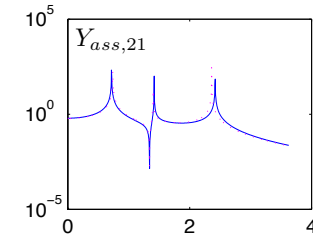
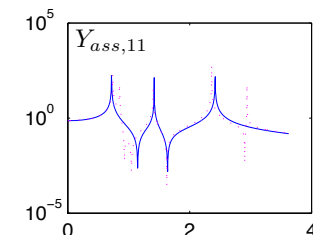
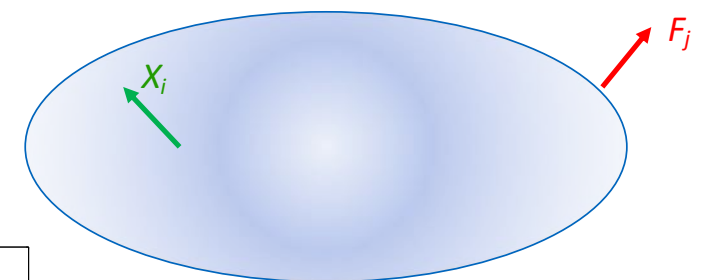
*Dynamic flexibility
"Admittance" / FRF*

Remarks:

- In practice, we like to work with admittances because that is what is measured when we excite at a location and measure the responses at several other locations

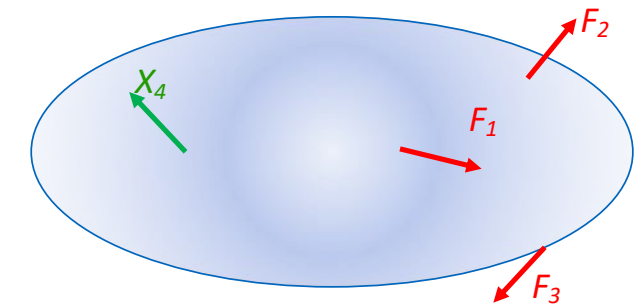
$$\boxed{\mathbf{X}} = \boxed{\mathbf{Y}} \quad \boxed{\mathbf{F}}$$

- We omit writing the damping, but similar if damping is included in measured admittances and impedances
- Admittance and impedance matrices are symmetric ("reciprocity")



Let us consider a system in which 3 different sources of excitations are present (F_1, F_2, F_3) and we are concerned by the vibration level X_4 at location 4.

If the sources' location and intensities are known and if the transfer path (admittance) between locations 1-4, 2-4, 3-4 are known, we can estimate the vibration response by

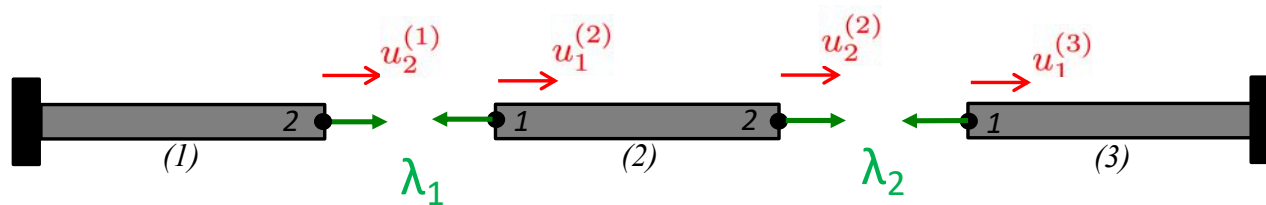


$$\mathbf{X} = \mathbf{Y}\mathbf{F} \quad \longrightarrow \quad x_4 = [Y_{41} \quad Y_{42} \quad Y_{43}] \begin{bmatrix} F_1 \\ F_2 \\ F_3 \end{bmatrix} = Y_{41}F_1 + Y_{42}F_2 + Y_{43}F_3$$

- The contribution of each force and each path to the response can be evaluated
- The contribution analysis should be evaluated for different frequency ranges.
- With this understanding, one can change the vibration level at the output by
 - modifying the transfer paths Y_{41}, Y_{42}, Y_{43} \longrightarrow *Understand the contribution of components to the path*
 - modifying the excitation sources F_1, F_2, F_3 \longrightarrow *Characterization of the source by equivalent forces*

Assembling substructures

Dual assembly



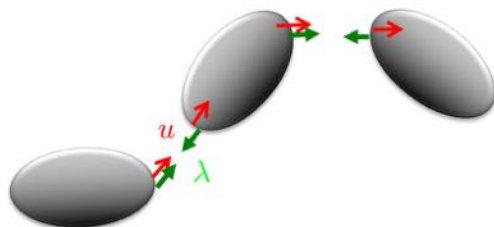
$$\begin{bmatrix} \mathbf{K} & \mathbf{B}^T \\ \mathbf{B} & \mathbf{o} \end{bmatrix} \begin{bmatrix} \mathbf{u} \\ \boldsymbol{\lambda} \end{bmatrix} = \begin{bmatrix} \begin{bmatrix} k^{(1)} & & & \\ 0 & 0 & -k^{(2)} & 0 \\ 0 & k^{(2)} & k^{(2)} & 0 \\ 0 & -k^{(2)} & 0 & 0 \end{bmatrix} & \begin{bmatrix} 1 & 0 \\ -1 & 0 \\ 0 & 1 \\ 0 & -1 \end{bmatrix} \\ \begin{bmatrix} 1 & -1 & 0 & 0 \\ 0 & 0 & 1 & -1 \end{bmatrix} & \mathbf{o} \end{bmatrix} \begin{bmatrix} \begin{bmatrix} u_2^{(1)} \\ u_1^{(2)} \\ u_2^{(2)} \\ u_1^{(3)} \end{bmatrix} \\ \begin{bmatrix} \lambda_1 \\ \lambda_2 \end{bmatrix} \end{bmatrix}$$

Dual assembly

Assembling substructures

Generally written, when assembling N_s substructures in the frequency domain:

Dual assembly

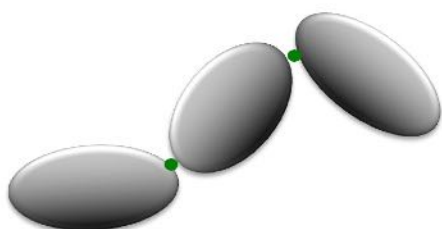


$$\begin{bmatrix} Z & B^T \\ B & \mathbf{o} \end{bmatrix} \begin{bmatrix} u \\ \lambda \end{bmatrix} = \begin{bmatrix} f \\ \mathbf{o} \end{bmatrix} \quad \text{where} \quad Z = \begin{bmatrix} Z^{(1)} & & \mathbf{o} \\ & \ddots & \\ \mathbf{o} & & Z^{(N_s)} \end{bmatrix} \quad u = \begin{bmatrix} u^{(1)} \\ \vdots \\ u^{(N_s)} \end{bmatrix}$$

B signed Boolean

$$f = \begin{bmatrix} f^{(1)} \\ \vdots \\ f^{(N_s)} \end{bmatrix}$$

Primal assembly



$$Z_{glob} \ u_{glob} = f_{glob} \quad \text{where } L \text{ is a Boolean such that} \quad u = Lu_{glob}$$

$$BL = \mathbf{o}$$

$$K_{glob} = L^T KL$$

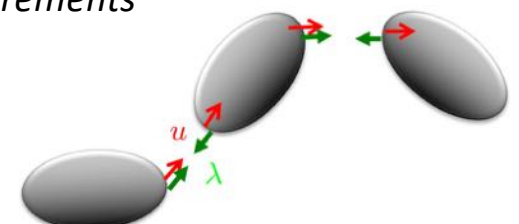
Why can it be handy to use dual vs. primal assembly ?

Mathematically equivalent, but different mechanical interpretation

$$\begin{bmatrix} Z & B^T \\ B & \mathbf{0} \end{bmatrix} \begin{bmatrix} u \\ \lambda \end{bmatrix} = \begin{bmatrix} f \\ \mathbf{0} \end{bmatrix}$$

Dual: + can be interpreted as combining interface admittances as obtained by measurements
(response of substructure to interface connection forces)

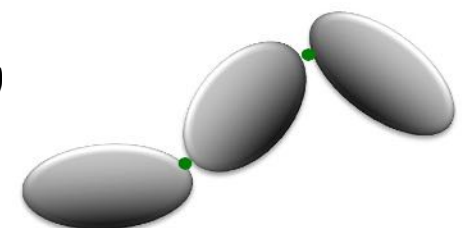
- + allows approximation of interface compatibility
(very useful in experimental substructuring, see later)
- more unknowns in the computations



$$Z_{glob} \ u_{glob} = f_{glob}$$

Primal: + can be seen as summing interface impedances (similar to Finite Element assembly)

- + minimum set of unknown
- impedances is not what is measured



Course outline

0. Introduction

- Some history
- Basic notations

1. Frequency-based Substructuring for starters

- Assembly of admittances (2 subdomains)
- Example of a guitar
- Generalization to more subdomains

2. Some important tricks to make FBS work

- Weakening of compatibility: the virtual point transformation
- Example of the AM-structure in PyFBS
- Decoupling
- Example of a rubber mount

3. Blocked forces and transfer path analysis

- The concept of blocked forces
- In-situ measurements of blocked forces
- example

4. Some other tastes of experimental substructuring

- Numerical substructures – model reduction
- Impulse-Based Substructuring

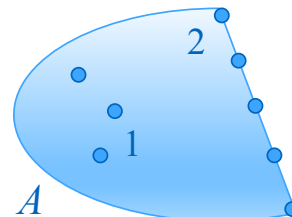
1. Frequency-based Substructuring for starters



Assembling admittances

Here, we assume that we know the dynamics of 2 components from their admittances obtained from a numerical model or from measurements:

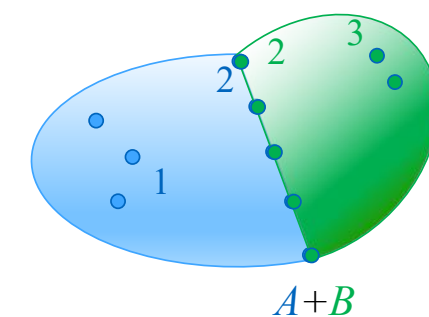
$$Y^A = \begin{bmatrix} Y_{11}^A & Y_{12}^A \\ Y_{21}^A & Y_{22}^A \end{bmatrix}$$



$$Y^B = \begin{bmatrix} Y_{22}^B & Y_{23}^B \\ Y_{32}^B & Y_{33}^B \end{bmatrix}$$



$$Y^{A+B} = \begin{bmatrix} Y_{11}^{A+B} & Y_{12}^{A+B} & Y_{13}^{A+B} \\ Y_{21}^{A+B} & Y_{22}^{A+B} & Y_{23}^{A+B} \\ Y_{31}^{A+B} & Y_{32}^{A+B} & Y_{33}^{A+B} \end{bmatrix}$$



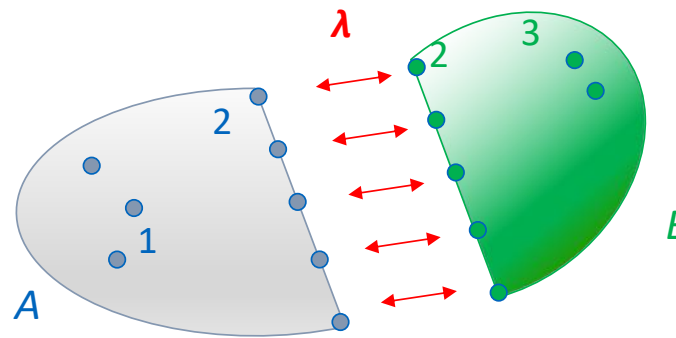
We use here block notations in the matrices and call

x_1 all internal dofs in substructure A (where later a force will be applied)

x_2 all interface dofs in substructure A, coinciding with all interface dofs in substructure B.

x_3 all internal dofs in substructure B (where later the output response will be analyzed)

$$Y^A = \begin{bmatrix} Y_{11}^A & Y_{12}^A \\ Y_{21}^A & Y_{22}^A \end{bmatrix}$$



$$Y^B = \begin{bmatrix} Y_{22}^B & Y_{23}^B \\ Y_{32}^B & Y_{33}^B \end{bmatrix}$$

The dynamic equation of each substructure in the frequency domain when it is assembled writes

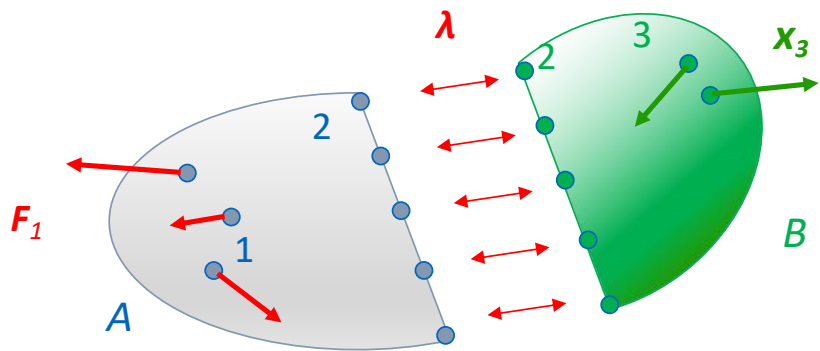
where the Lagrange multipliers λ are the internal forces satisfying by construction the action-reaction principle and ensuring the satisfaction of the compatibility condition

$$\begin{aligned} \begin{bmatrix} x_1^A \\ x_2^A \end{bmatrix} &= \begin{bmatrix} Y_{11}^A & Y_{12}^A \\ Y_{21}^A & Y_{22}^A \end{bmatrix} \begin{bmatrix} f_1^A \\ \lambda \end{bmatrix} \\ \begin{bmatrix} x_2^B \\ x_3^B \end{bmatrix} &= \begin{bmatrix} Y_{22}^B & Y_{23}^B \\ Y_{32}^B & Y_{33}^B \end{bmatrix} \begin{bmatrix} -\lambda \\ f_3^B \end{bmatrix} \end{aligned}$$

$$x_2^A - x_2^B = 0$$

These sets of equations (dynamic equilibrium and compatibility) are the *dually assembled form* as seen in the introduction if we assume the interface dofs to have corresponding numbering ($B = [0 \ -I \ I \ 0]$).

$$\begin{bmatrix} Z^{(1)} & \mathbf{0} \\ \mathbf{0} & Z^{(2)} \\ [\mathbf{0} \quad -I] & [I \quad \mathbf{0}] \end{bmatrix} \begin{bmatrix} \mathbf{0} \\ -I \\ I \\ \mathbf{0} \\ \mathbf{0} \end{bmatrix} \begin{bmatrix} u^{(1)} \\ u^{(2)} \\ \lambda \end{bmatrix} = \begin{bmatrix} f^{(1)} \\ f^{(2)} \\ \mathbf{0} \end{bmatrix}$$



$$\begin{aligned} \begin{bmatrix} \mathbf{x}_1^A \\ \mathbf{x}_2^A \end{bmatrix} &= \begin{bmatrix} \mathbf{Y}_{11}^A & \mathbf{Y}_{12}^A \\ \mathbf{Y}_{21}^A & \mathbf{Y}_{22}^A \end{bmatrix} \begin{bmatrix} \mathbf{f}_1^A \\ \boldsymbol{\lambda} \end{bmatrix} \\ \begin{bmatrix} \mathbf{x}_2^B \\ \mathbf{x}_3^B \end{bmatrix} &= \begin{bmatrix} \mathbf{Y}_{22}^B & \mathbf{Y}_{23}^B \\ \mathbf{Y}_{32}^B & \mathbf{Y}_{33}^B \end{bmatrix} \begin{bmatrix} -\boldsymbol{\lambda} \\ 0 \end{bmatrix} \end{aligned}$$

$$\mathbf{x}_2^A - \mathbf{x}_2^B = 0$$

Dually assembled form

Assume now that we only have applied forces on dofs 1 in A , and that we are interested to know the response at dofs 3 in B .

To compute the admittance of the assembled system $A+B$, we will eliminate the internal forces $\boldsymbol{\lambda}$ in the interface as follows:

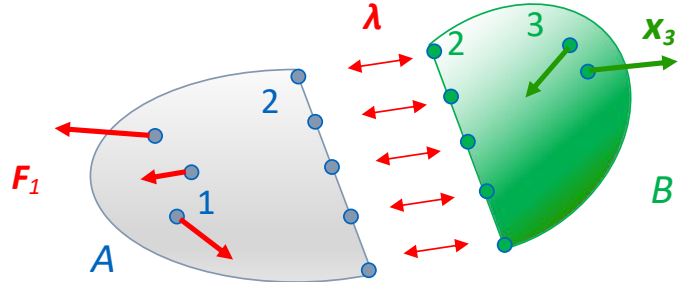
- From the dynamic equations of each substructure, the interface displacements as function of the interface forces are:

$$\begin{aligned} \mathbf{x}_2^A &= \mathbf{Y}_{21}^A \mathbf{f}_1^A + \mathbf{Y}_{22}^A \boldsymbol{\lambda} \\ \mathbf{x}_2^B &= -\mathbf{Y}_{22}^B \boldsymbol{\lambda} \end{aligned}$$

- Replacing then in the interface compatibility condition, we find the so-called *dual interface problem*

$$(\mathbf{Y}_{22}^A + \mathbf{Y}_{22}^B) \boldsymbol{\lambda} = -\mathbf{Y}_{21}^A \mathbf{f}_1^A$$

that determines the amplitude of the interface forces needed to close the gap created by the applied forces



$$\begin{aligned} \begin{bmatrix} \mathbf{x}_1^A \\ \mathbf{x}_2^A \end{bmatrix} &= \begin{bmatrix} \mathbf{Y}_{11}^A & \mathbf{Y}_{12}^A \\ \mathbf{Y}_{21}^A & \mathbf{Y}_{22}^A \end{bmatrix} \begin{bmatrix} \mathbf{f}_1^A \\ \boldsymbol{\lambda} \end{bmatrix} \\ \begin{bmatrix} \mathbf{x}_2^B \\ \mathbf{x}_3^B \end{bmatrix} &= \begin{bmatrix} \mathbf{Y}_{22}^B & \mathbf{Y}_{23}^B \\ \mathbf{Y}_{32}^B & \mathbf{Y}_{33}^B \end{bmatrix} \begin{bmatrix} -\boldsymbol{\lambda} \\ 0 \end{bmatrix} \end{aligned}$$

Dually assembled form

$$\mathbf{x}_2^A - \mathbf{x}_2^B = 0$$

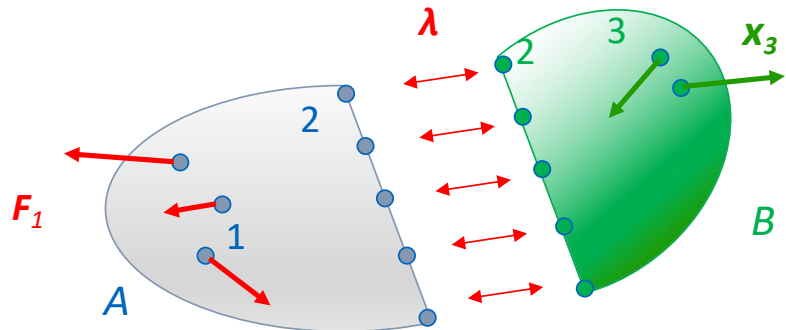
Solving then for the interface forces:

$$(\mathbf{Y}_{22}^A + \mathbf{Y}_{22}^B) \boldsymbol{\lambda} = -\mathbf{Y}_{21}^A \mathbf{f}_1^A \quad \longrightarrow \quad \boldsymbol{\lambda} = -(\mathbf{Y}_{22}^A + \mathbf{Y}_{22}^B)^{-1} \mathbf{Y}_{21}^A \mathbf{f}_1^A$$

Dual Interface Problem

and replacing in the dynamic response at the output 3 in substructure B:

$$\mathbf{x}_3^B = -\mathbf{Y}_{32}^B \boldsymbol{\lambda} \quad \longrightarrow \quad \mathbf{x}_3^B = \mathbf{Y}_{32}^B (\mathbf{Y}_{22}^A + \mathbf{Y}_{22}^B)^{-1} \mathbf{Y}_{21}^A \mathbf{f}_1^A$$



$$\mathbf{x}_3^B = \underbrace{\mathbf{Y}_{32}^B (\mathbf{Y}_{22}^A + \mathbf{Y}_{22}^B)^{-1} \mathbf{Y}_{21}^A \mathbf{f}_1^A}_{\substack{Y_{31}^{A+B} \\ \text{Gap in the interface due to applied forces,} \\ \text{when no interface force is present}}} \quad \boxed{\mathbf{x}_3^B = \underbrace{\mathbf{Y}_{32}^B (\mathbf{Y}_{22}^A + \mathbf{Y}_{22}^B)^{-1} \mathbf{Y}_{21}^A \mathbf{f}_1^A}_{\substack{Y_{31}^{A+B} \\ \text{Gap in the interface due to applied forces,} \\ \text{when no interface force is present}}}}$$

*Frequency-Based
Substructuring
(FBS)*

*Gap in the interface due to applied forces,
when no interface force is present*

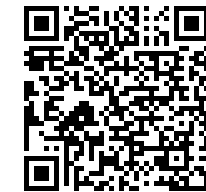
Internal interface forces λ to close the gap

Remarks:

- The admittance of the components can be measured or obtained from a FE model (“hybrid” models).
- If the interface admittances \mathbf{Y}_{22}^A , \mathbf{Y}_{22}^B are obtained from measurements, they will always be noisy and slightly wrong. Those errors will usually be strongly amplified when computing the inverse $(\mathbf{Y}_{22}^A + \mathbf{Y}_{22}^B)^{-1}$. **This is one of the biggest challenges in experimental substructuring.** There are several mathematical techniques to alleviate this problem (see later)
- The approach shown here can be called *Dual or Lagrange-Multiplier FBS (LM-FBS)*.

Check yourself

pingo.coactum.de
Code 756413



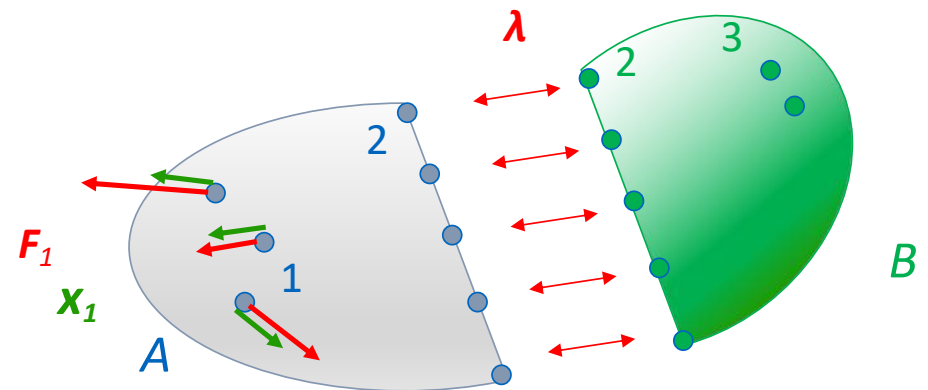
In case one would be interested in the vibration response observed in the assembled system on dofs 1 (in the same substructure as where the forces are applied), the formula of the Frequency-Based Substructuring (FBS) would be:

a. $x_1^A = \mathbf{Y}_{11}^A f_1^A$

b. $x_1^A = \mathbf{Y}_{12}^A (\mathbf{Y}_{22}^A + \mathbf{Y}_{22}^B)^{-1} \mathbf{Y}_{21}^A f_1^A$

c. $x_1^A = \left(\mathbf{Y}_{11}^A - \mathbf{Y}_{12}^A (\mathbf{Y}_{22}^A + \mathbf{Y}_{22}^B)^{-1} \mathbf{Y}_{21}^A \right) f_1^A$

d. $x_1^A = \mathbf{Y}_{12}^A (\mathbf{Y}_{22}^A)^{-1} \mathbf{Y}_{21}^A f_1^A$



$$x_3^B = \mathbf{Y}_{32}^B (\mathbf{Y}_{22}^A + \mathbf{Y}_{22}^B)^{-1} \mathbf{Y}_{21}^A f_1^A$$

Check yourself

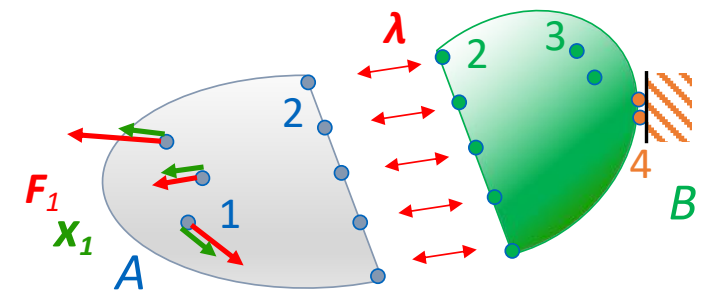
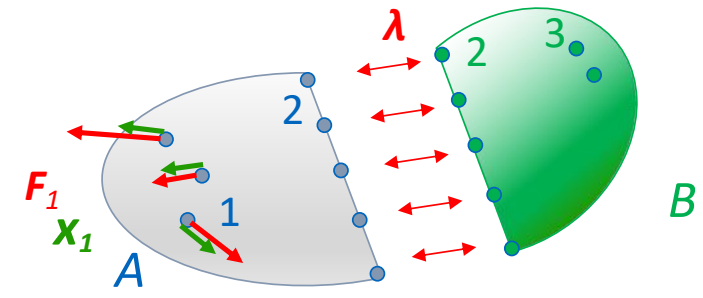
When the FRF of substructure B is measured as fully free, the assembly with substructure A yields

$$\mathbf{x}_3^B = \mathbf{Y}_{32}^B (\mathbf{Y}_{22}^A + \mathbf{Y}_{22}^B)^{-1} \mathbf{Y}_{21}^A \mathbf{f}_1^A$$

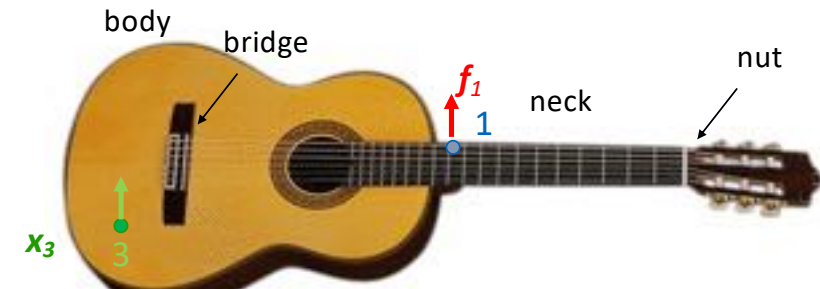
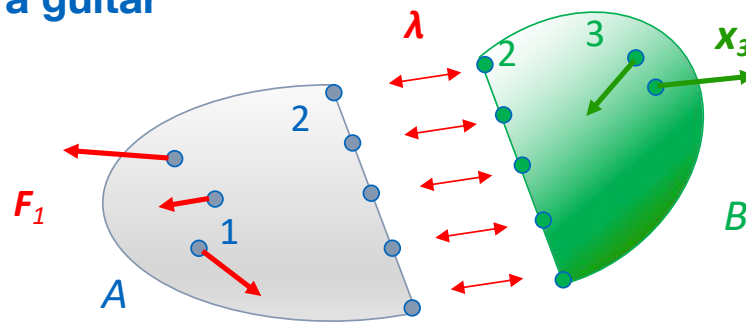
If we want to compute the assembly of A+B, but where B is fixed to the outside world at some dofs 4, how can we proceed? (3 correct answers)

- a. Measure \mathbf{Y}_{fix}^B (dofs 4 fixed) and apply the same formula as before where \mathbf{Y}^B is replaced by \mathbf{Y}_{fix}^B
- b. Measure $\mathbf{Y}_{fix,fix}^B$ (dofs 2 and 4 fixed) and apply the same formula as before where \mathbf{Y}^B is replaced by $\mathbf{Y}_{fix,fix}^B$
- c. Measure \mathbf{Y}^B (all dofs free), transform it to \mathbf{Y}_{fix}^B (dofs 4 fixed) and apply the same formula as before where \mathbf{Y}^B is replaced by \mathbf{Y}_{fix}^B
- d. Measure \mathbf{Y}^B (for all dofs free) and apply the same formula as before with, instead of just dofs 3, dofs 3+4 as interface dofs.

pingo.coactum.de
Code 756413



Example of a guitar



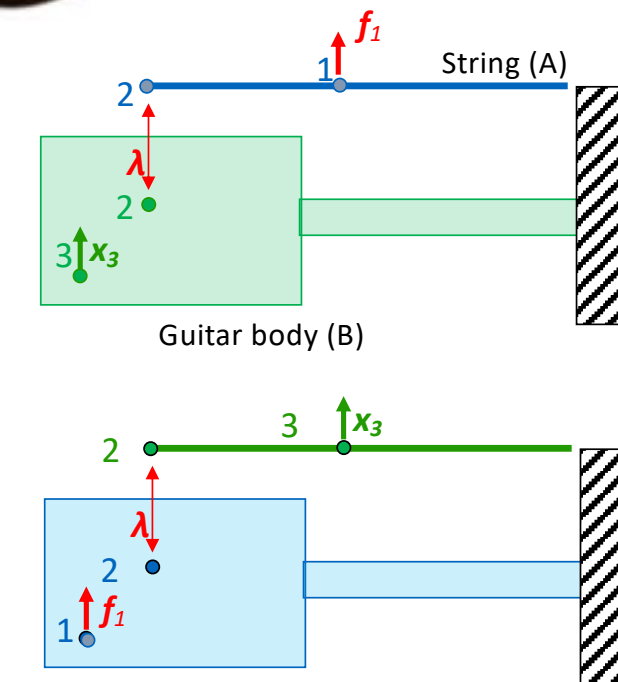
In order to investigate the timber of a guitar, we want to analyze the dynamic interaction between the vibration of a string on the body of a guitar.

In particular, we are interested to see how the admittance of the string and the body combine to create the global guitar dynamics from an excitation of the string to the output vibration on a point of the body (exemplary for the sound that will be radiated by the guitar)

Since it is difficult to precisely apply a force on the string, we actually investigate the case where a force is given on the body and the vibration of the string is measured (equivalent due to symmetry/reciprocity)

Assumptions

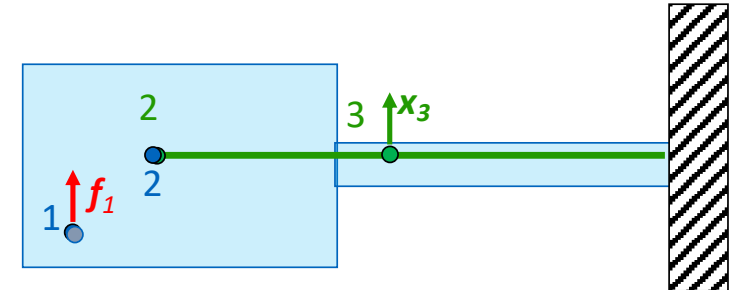
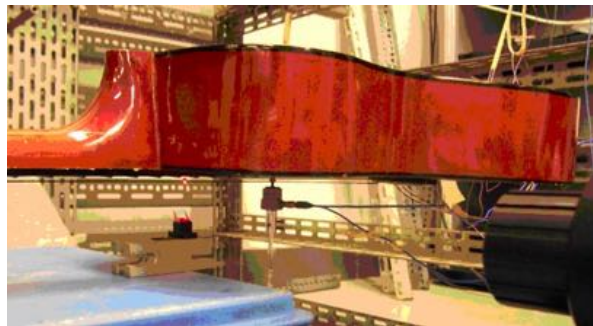
- string and nut clamped (no dynamic contribution)
- in-plane vibrations of the sound board and bridge assumed irrelevant



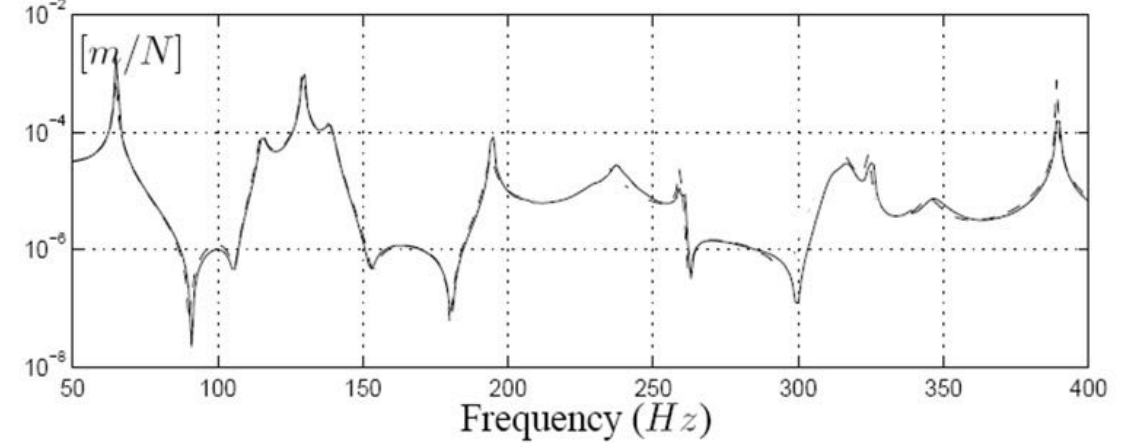
Measuring the admittance of the full guitar (assembled system) for validation

To validate the result from Frequency-Based Substructuring:

- shaker with impedance head (measures force and acceleration) on 1
- laser vibrometer to measure the vibration of the string on 3



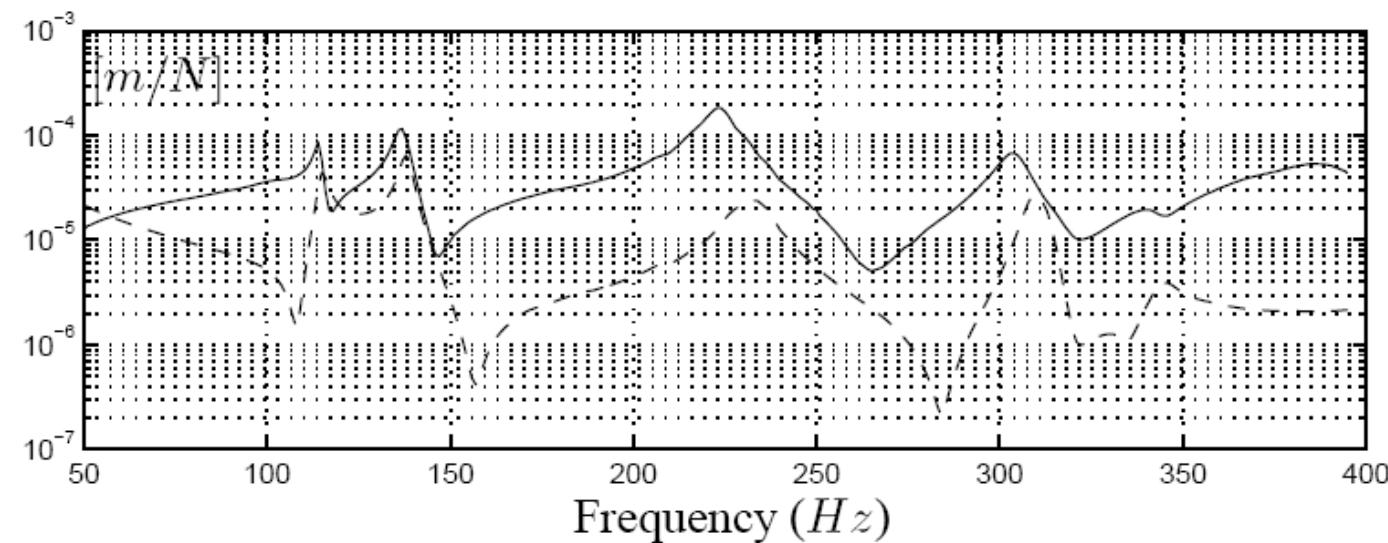
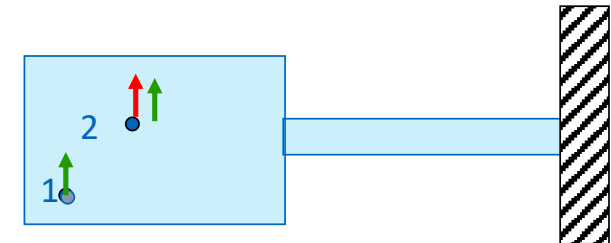
$$|Y_{31}| = \left| \frac{x_3}{f_1} \right|$$



Measuring the Admittance of the guitar body alone (Substructure A)

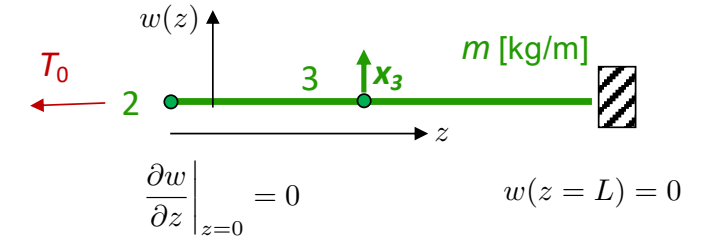
Measuring \mathbf{Y}_{22}^A and \mathbf{Y}_{21}^A with

- shaker with impedance head on 2 (bridge)
- laser vibrometer on 1



Admittance of string (alone)

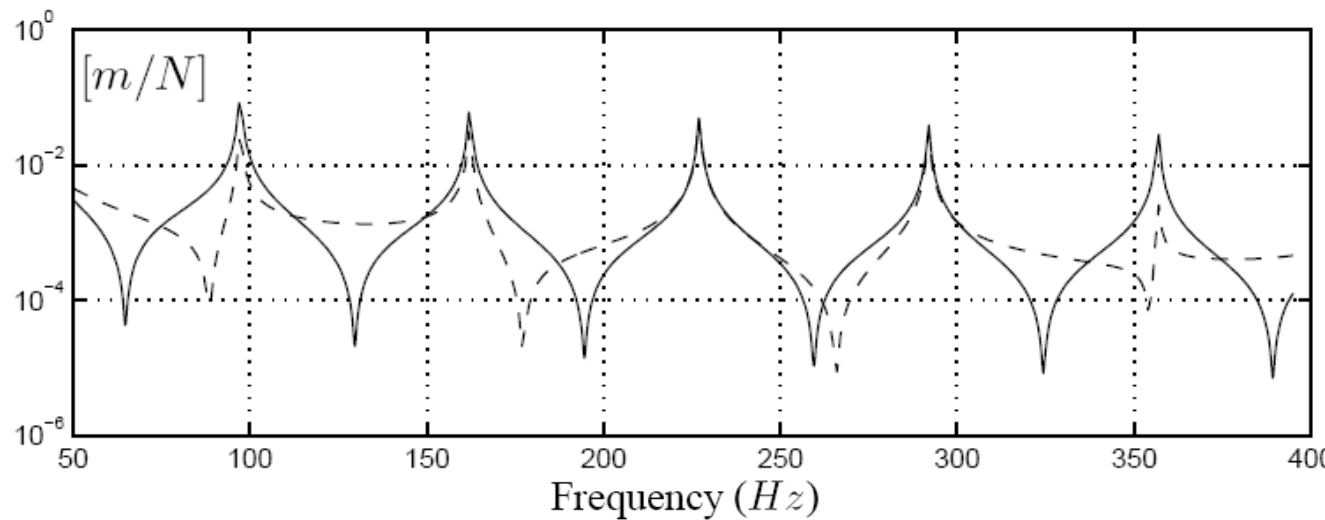
It is hard to obtain \mathbf{Y}_{22}^B and \mathbf{Y}_{23}^B for the string from experiment since it would require leaving the end of the strings free in the transverse direction while keeping it under tension ...



So the string dynamics is obtained from an analytical model:

$$T_0 \frac{\partial^2 w}{\partial z^2} + \Omega^2 m w = 0$$

Can be solved analytically :



String

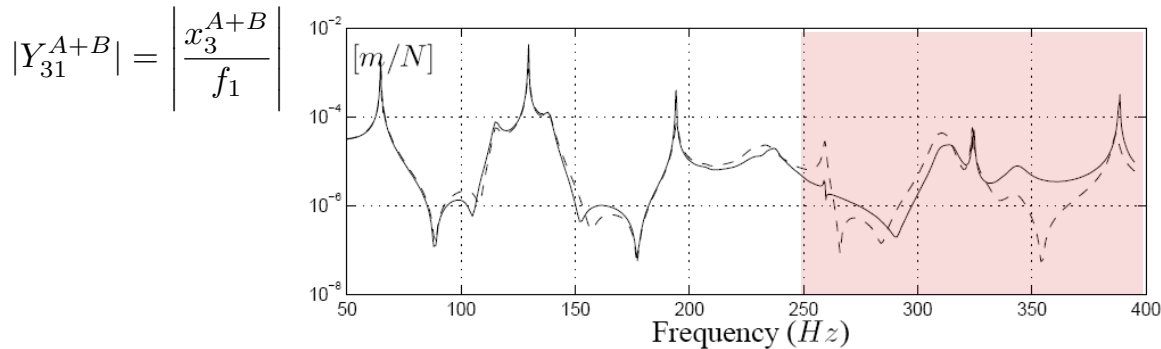
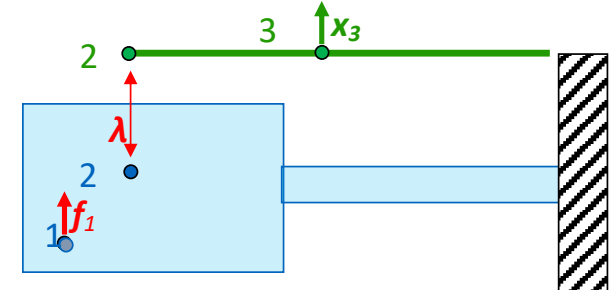
$$\text{--- } |Y_{22}^B| = \left| \frac{x_2^B}{f_2} \right|$$

$$\text{--- } |Y_{32}^B| = \left| \frac{x_3^B}{f_2} \right|$$

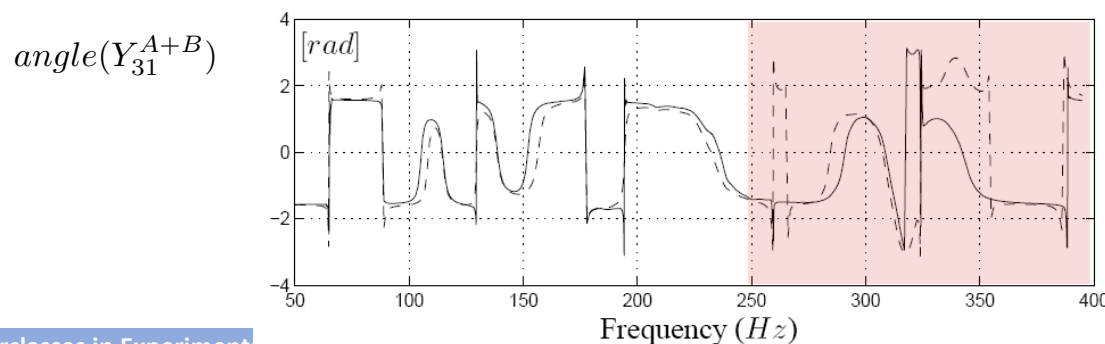
Result of the assembly of the components (Frequency-based substructuring)

$$\mathbf{x}_3^B = \mathbf{Y}_{32}^B (\mathbf{Y}_{22}^A + \mathbf{Y}_{22}^B)^{-1} \mathbf{Y}_{21}^A \mathbf{f}_1^A$$

Applied for each frequency step between 50 Hz and 400 Hz :



- Measured on assembly (validation)
- Computed by Frequency-based Subst.



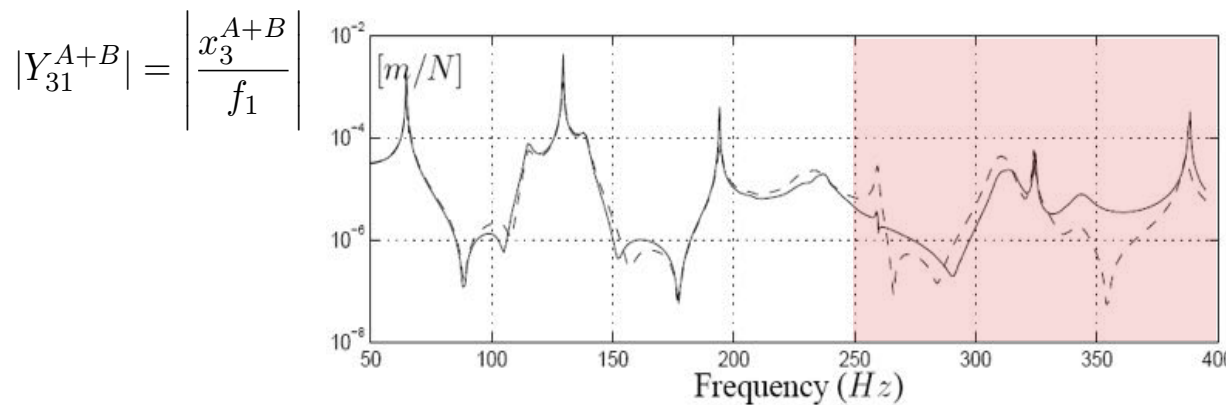
Prediction of the FBS assembly very good in low frequencies, **but not above 250 Hz !**

Check yourself

pingo.coactum.de
Code 756413



Why is the prediction of the FBS bad for frequencies higher than 250 Hz ?

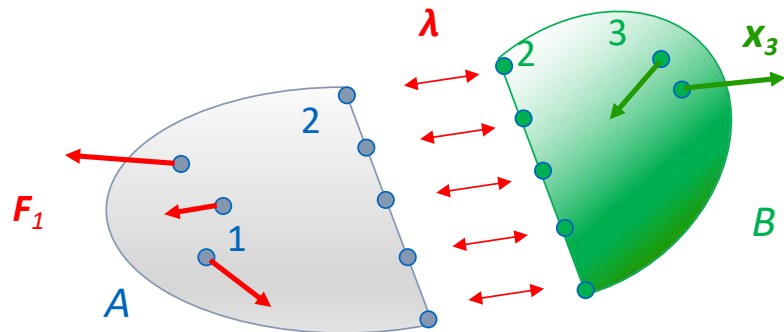


- Measured on assembly (validation)
- Computed by Frequency-based Subst.

- a. The boundary conditions assumed for our substructured model is bad for higher frequencies.
- b. The measurements of the FRFs of the guitar body were too noisy at higher frequencies.
- c. The interaction with the air (vibro-acoustics) becomes important at higher frequencies.

Generalization to more than 2 substructures

Remember, for 2 substructures



$$\boldsymbol{x}_3^B = \underbrace{\boldsymbol{Y}_{32}^B (\boldsymbol{Y}_{22}^A + \boldsymbol{Y}_{22}^B)^{-1} \boldsymbol{Y}_{21}^A \boldsymbol{f}_1^A}_{\substack{\text{Gap in the interface due to applied forces,} \\ \text{when no interface force is present}}} + \underbrace{\boldsymbol{Y}_{31}^{A+B}}_{\text{Internal interface forces } \lambda \text{ to close the gap}}$$

If many substructures, let us consider again the general dually assembled form (Chapter 1)

$$\begin{bmatrix} \mathbf{Z} & \mathbf{B}^T \\ \mathbf{B} & \mathbf{o} \end{bmatrix} \begin{bmatrix} \mathbf{u} \\ \lambda \end{bmatrix} = \begin{bmatrix} \mathbf{f} \\ \mathbf{o} \end{bmatrix}$$

where

$$\mathbf{Z} = \begin{bmatrix} \mathbf{Z}^{(1)} & & \mathbf{o} \\ & \ddots & \\ \mathbf{o} & & \mathbf{Z}^{(N_s)} \end{bmatrix} \quad \mathbf{u} = \begin{bmatrix} \mathbf{u}^{(1)} \\ \vdots \\ \mathbf{u}^{(N_s)} \end{bmatrix} \quad \mathbf{f} = \begin{bmatrix} \mathbf{f}^{(1)} \\ \vdots \\ \mathbf{f}^{(N_s)} \end{bmatrix}$$

$$\begin{bmatrix} Z & B^T \\ B & \mathbf{o} \end{bmatrix} \begin{bmatrix} u \\ \lambda \end{bmatrix} = \begin{bmatrix} f \\ \mathbf{o} \end{bmatrix}$$

➡ $B(Yf - YB^T\lambda) = \mathbf{o}$

\downarrow

$(BYB^T)\lambda = BYf$

Dual Interface Problem

“what interface forces are needed to close the interface gap created by the external force?”

a. Substructured problem

b. Effect of local force in $\Omega^{(1)}$

c. Global effect of λ to enforce compatibility

$$(\mathbf{B}\mathbf{Y}\mathbf{B}^T)\lambda = \mathbf{B}\mathbf{Y}\mathbf{f}$$

Dual Interface Problem



$$\boldsymbol{\lambda} = (\mathbf{B}\mathbf{Y}\mathbf{B}^T)^{-1}\mathbf{B}\mathbf{Y}\mathbf{f}$$

$$\mathbf{u} = \mathbf{Y}(\mathbf{f} - \mathbf{B}^T \boldsymbol{\lambda})$$



$$\mathbf{u} = \left(\mathbf{Y} - \mathbf{Y}\mathbf{B}^T(\mathbf{B}\mathbf{Y}\mathbf{B}^T)^{-1}\mathbf{B}\mathbf{Y} \right) \mathbf{f}$$

$$\mathbf{Y}_{g,dual}$$

Lagrange Multiplier FBS
(LM-FBS)

Interpretation of dually assembled admittance

$$\mathbf{u} = \left(\underbrace{\mathbf{Y}}_{uncoupl.} - \underbrace{\mathbf{Y}\mathbf{B}^T(\mathbf{B}\mathbf{Y}\mathbf{B}^T)^{-1}\mathbf{B}\mathbf{Y}}_{\underbrace{\Delta}_{coupling}} \right) \mathbf{f}$$

2. Some important tricks to make FBS work



Course outline

0. Introduction

- Some history
- Basic notations

1. Frequency-based Substructuring for starters

- Assembly of admittances (2 subdomains)
- Example of a guitar
- Generalization to more subdomains

2. Some important tricks to make FBS work

- **Weakening of compatibility: the virtual point transformation**
- **Example of the AM-structure in PyFBS**
- **Decoupling**
- **Example of a rubber mount**

3. Blocked forces and transfer path analysis

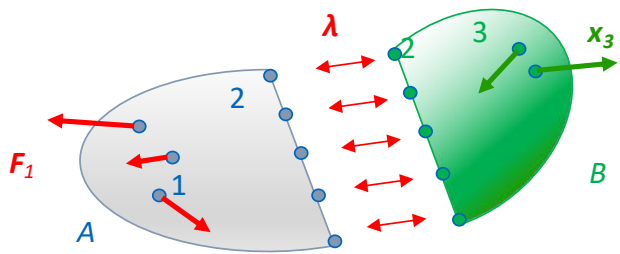
- The concept of blocked forces
- In-situ measurements of blocked forces
- example

4. Some other tastes of experimental substructuring

- Numerical substructures – model reduction
- Impulse-Based Substructuring

Weakening of the interface compatibility: the virtual point transformation

“trick” to alleviate problems arising from inaccuracies in the measurement of components:



$$\mathbf{x}_3^B = \mathbf{Y}_{32}^B (\mathbf{Y}_{22}^A + \mathbf{Y}_{22}^B)^{-1} \mathbf{Y}_{21}^A \mathbf{f}_1^A$$

Internal interface forces λ to close the gap

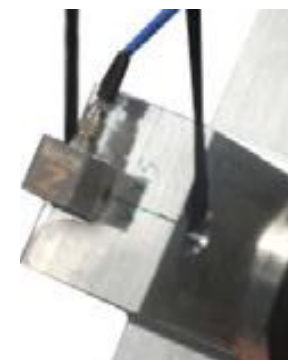
Frequency-Based
Substructuring
(FBS)

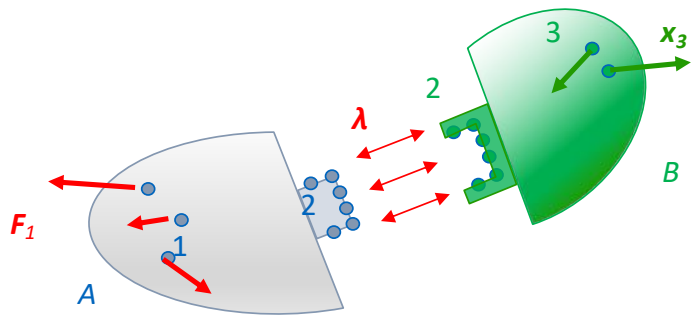
Computation of the interface forces requires summing interface admittances and inverting.

If \mathbf{Y}_{22}^A and/or \mathbf{Y}_{22}^B are obtained from measurements, they will slightly inexact due to

- calibration errors of the force and displacement sensors
- noise in the signal and data acquisition errors (windowing, filters)
- added mass of the vibration sensors, damping of sensor cables ...
- errors in the positioning/orientation of the sensors

→ Errors amplified in the FBS formulas





$$\boldsymbol{x}_3^B = \mathbf{Y}_{32}^B (\mathbf{Y}_{22}^A + \mathbf{Y}_{22}^B)^{-1} \mathbf{Y}_{21}^A \boldsymbol{f}_1^A$$

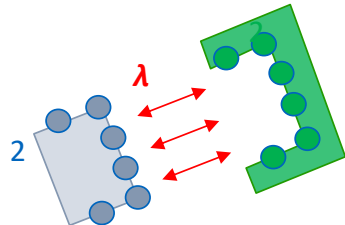
Internal interface forces λ to close the gap

Frequency-Based
Substructuring
(FBS)

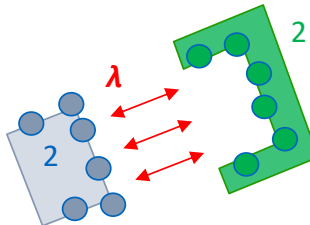
Assume that the interface motion is nearly a rigid body motion:

Usually, one measures many more degrees of freedom to have a good representation of the interface.

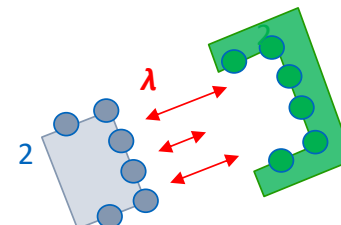
If one then tries to connect all dofs measured on the interface, then any small error in the measurements will generate very large and erroneous interface forces:



Correct interface forces
when dofs move as a rigid body

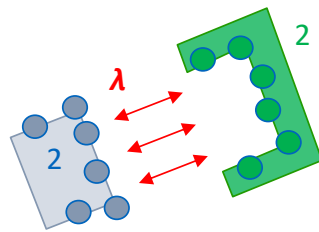


Dofs motion according to measured admittance
when correct interface forces are applied

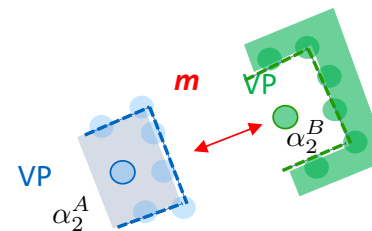


Interface forces needed to ensure
compatibility according to measured admittances

To avoid big errors, estimate an average and impose that **only the average motion** should be compatible, leaving detailed measurement **errors unmatched** (so not influencing the interface forces):



Dofs motion according to measured admittance
when correct interface forces are applied



Matching only the rigid motion part of the interface

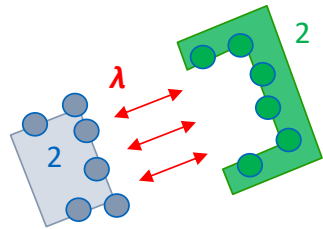
The motion of the interface on each side is then represented by a **virtual point** (VP) that has 6 dofs.
Only 3 forces and 3 moments on interface

$$\mathbf{x}_2^A = \mathbf{R}_2^A \alpha_2^A + \boldsymbol{\mu}^A$$

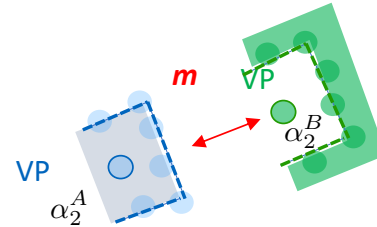
Asking the error to be orthogonal to the rigid body modes (so 0 in an average sense):

$$\begin{aligned} \mathbf{R}_2^{A^T} \boldsymbol{\mu}^A &= 0 \rightarrow \mathbf{R}_2^{A^T} \mathbf{x}_2^A = \mathbf{R}_2^{A^T} \mathbf{R}_2^A \alpha_2^A \\ &\rightarrow \alpha_2^A = (\mathbf{R}_2^{A^T} \mathbf{R}_2^A)^{-1} \mathbf{R}_2^{A^T} \mathbf{x}_2^A = \mathbf{T}_{VPT}^A \mathbf{x}_2^A \end{aligned}$$

Transformation (reduction) matrix that computes
in a least-square sense the rigid motion amplitudes



Dofs motion according to measured admittance
when correct interface forces are applied



Matching only the rigid motion part of the interface

This [virtual point transformation](#) (VPT) can also be applied on the B side.

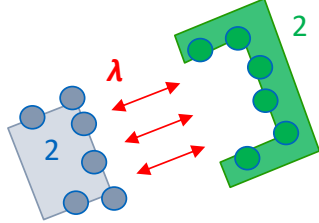
A similar transformation needed to transform the resulting forces and moments for the VP :

$$\mathbf{f}_2^A = \mathbf{T}_{VPT}^{A^T} \mathbf{m}$$

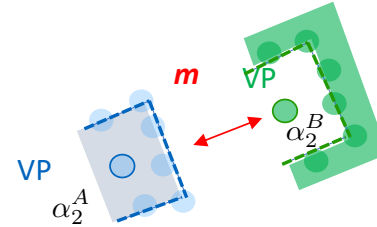
$$\mathbf{f}_2^B = \mathbf{T}_{VPT}^{B^T} (-\mathbf{m})$$

→ finds the force distribution with minimum amplitude along the interface that has resultant forces/moments **m**.

→ **m** used as internal interface forces (Lagrange multipliers) between the VP.



Dofs motion according to measured admittance
when correct interface forces are applied



Matching only the rigid motion part of the interface

$$\begin{aligned}\alpha_2^A &= (\mathbf{R}_2^{A^T} \mathbf{R}_2^A)^{-1} \mathbf{R}_2^{A^T} \mathbf{x}_2^A = \mathbf{T}_{VPT}^A \mathbf{x}_2^A \\ \alpha_2^B &= (\mathbf{R}_2^{B^T} \mathbf{R}_2^B)^{-1} \mathbf{R}_2^{B^T} \mathbf{x}_2^B = \mathbf{T}_{VPT}^B \mathbf{x}_2^B \\ \mathbf{f}_2^A &= \mathbf{T}_{VPT}^{A^T} \mathbf{m} \\ \mathbf{f}_2^B &= \mathbf{T}_{VPT}^{B^T} (-\mathbf{m})\end{aligned}$$

Enforcing then the compatibility only for the VPs and using the resulting forces \mathbf{m} as interface forces, one obtains to the modified FBS formula

$$\mathbf{x}_3^B = \mathbf{Y}_{32}^B (\mathbf{Y}_{22}^A + \mathbf{Y}_{22}^B)^{-1} \mathbf{Y}_{21}^A \mathbf{f}_1^A$$



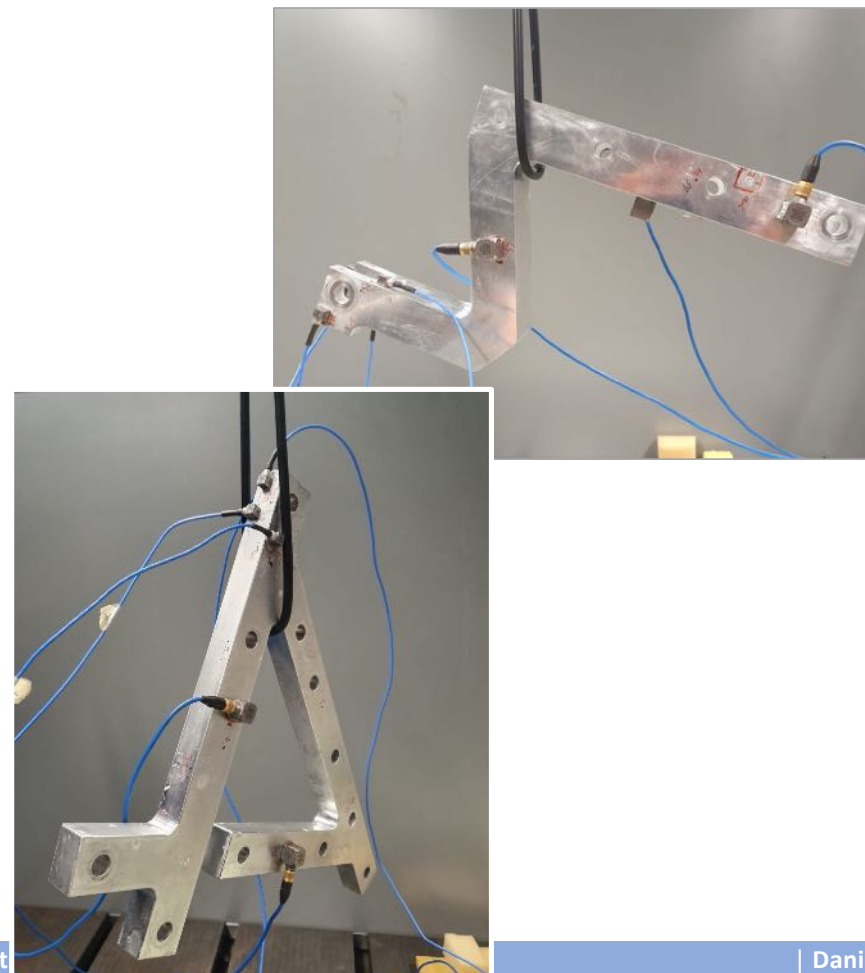
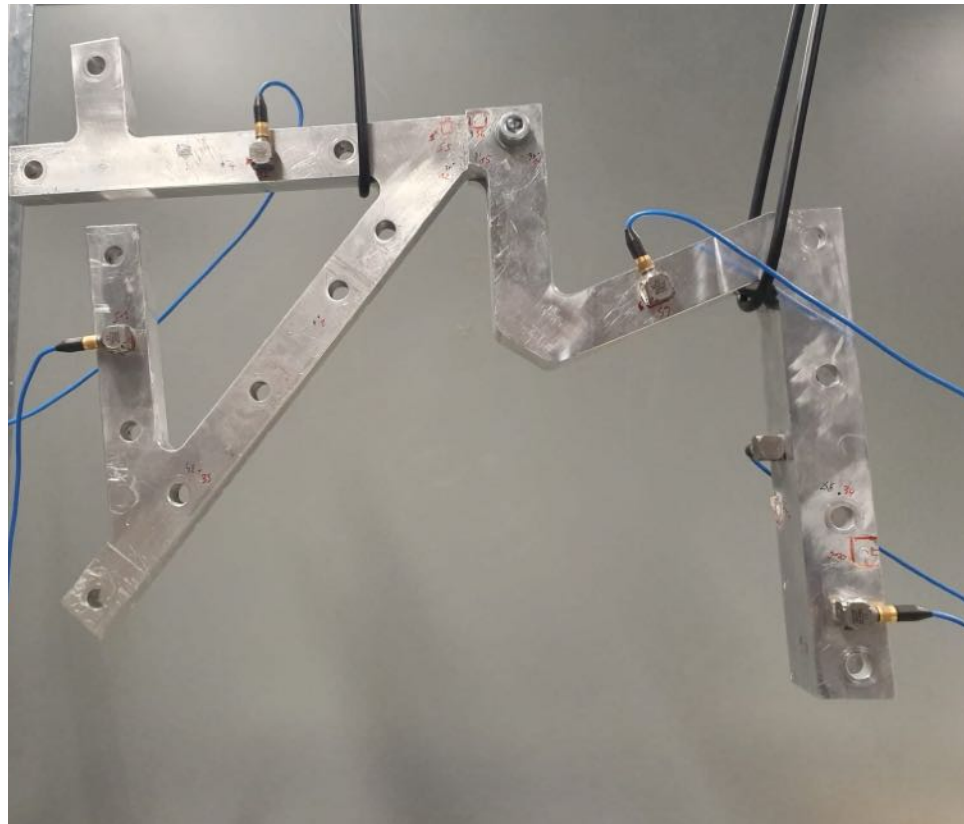
$$\mathbf{x}_3^B = \mathbf{Y}_{32}^B \mathbf{T}_{VPT}^{B^T} \left(\mathbf{T}_{VPT}^A \mathbf{Y}_{22}^A \mathbf{T}_{VPT}^{A^T} + \mathbf{T}_{VPT}^B \mathbf{Y}_{22}^B \mathbf{T}_{VPT}^{B^T} \right)^{-1} \mathbf{T}_{VPT}^A \mathbf{Y}_{21}^A \mathbf{f}_1^A$$

*Internal interface \mathbf{m} to make the interface compatible in average
→ Much better conditioned !*

Remarks:

1. **weakening** of the interface compatibility that avoids small measurement errors to affect too much the assembly result (technique similar to RBE3 elements in commercial codes).
2. no need anymore to measure $\mathbf{x}_2^A, \mathbf{x}_2^B$ on matching locations! Simplifies significantly the measurement campaign !
3. Locations for the force input and for the displacements on 2 can be different !

Example of an assembly by Frequency Based Substructuring (FBS)

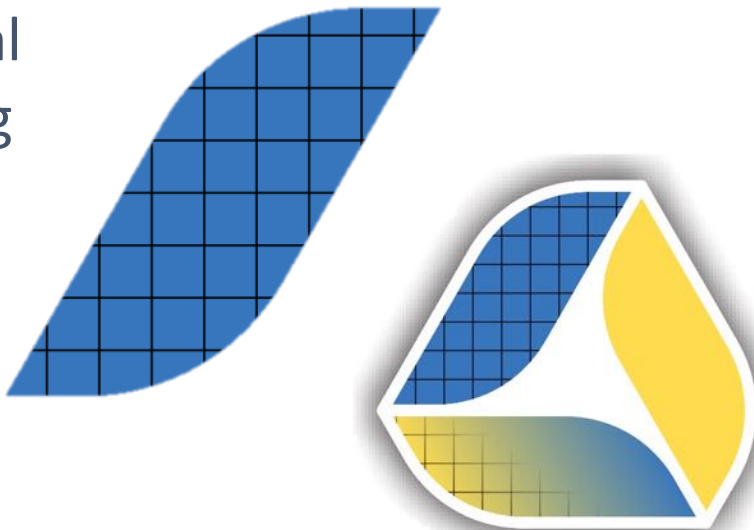


PyFBS: open-source DS



Numerical modelling

- FEM import
- Model reduction
- Eigenvalue extraction
- FRF synthesis



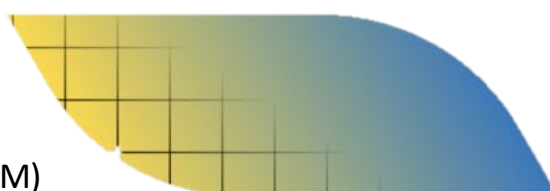
Experimental modelling

- Data Import (*.uff, *.hdf, ...)
- Sensor/impact positioning
- Interface reduction: VPT...
- ODS animation
- Mode shape animation



Hybrid modelling

- System equivalent model mixing (SEMM)
 - System equivalent reduction and expansion process (SEREP)

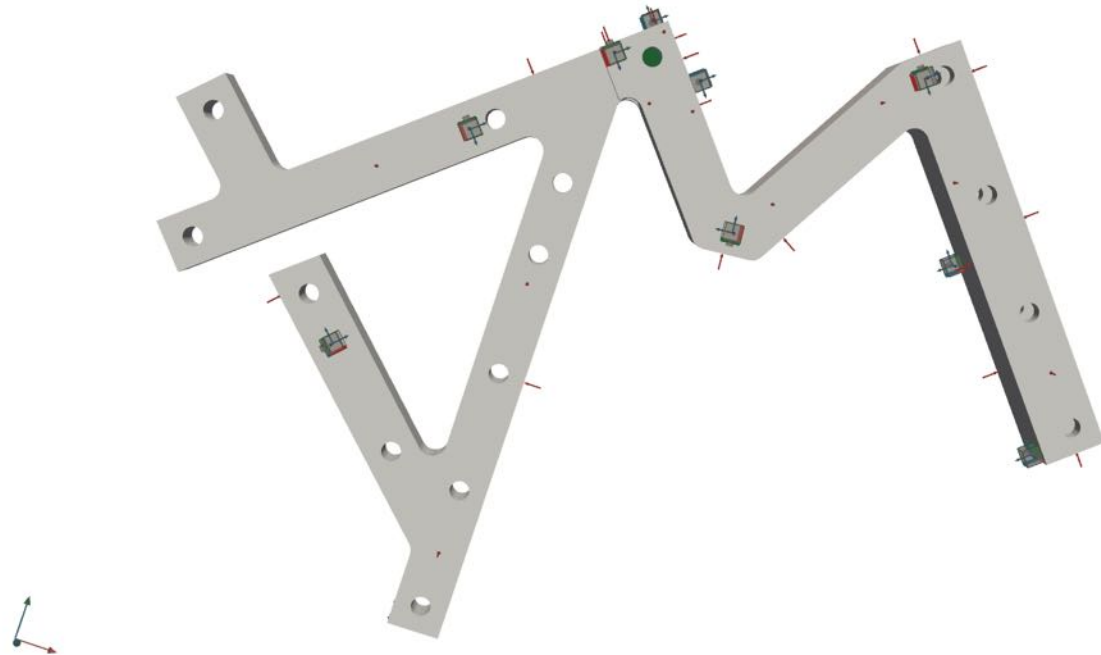


<https://gitlab.com/pyFBS/pyFBS>

PyFBS: open-source DS



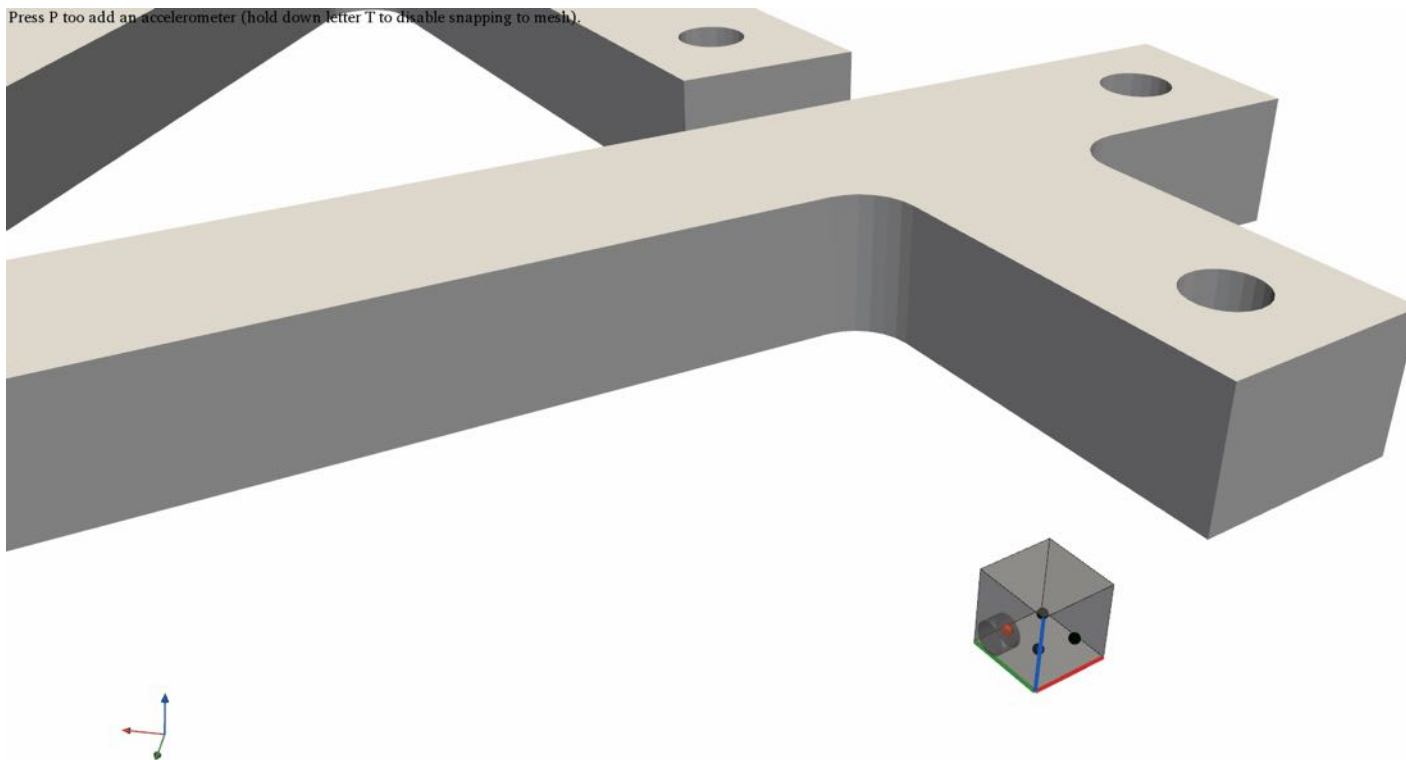
- Easy organization of data
- Design of Experiment using CAD models



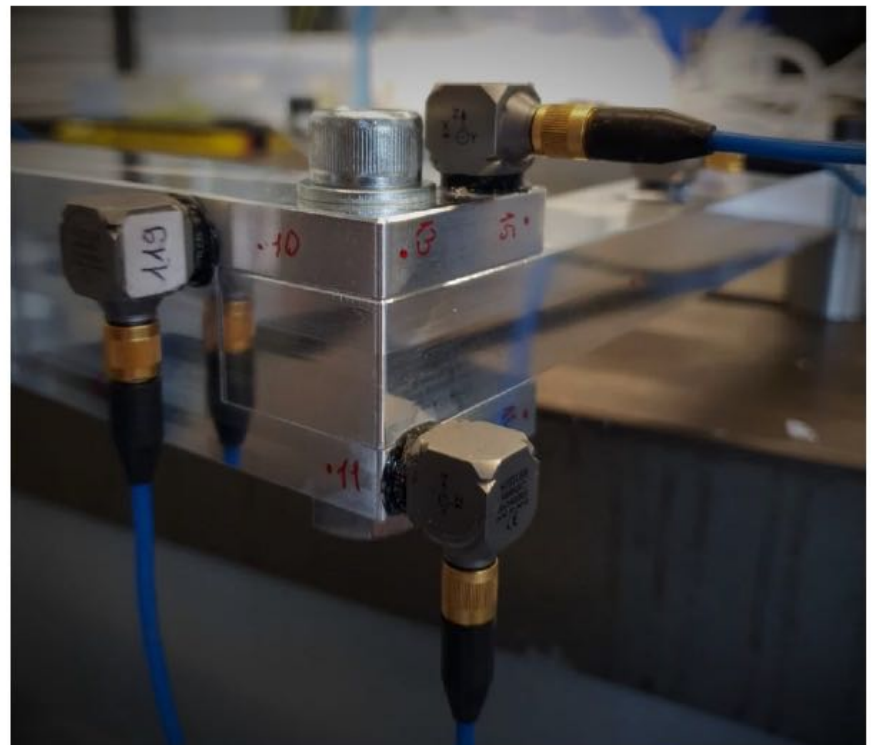
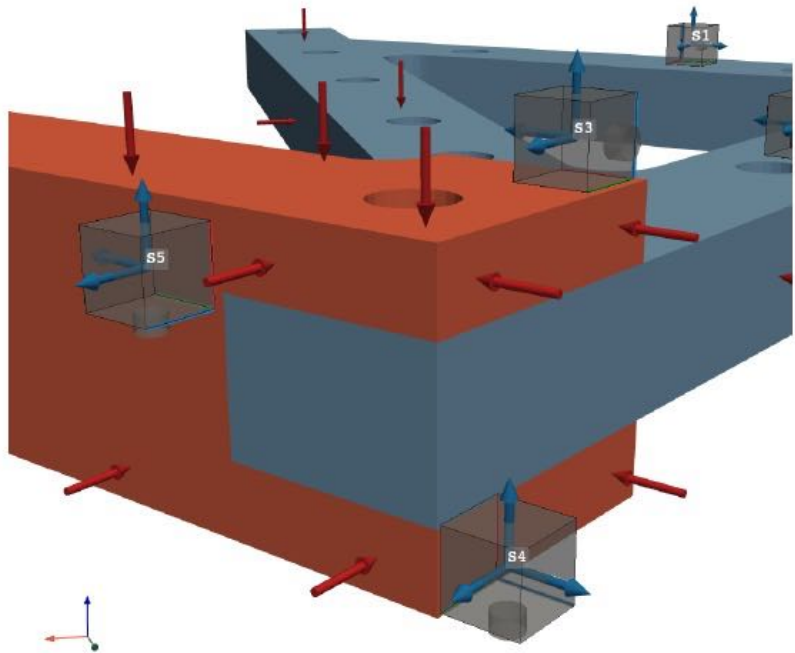
PyFBS: open-source DS



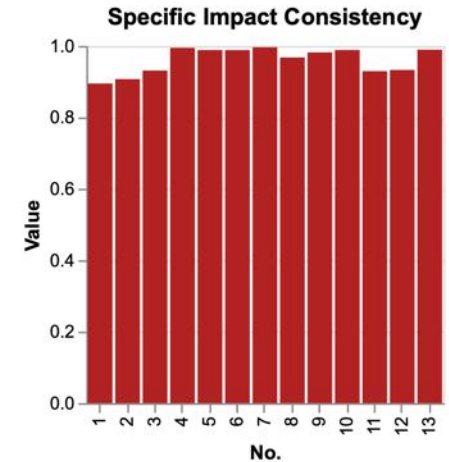
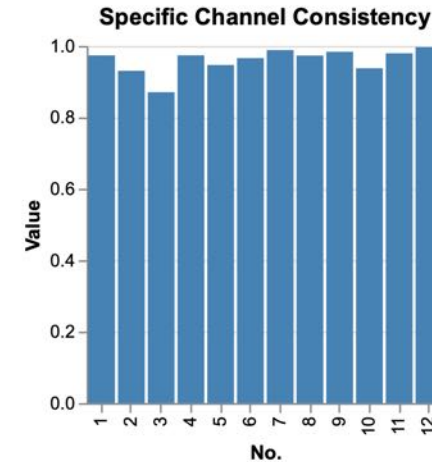
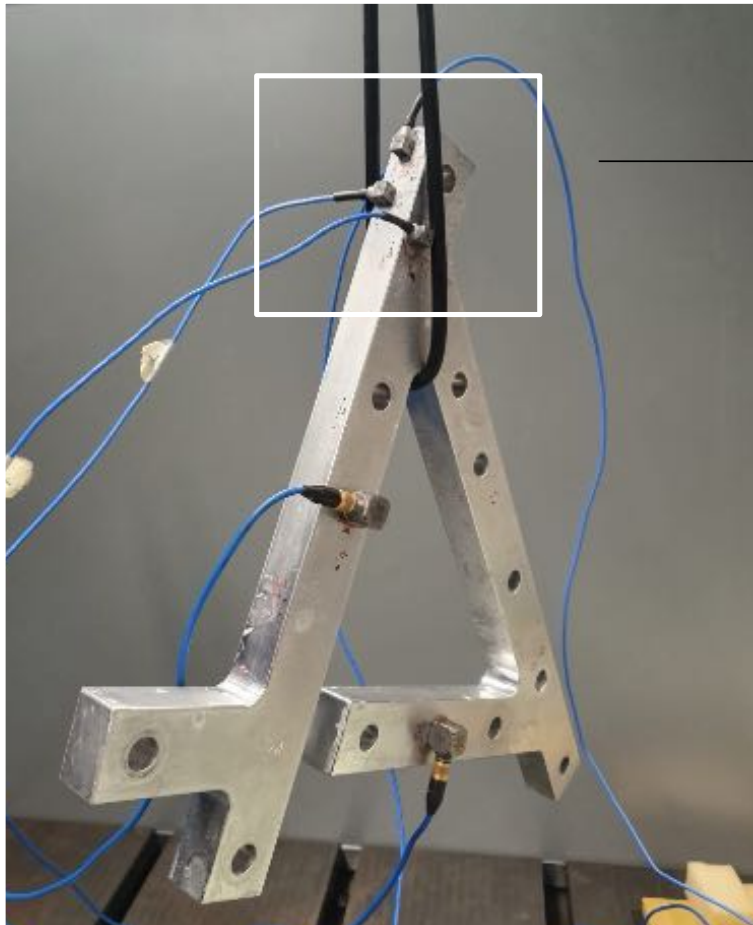
Interactive DOE



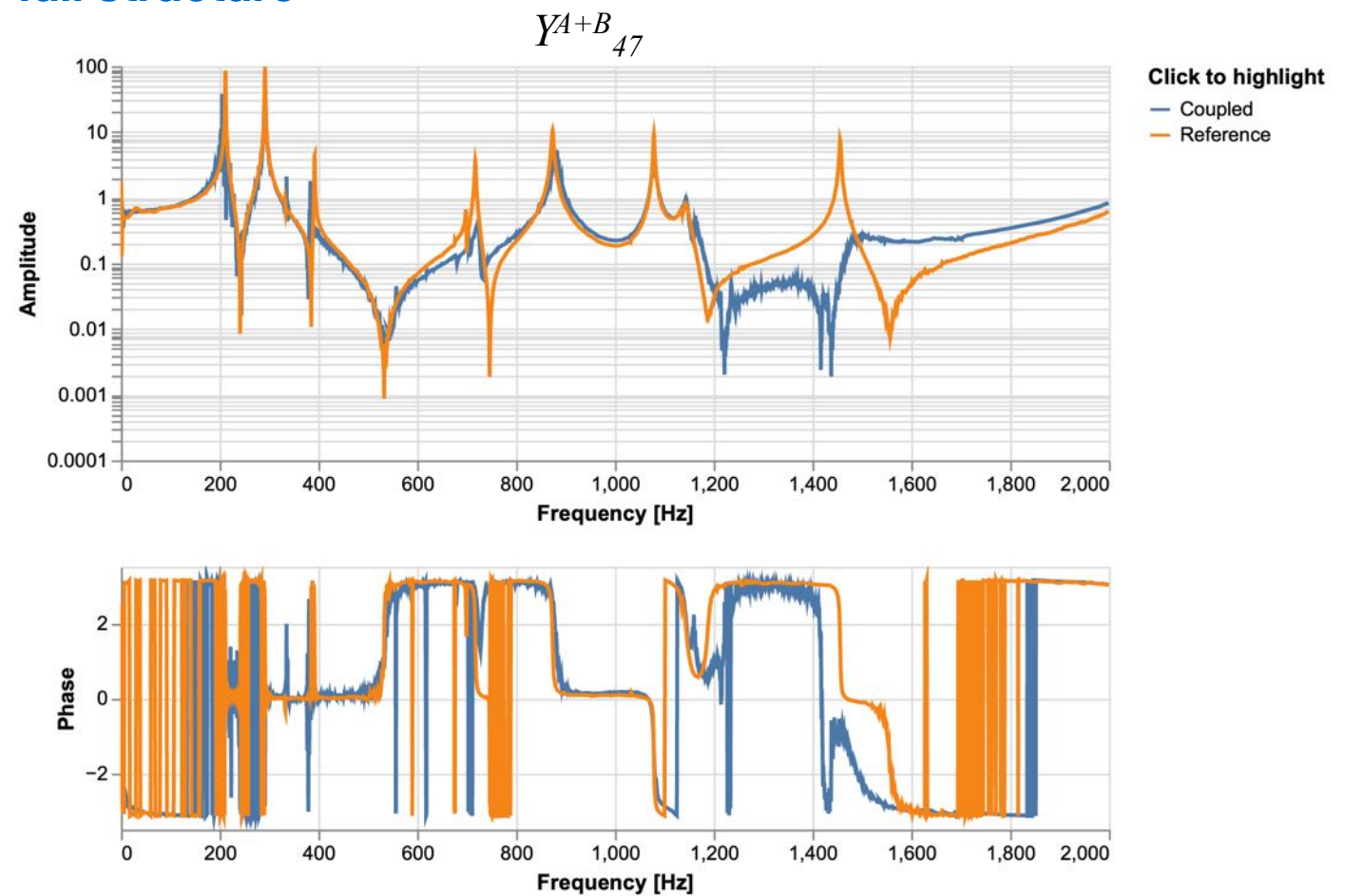
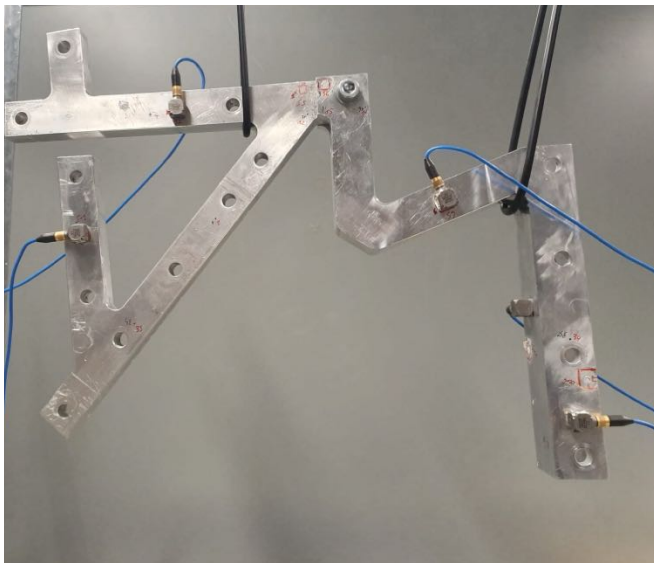
PyFBS: open-source DS



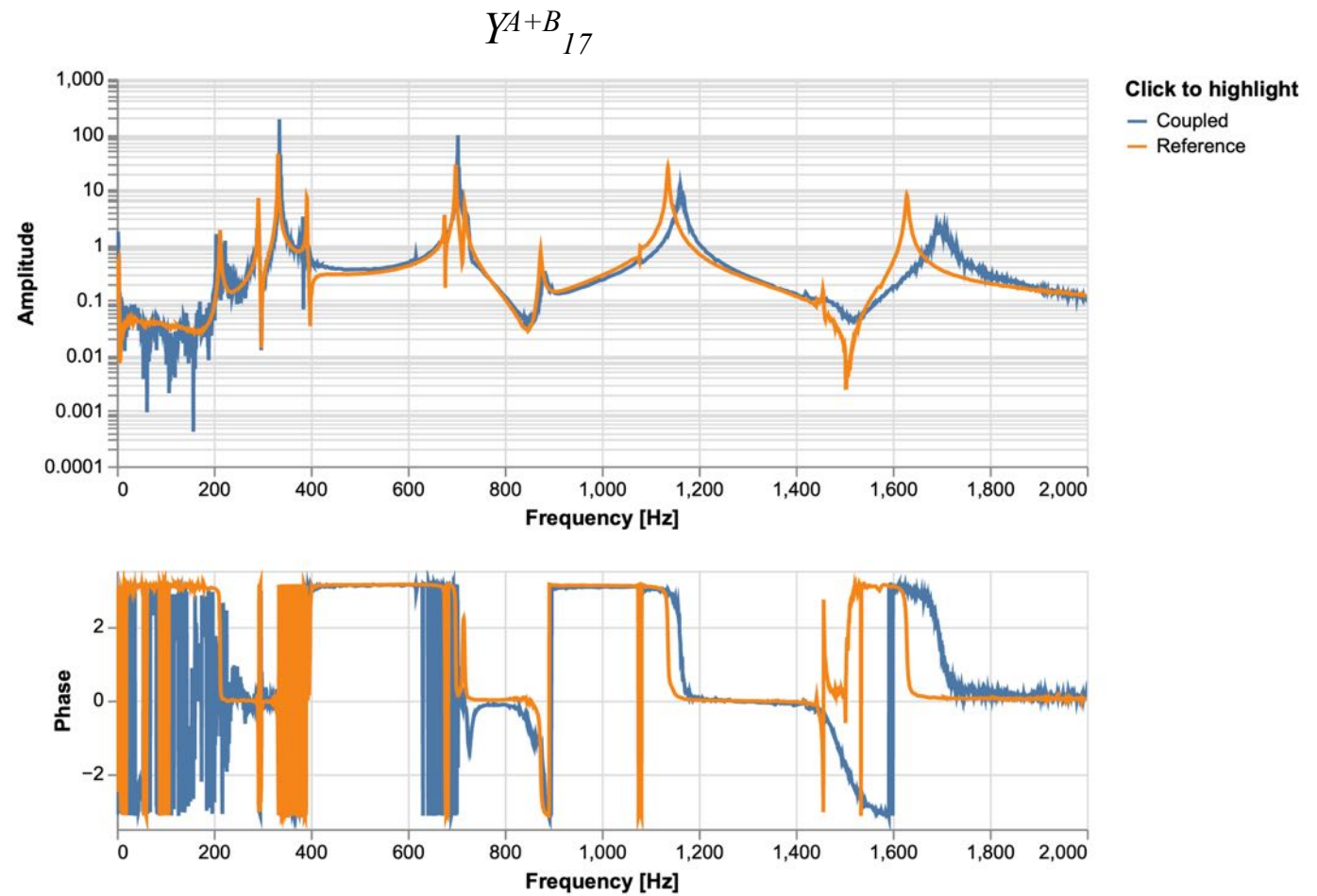
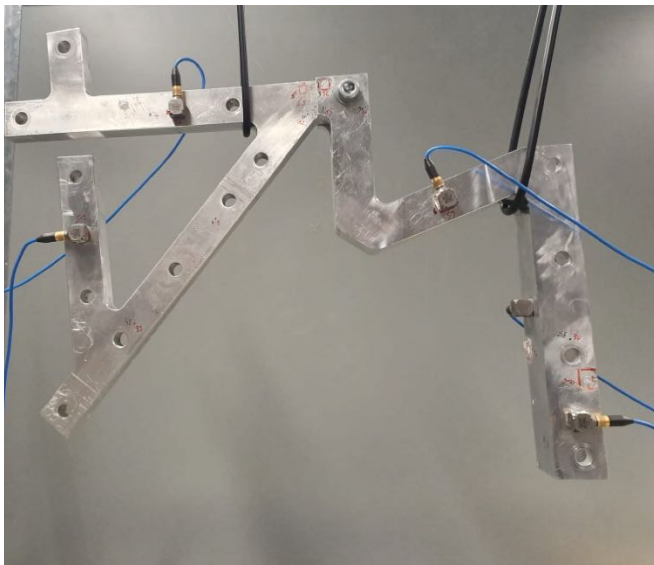
Verifying rigidity of interfaces



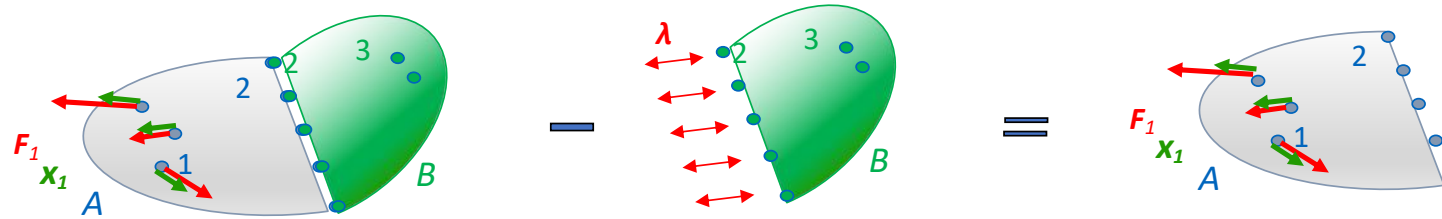
Assemble and compare to full structure



Assemble and compare to full structure

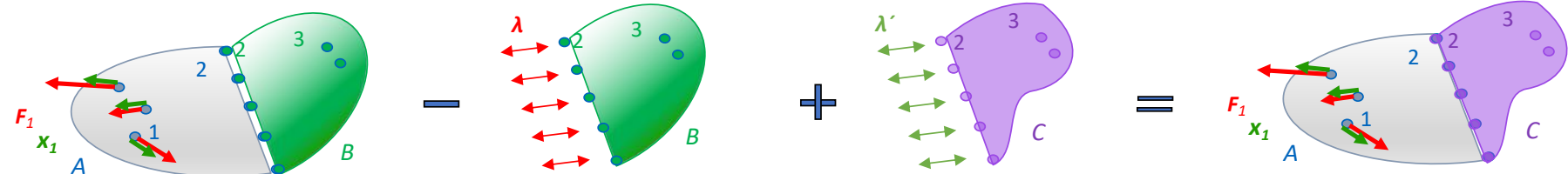


Decoupling

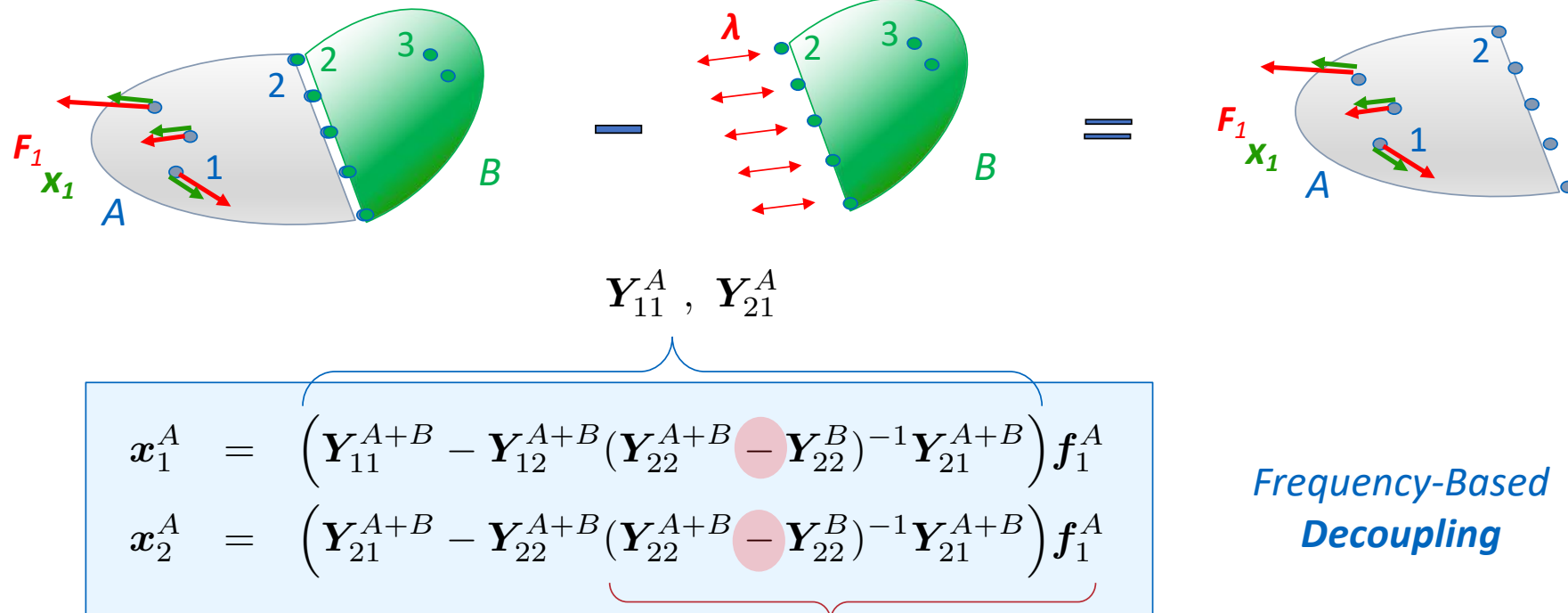


Interesting when:

- a component A has too big amplitudes during the test or cannot be well excited because it is too small
- to analyse dynamic changes when a component is replaced by another:



Decoupling = adding a “negative” substructure B to the assembly $A+B$:

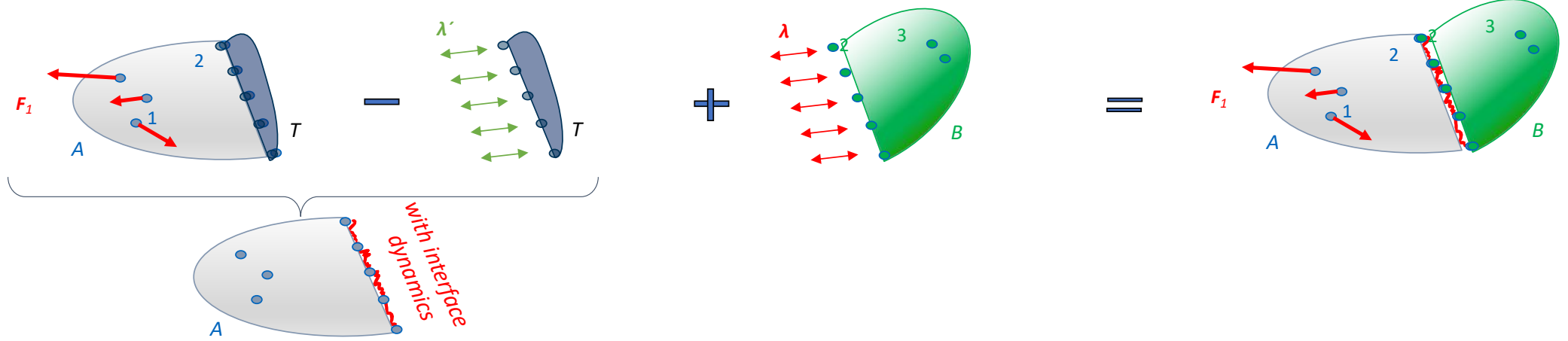


*Frequency-Based
Decoupling*

Internal interface forces λ present in the assembly, that must be removed to have the behavior of A without coupling

Decoupling: Transmission simulator

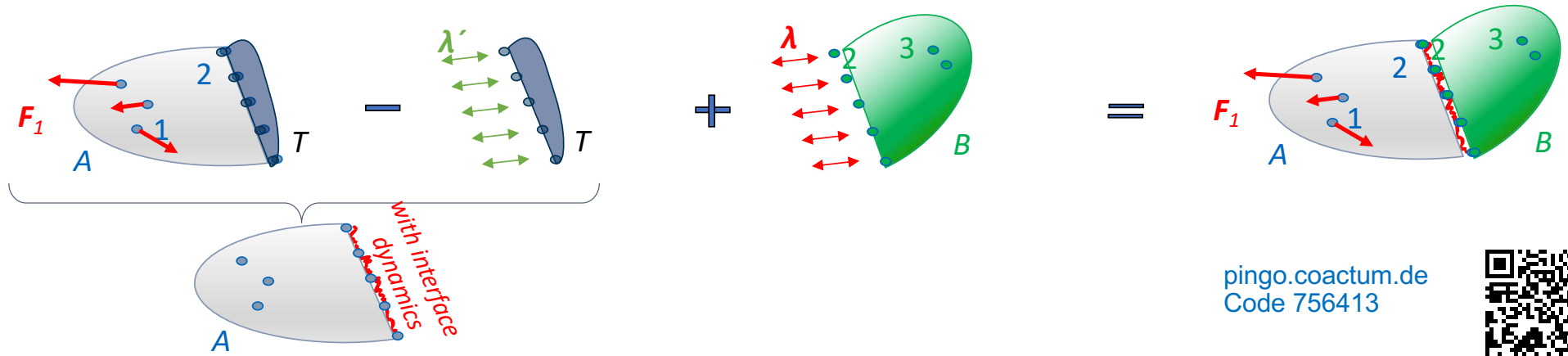
When the interface dynamics is important (bolted joints, glued interface ...)



The transmission simulator should have an interface dynamics similar to what will be observed when substructure B is coupled

* The name “transmission simulator” was first coined in
R. L. Mayes and M. Arviso. Design studies for the transmission simulator method of experimental dynamic substructuring. In International seminar on modal analysis, ISMA, Leuven, 2010. KUL.

Check yourself



pingo.coactum.de
Code 756413



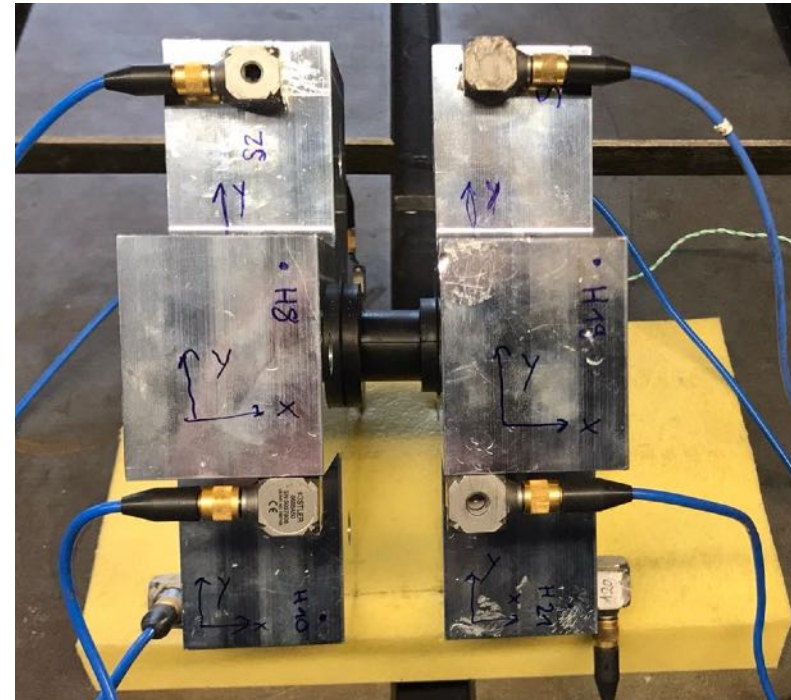
What is another interesting advantage of the transmission simulator?

- The dynamics of the component is measured for vibrations close to what will be seen in the final assembly, thereby reducing the errors when applying the FBS for future assemblies.
- It allows accounting for non-linear effects in the interface.
- It reduces the number of operations when building the assembled dynamics.

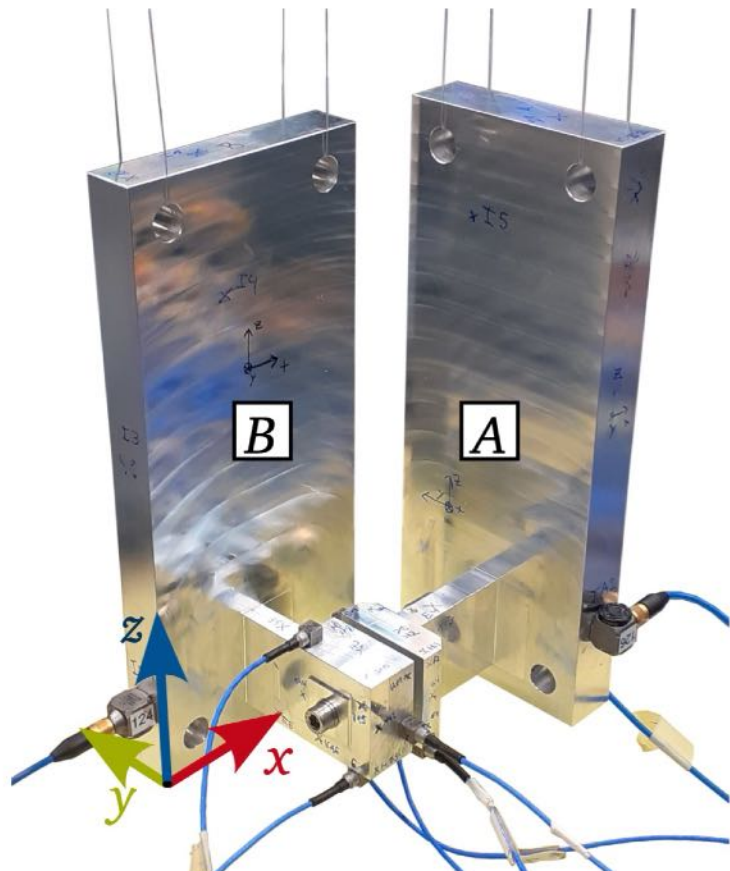
Decoupling: Joint identification



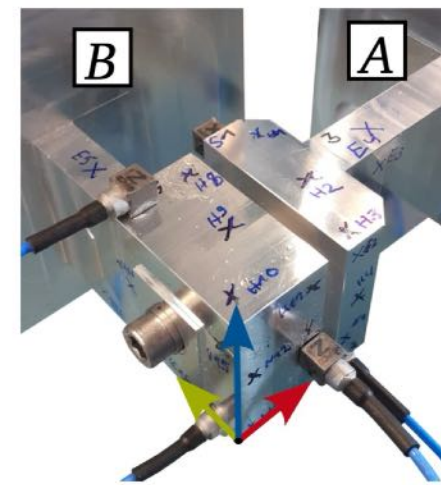
[2]



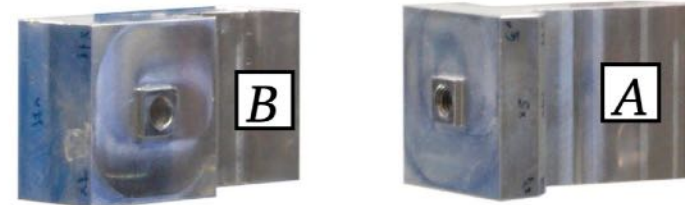
[2] Brake, Matthew RW, and Pascal Reuß. "The Brake-Reuß beams: a system designed for the measurements and modeling of variability and repeatability of jointed structures with frictional interfaces." *The Mechanics of Jointed Structures: Recent Research and Open Challenges for Developing Predictive Models for Structural Dynamics* (2018): 99-107.



(a) Measurement setup with suspension.

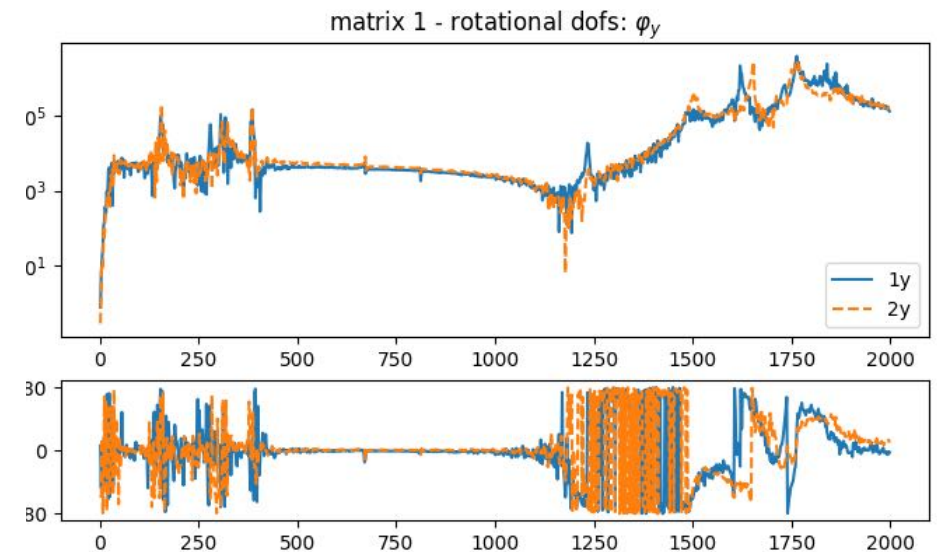
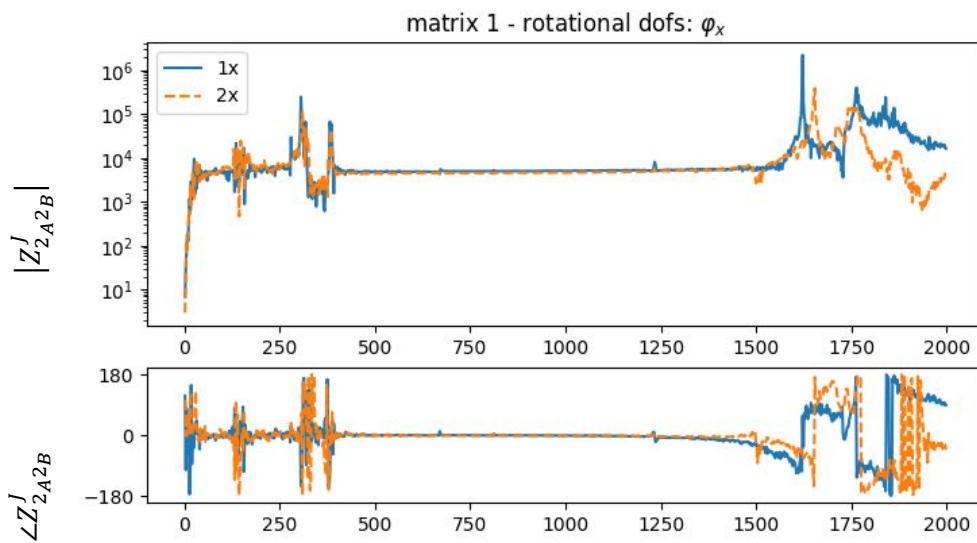
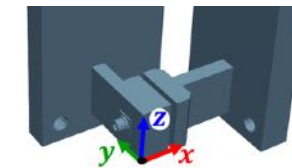


(b) Close-up of the assembled interface.



(c) Close-up on disassembled A and B.

- Interface impedance (including repeatability): translational dofs



M. Kreutz, F. Trainotti, V. Gimpl, and D. J. Rixen. On the robust experimental multi-degree-of-freedom identification of bolted joints using frequency-based substructuring. *Mechanical Systems and Signal Processing*, 203:110626, 2023.

Course outline

0. Introduction

- Some history
- Basic notations

1. Frequency-based Substructuring for starters

- Assembly of admittances (2 subdomains)
- Example of a guitar
- Generalization to more subdomains

2. Some important tricks to make FBS work

- Weakening of compatibility: the virtual point transformation
- Example of the AM-structure in PyFBS
- Decoupling
- Example of a rubber mount

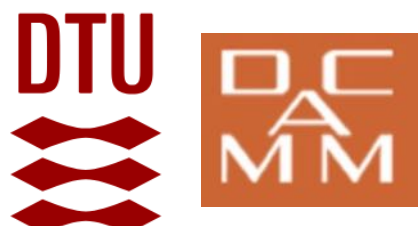
3. Blocked forces and transfer path analysis

- **The concept of blocked forces**
- **In-situ measurements of blocked forces**
- **example**

4. Some other tastes of experimental substructuring

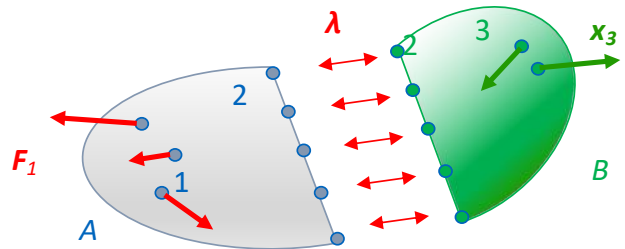
- Numerical substructures – model reduction
- Impulse-Based Substructuring

3. Blocked forces and transfer path analysis



The concept of blocked forces

How to measure the excitation source? Usually not possible (internal forces)



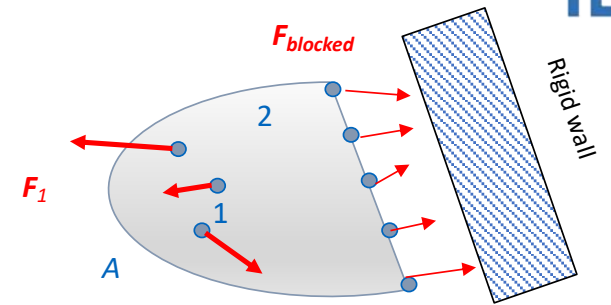
$$\mathbf{x}_3^B = \mathbf{Y}_{32}^B (\mathbf{Y}_{22}^A + \mathbf{Y}_{22}^B)^{-1} \mathbf{Y}_{21}^A \mathbf{f}_1^A$$

One idea would be to measure the interface force λ to characterize the source. Not a good idea, since interface force depend on the structure dynamics ! Change if substructure B changes.

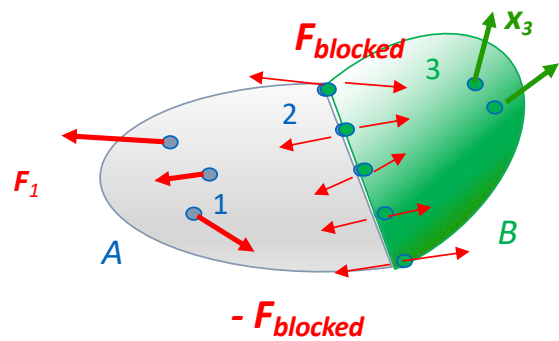
A much better and independent characterisation of the source excitation can be done with “*blocked forces*”.

Imagine that one measures the force that the source substructure A would apply on a fully rigid wall

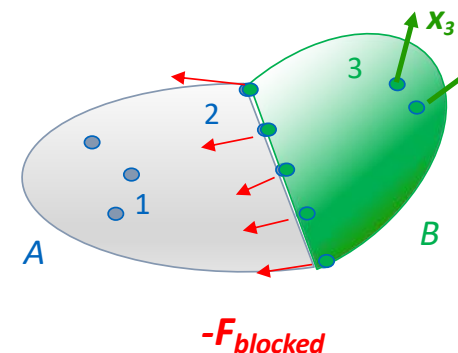
→ blocked forces F_{blocked} : forces that must be applied to fix the interface



Let us now make the following “thought experiment”:

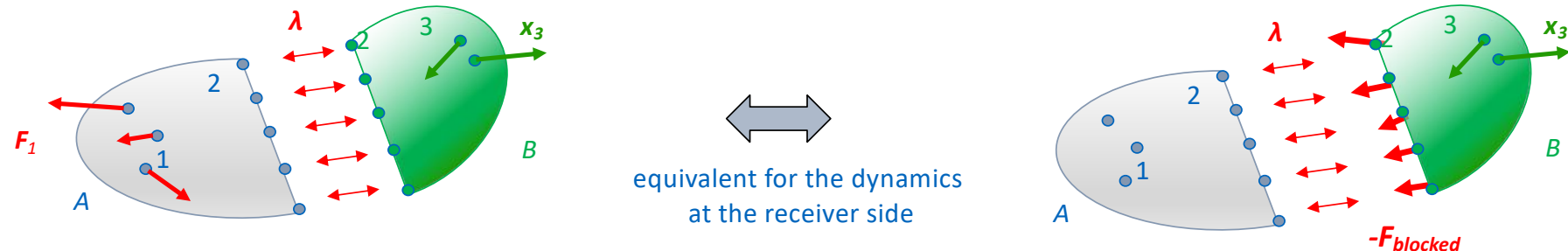


Apply F_{blocked} and $-F_{\text{blocked}}$ on the interface.
This leaves obviously the dynamics unchanged



Remove F_{blocked} and *the true source force F_1*
This also leaves the dynamics unchanged for the receiver B
since the combination of these two forces keeps the interface still
by definition of the blocked force.

Hence, it is equivalent (for the receiver) to excite the assembly with the true source force or with $-F_{blocked}$



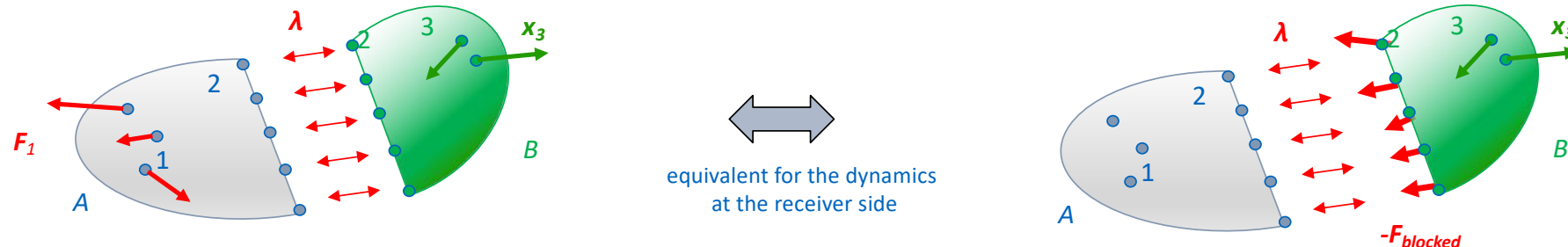
ATTENTION: $-F_{blocked}$ must be seen as a fictitious external force applied to the assembly.

Applying the blocked force as external force to the interface instead of applied the true source force is then (for the receiver) fully equivalent !

So the procedure for a TPA can be summarized as follows:

1. Measure (or estimate) the blocked force of the source
2. Measure the admittance of the assembly or build it from the dynamics from its components (using FBS)
3. Evaluate the vibration at the receiver from $x_3^B = Y_{32}^{A+B}(-F_{blocked})$

The concept of blocked forces can also be explained mathematically:



The response in B due to the real excitation is

$$\mathbf{x}_3^B = \mathbf{Y}_{31}^{A+B} \mathbf{F}_1 = [\mathbf{Y}_{32}^B (\mathbf{Y}_{22}^A + \mathbf{Y}_{22}^B)^{-1} \mathbf{Y}_{21}^A] \mathbf{F}_1^A$$

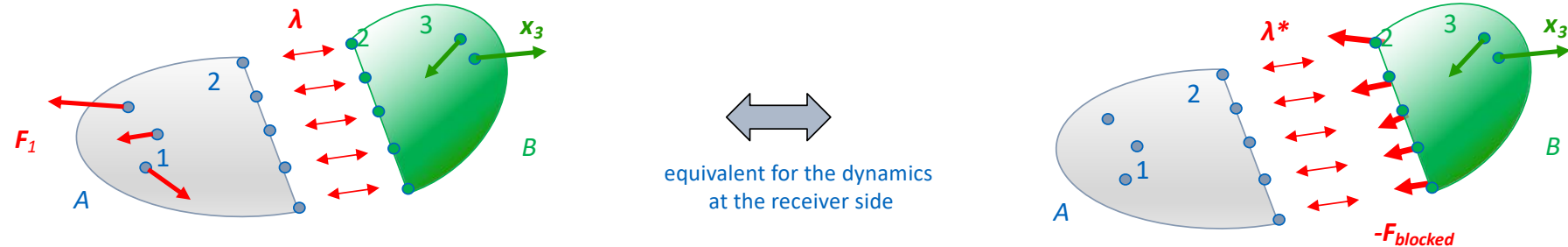
The response in B due to an equivalent external force on the interface is

$$\mathbf{x}_3^B = \mathbf{Y}_{32}^{A+B} \mathbf{F}_2^{eq} = [\mathbf{Y}_{32}^B (\mathbf{Y}_{22}^A + \mathbf{Y}_{22}^B)^{-1} \mathbf{Y}_{22}^A] \mathbf{F}_2^{eq}$$

The response in B will be identical if

$$\mathbf{F}_2^{eq} = (\mathbf{Y}_{22}^A)^{-1} \underbrace{\mathbf{Y}_{21}^A \mathbf{F}_1^A}_{\substack{\text{Motion of the free interface} \\ \text{Forces needed on the interface} \\ \text{to fix the free interface motion}}}= -\mathbf{F}_{\text{blocked}}$$

Check yourself



When applying the blocked force approach, the source excitation is characterized independently of the receiver by F_{blocked}

What statement is then true when using $-F_{\text{blocked}}$ in the TPA analysis ?

- The vibration of the source is not equivalent to the original problem
- The admittance of the source substructure does not need to be known



pingo.coactum.de
Code 756413

Check yourself

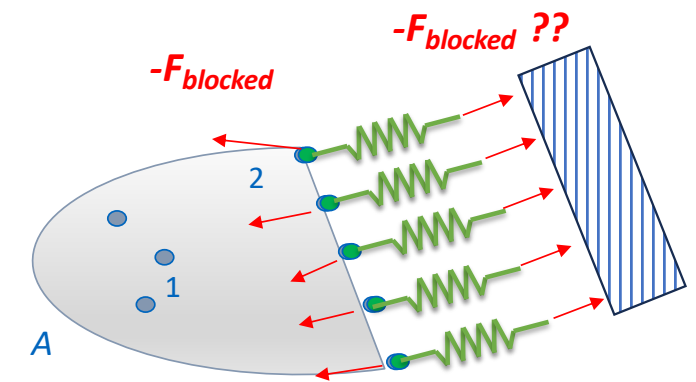
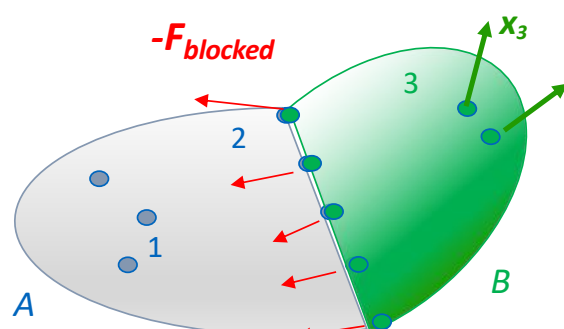
pingo.coactum.de
Code 756413



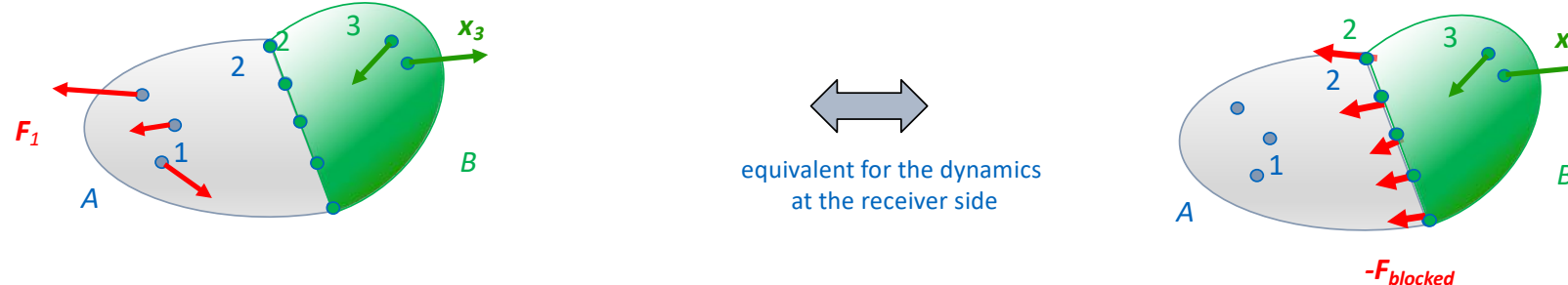
Imagine we attach the source to the fixed world through a massless spring.

The forces measured on the other side of the springs are also the blocked forces

- a. Yes
- b. No

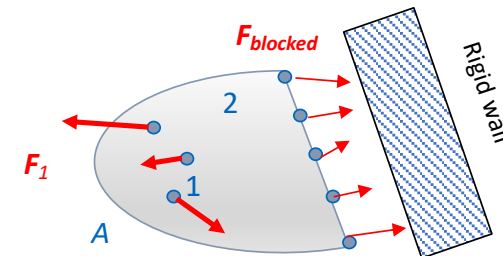


In-situ measurement of blocked forces



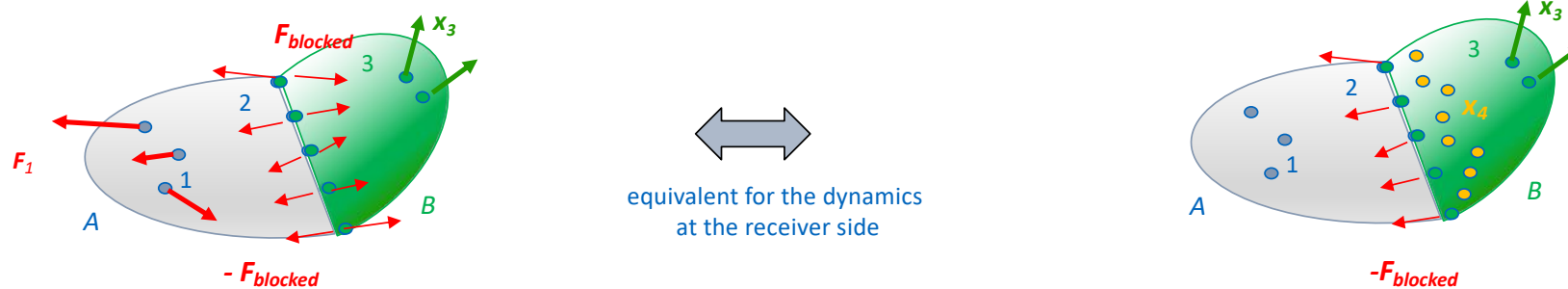
Measuring blocked forces on a rigid rig is very hard:

- A test rig is never fully rigid
- One needs to install several force sensors between the source and the test rig, thereby influencing the dynamics of the source ...



Hence, identify *during the operation of the assembled system ("in-situ")* the force on the interface that would create the observed output in the receiver (so the blocked force):

A. Moorhouse, A. Elliott, and T. Evans. In situ measurement of the blocked force of structure-borne sound sources. *Journal of Sound and Vibration*, 325(4–5):679 – 685, 2009.



The equivalent force is then obtain as

- + No need to uncouple the source
- + The source is measured in a realistic coupled setting
- + No need for force sensors in the operational measurement

- Requires measuring enough indicators to fully “observe” the interface
- Need to excite \mathbf{x}_2 or \mathbf{x}_4 to measure \mathbf{Y}_{42}^{A+B}
- Indirect measurement of the blocked force, can be bad if \mathbf{Y}_{42}^{A+B} not precisely measured



$$\mathbf{F}_2^{eq} = -\mathbf{F}_{blocked} = (\mathbf{Y}_{42}^{A+B})^+ \mathbf{x}_4^{op}$$

FRF from interface forces to indicators

Vibration measured in operation at the indicators

- Use a redundant number of indicators (regularization by the pseudo-inverse)
- If the interface is very stiff, apply a VPT on the interface dofs to average the blocked force in resulting forces and moments

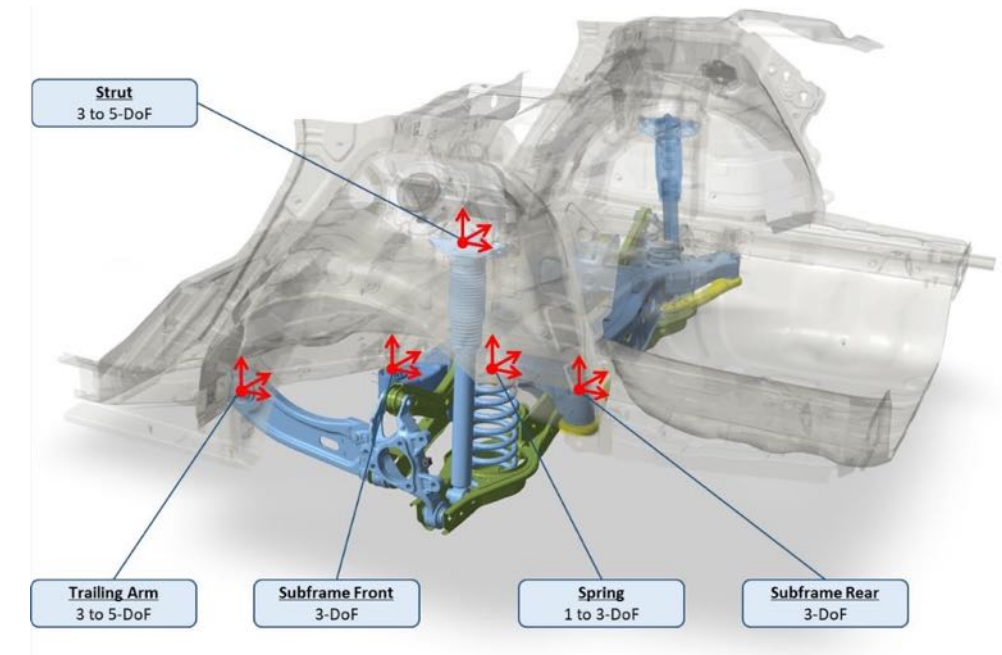
Example: blocked forces and TPA of tire excitation on a car

This example is taken from <https://www.vibestechology.com/case/vibes-hyundai-motor-company/> that was published in [vdSeijs,2021] van der Seijs, M. V., Harvie, J. M., & Song, D. P. (2021, February). Road noise NVH: embedding suspension test benches in NVH design using Virtual Points and the TPA framework. In Proceedings of the thirty-ninth international modal analysis conference.

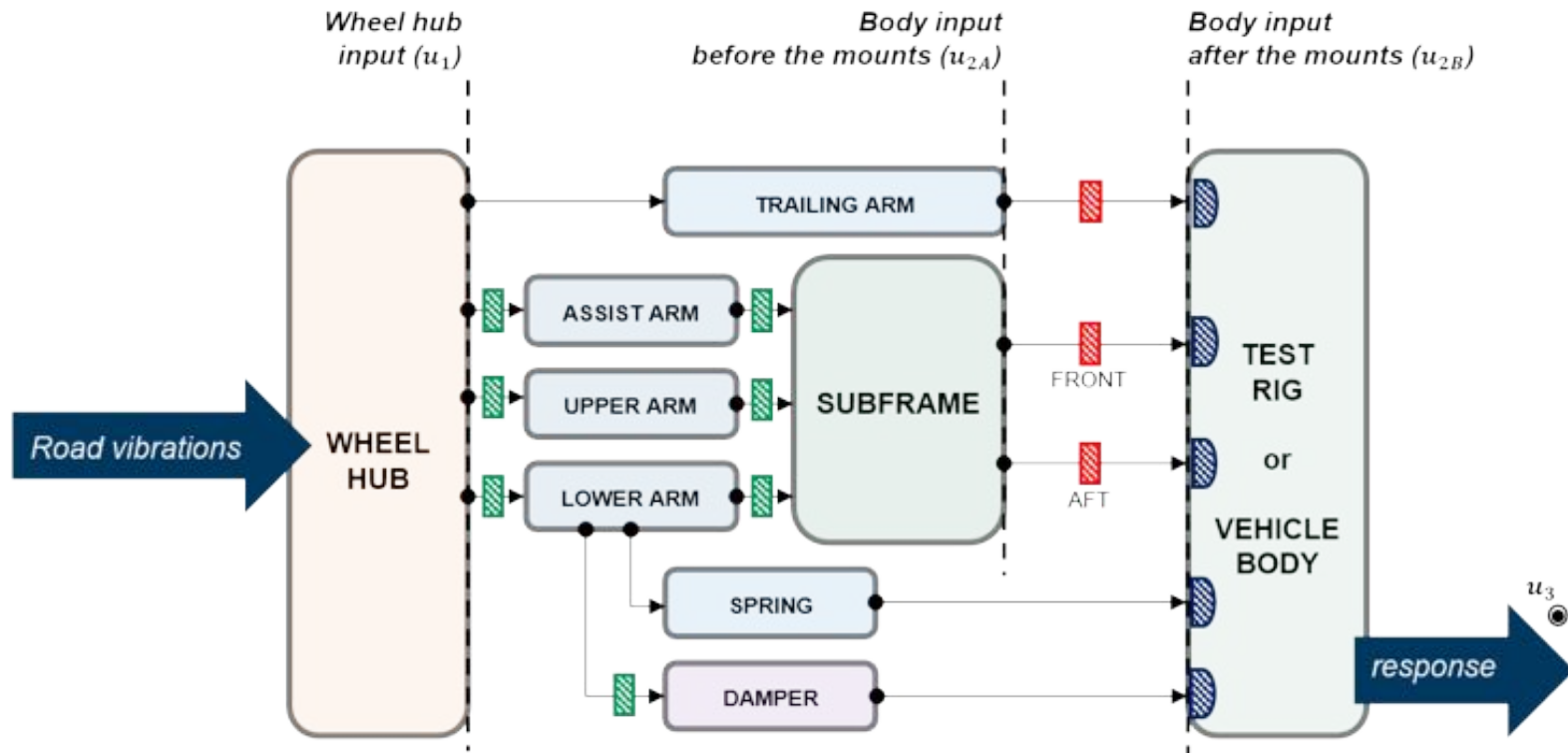


One of the aims of the study was to verify the use of blocked forces and of component-based TPA:

- Source: the rear suspension excited by a runup of the rear wheels on a “dyno” from 20 – 120 km/h.
- Receiver: car, from connection to rear suspension to driver’s ear (output: sound pressure levels)



The 5 connection points of the rear suspension and their modelling strategy using virtual points [vdSeijs,2021]

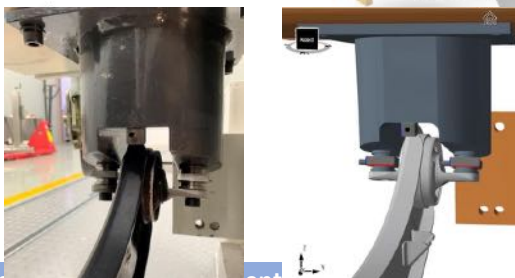
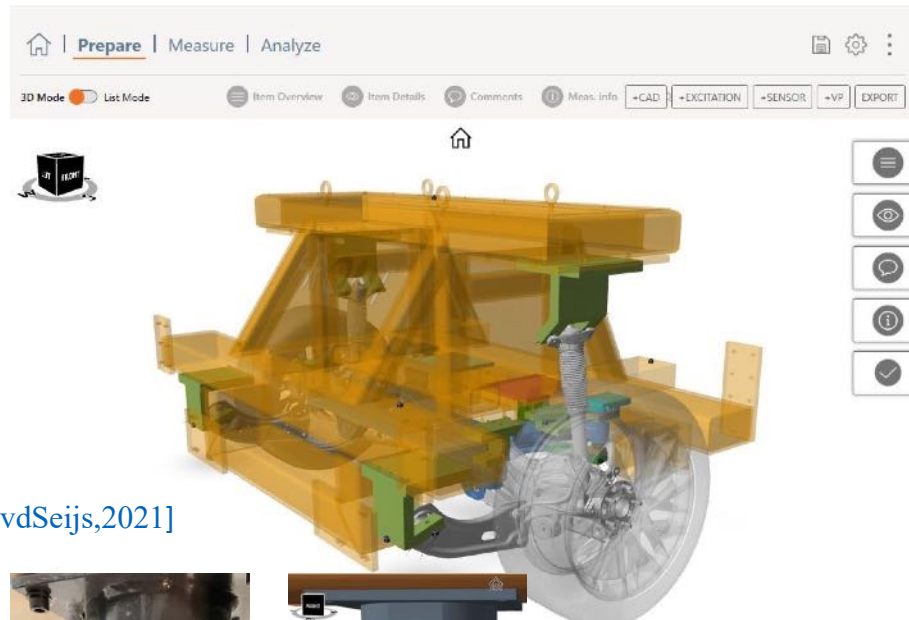


Schematic overview of the rear wheel suspension system for a single side [vdSeijs,2021]

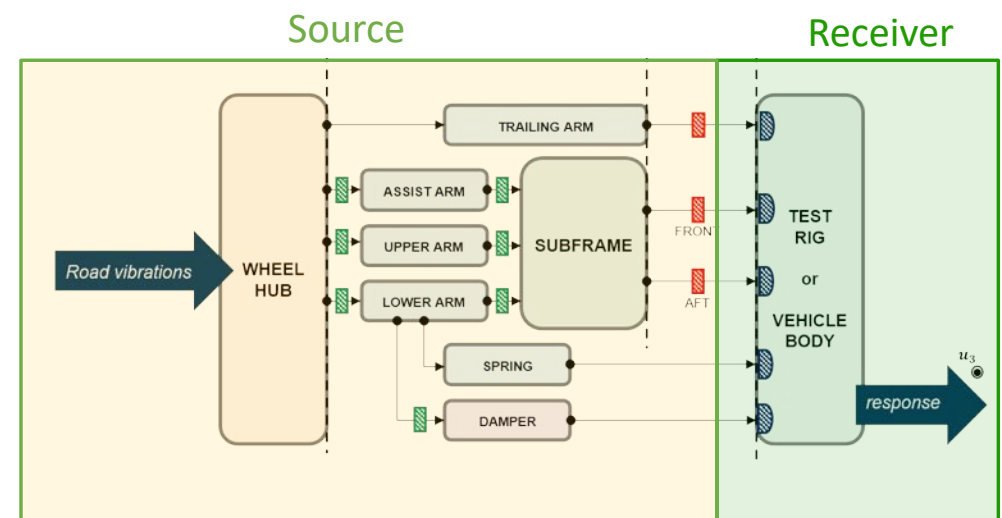
Several ways to apply the Blocked force TPA are tested

Validation case 1

- *interface after rubber mount*
- *blocked force from fixed interfaces (after rubber mounts)*
- *TPA : blocked force on $Y^{\text{full-car}}$ after the rubber mounts*

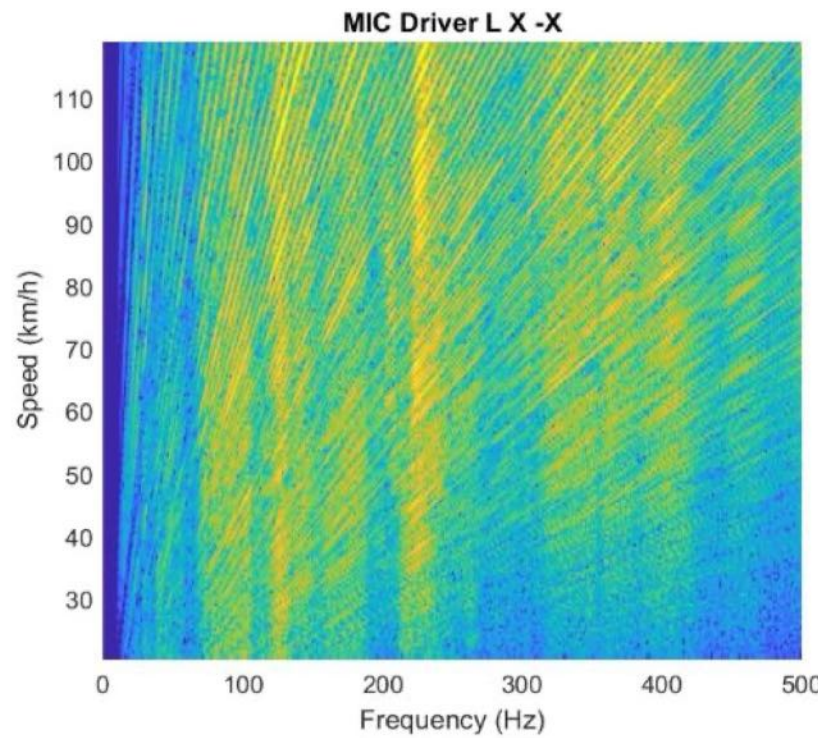


Blocked force measured on rigid test rig with force sensors (green connectors very rigid)

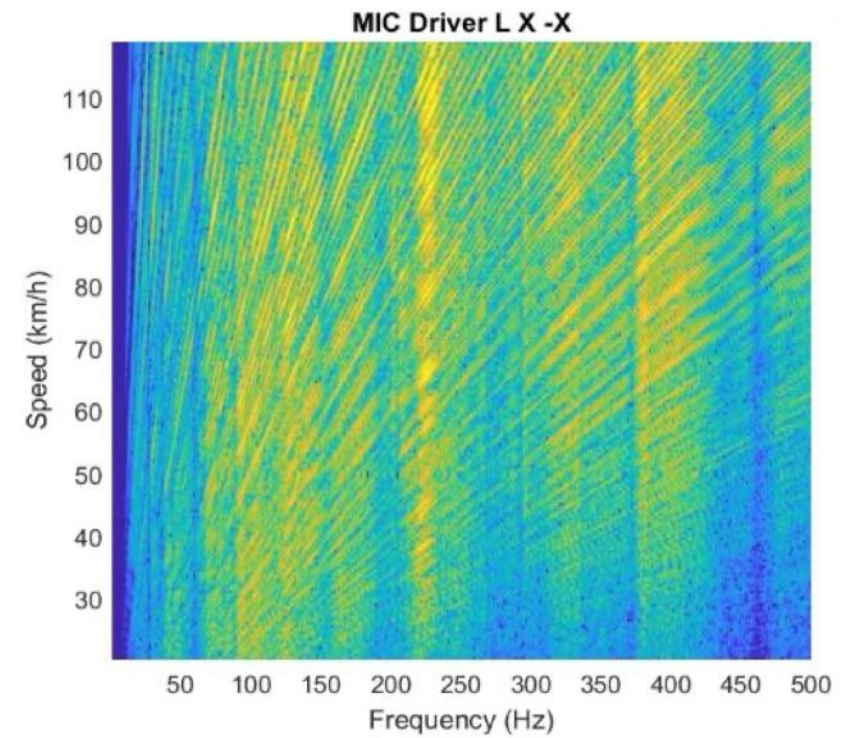


Validation case 1

Comparing microphone levels during run-up (ear driver) as computed through TPA with Blocked Forces from rigid interface, and validation measurements with the car on the dyno.



TPA with Blocked Forces from rigid interface

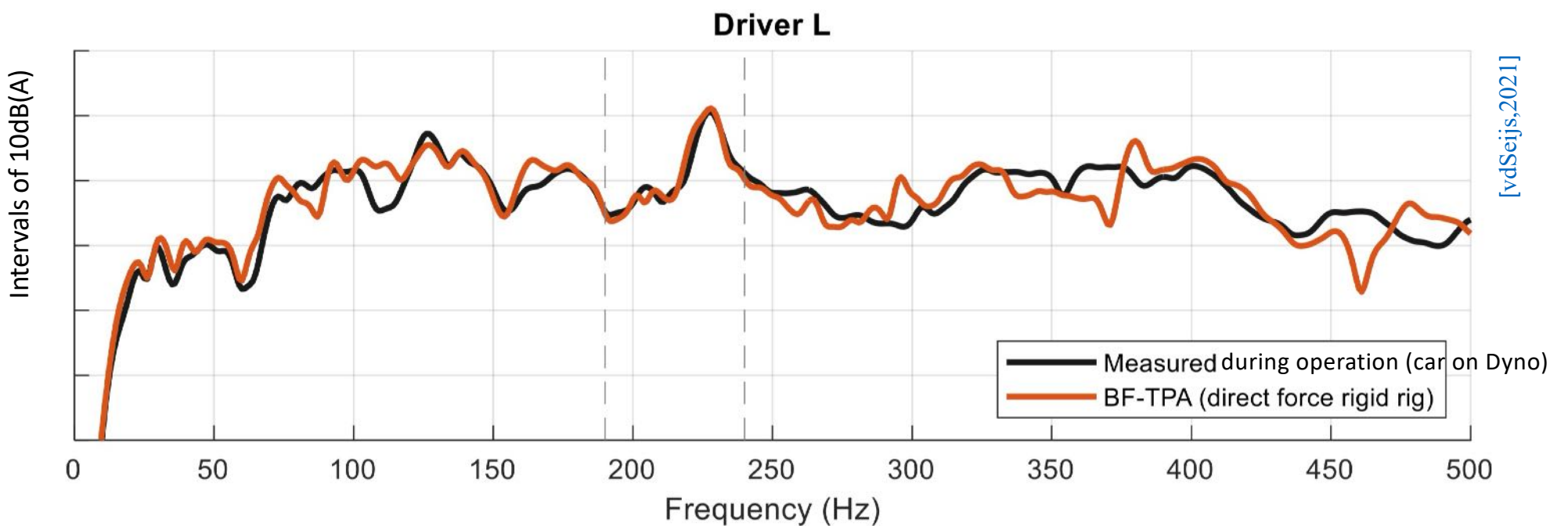


Validation measurement during operation
(car on Dyno)

[vdSeijss,2021]

Validation case 1

Comparing time-averaged spectra of driver-ear sound pressure levels in dB(A) over the full run-up from 20-120 km/h, as computed through TPA with Blocked Forces from rigid interface, and validation measurements with the car on the dyno.



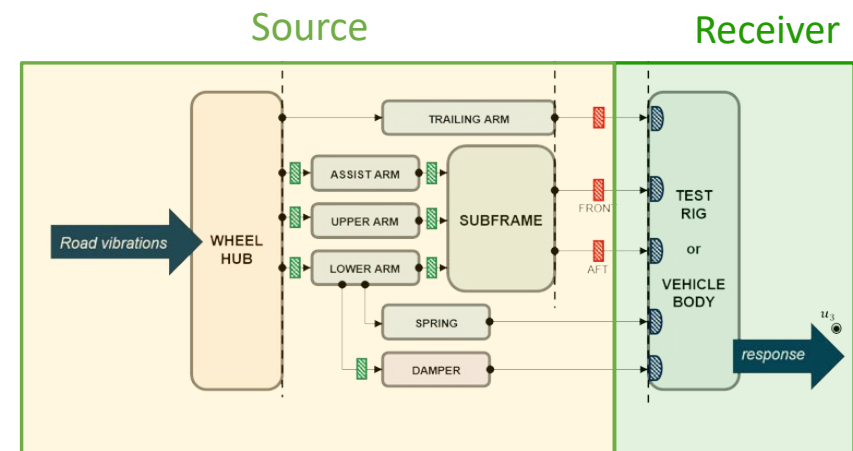
Validation case 2.a and 2.b

- interface after (2.a) and before (2.b) rubber mounts
- blocked force from soft test rig (after (2.a) and before (2.b) mounts)
- TPA : blocked force on $Y^{\text{full-car}}$ after (2.a) and before (2.b) mounts

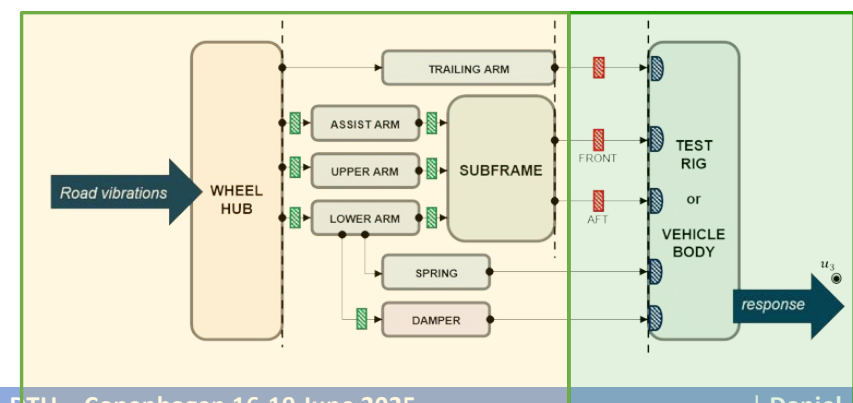


Blocked force measured on soft test rig with indicator sensors on soft test rig connections (in-situ)

(2.a)

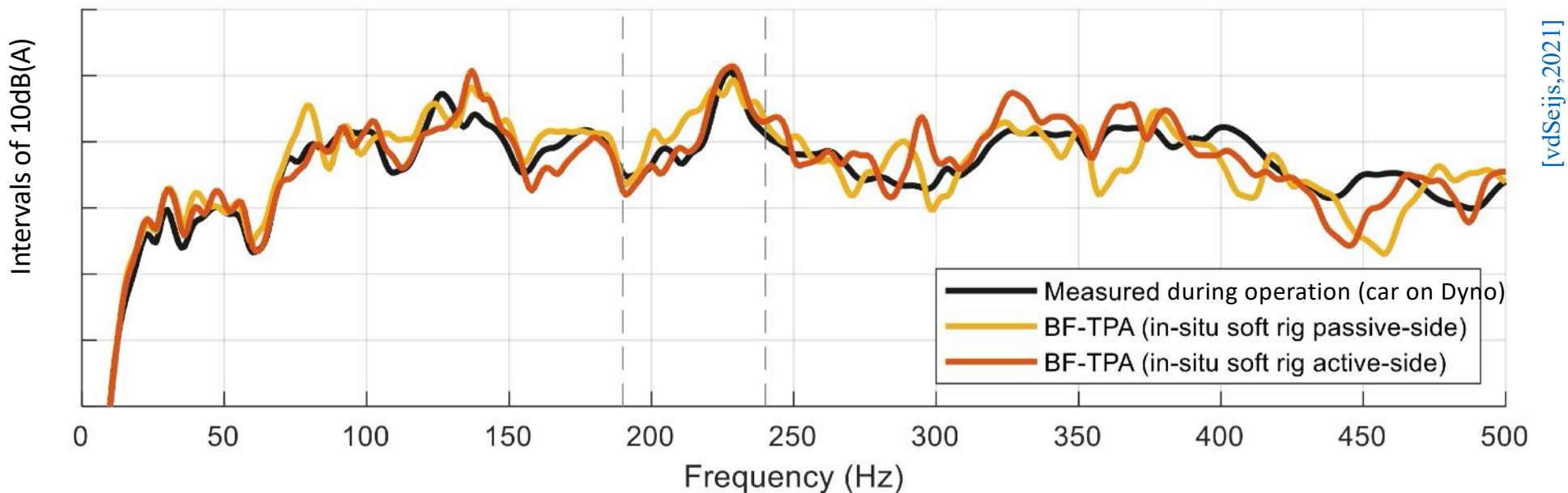


(2.b)



Validation case 2.a, 2.b

Comparing time-averaged spectra of driver-ear sound pressure levels in dB(A) over the full run-up from 20-120 km/h, as computed through TPA with Blocked Forces from soft test rig, and validation measurements with the car on the dyno.



Validation case 3.a and 3.b

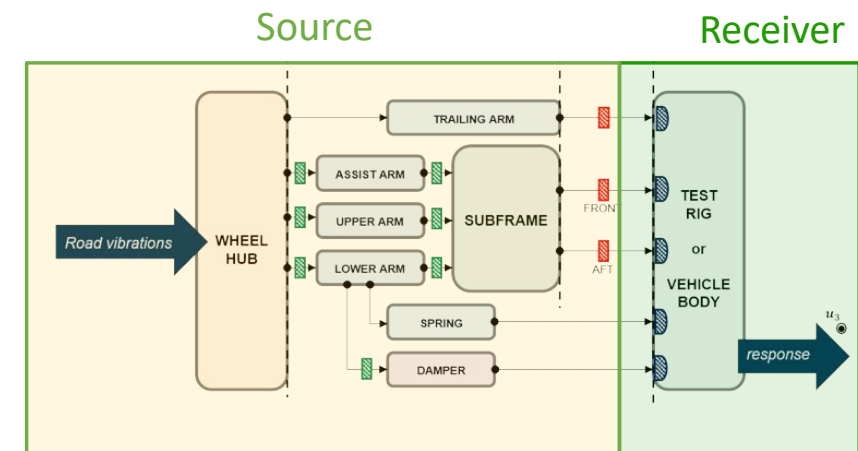
- interface after (3.a) and before (3.b) rubber mounts
- blocked force from car (after (3.a) and before (3.b) mounts)
- TPA : blocked force on $Y^{\text{full-car}}$ after (3.a) and before (3.b) mounts



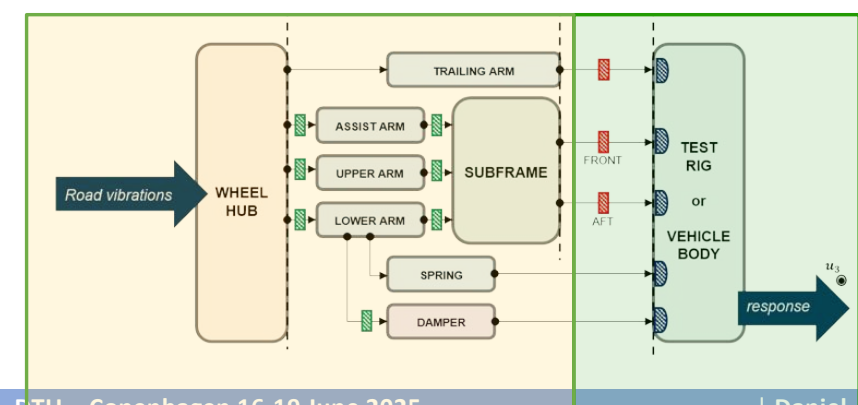
(3.a)

Blocked force measured in-situ directly on the car interface

(Note this case is called „on-board“ validation, since the blocked force is applied to the same system on which the blocked force was identified). This works often the best, but allows only to analyse the different path, not changing the receiver.

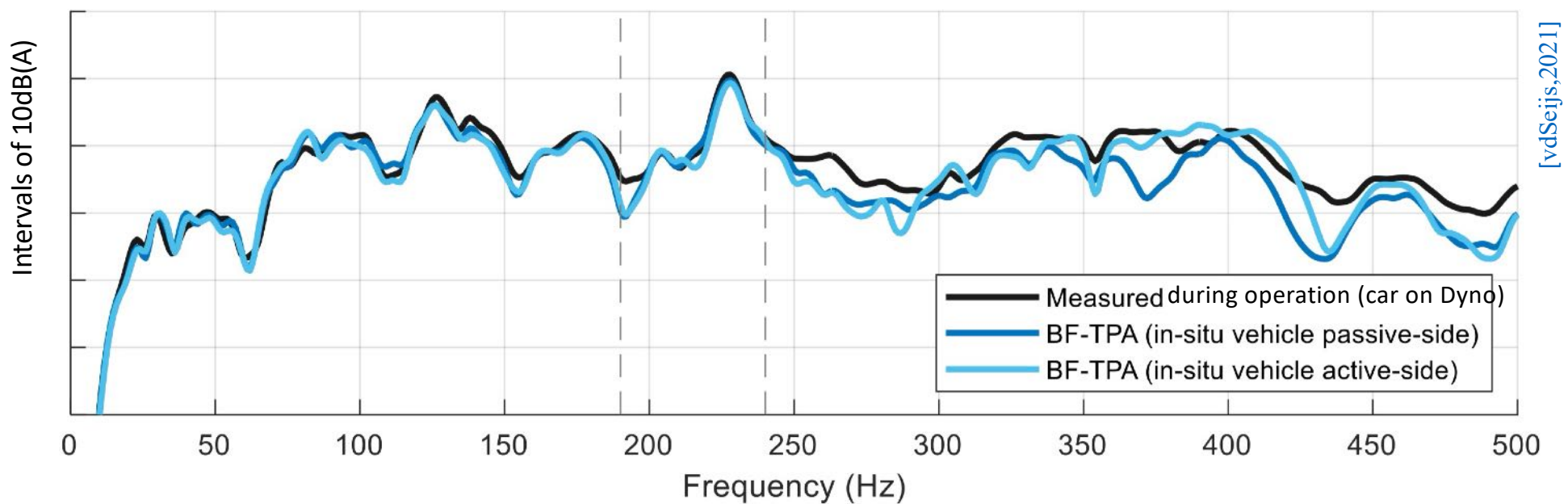


(3.b)



Validation case 3.a, 3.b

Comparing time-averaged spectra of driver-ear sound pressure levels in dB(A) over the full run-up from 20-120 km/h, as computed through TPA with Blocked Forces car-in-situ, and validation measurements with the car on the dyno.



Literature on FBS:

- S. Allen, D. Rixen, M. van der Seijs, P. Tiso, T. Abrahamsson, and R. L. Mayes. Substructuring in Engineering Dynamics, volume 594 of CISM International Centre for Mechanical Sciences. Springer, 2020.
- M. van der Seijs. Experimental Dynamic Substructuring, Analysis and Design Strategies for Vehicle Development. PhD thesis, Delft University of Technology, Delft, The Netherlands, June 2016.
- M. Häußler. Modular sound & vibration engineering by substructuring - Listening to machines during virtual design. PhD thesis, Technical University Munich - Department of Mechanical Engineering, April 2021.
- D. Rixen, T. Godeby, and E. Pagnacco. Dual assembly of substructures and the fbs method: Application to the dynamic testing of a guitar. In International Conference on Noise and Vibration Engineering, ISMA, Leuven, Belgium, September 18-20 2006. KUL.
- A. Moorhouse, A. Elliott, and T. Evans. In situ measurement of the blocked force of structure-borne sound sources. Journal of Sound and Vibration, 325(4–5):679 – 685, 2009.
- A. El Mahmoudi, F. Trainotti, K. Park, and D. J. Rixen. In-situ source characterization for nvh analysis of the engine-transmission unit. In IMAC-XXXVII: International Modal Analysis Conference, Houston, AR, Bethel, CT, February 2020. Society for Experimental Mechanics.
- van der Seijs, M. V., Harvie, J. M., & Song, D. P. (2021, February). Road noise NVH: embedding suspension test benches in NVH design using Virtual Points and the TPA framework. In Proceedings of the thirty-ninth international modal analysis conference.

Course outline

0. Introduction

- Some history
- Basic notations

1. Frequency-based Substructuring for starters

- Assembly of admittances (2 subdomains)
- Example of a guitar
- Generalization to more subdomains

2. Some important tricks to make FBS work

- Weakening of compatibility: the virtual point transformation
- Example of the AM-structure in PyFBS
- Decoupling
- Example of a rubber mount

3. Blocked forces and transfer path analysis

- The concept of blocked forces
- In-situ measurements of blocked forces
- example

4. Some other tastes of experimental substructuring

- Numerical substructures – model reduction
- Impulse-Based Substructuring

4. Some other tastes of experimental substructuring



Including numerical substructures (Hybrid Models)

2 ways to compute the FRF of a numerical substructures

- Compute responses for different force input, at different excitation frequencies

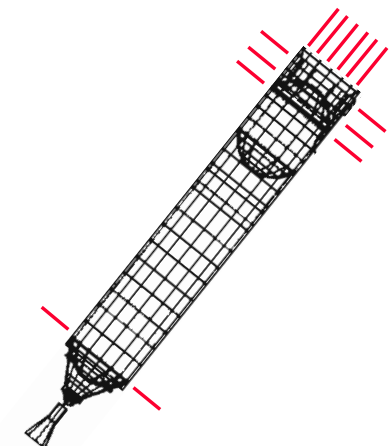
$$\mathbf{X} = (\mathbf{K} - \Omega^2 \mathbf{M})^{-1} \mathbf{F} = \mathbf{Y} \mathbf{F}$$

→ very expensive

- Modal superposition

$$\mathbf{Y} = \sum_{i=1}^n \frac{\Phi_{ji} \Phi_{ki}}{\mu_i(-\Omega^2 + j\Omega 2\epsilon_i \omega_i + \omega_i^2)}$$

→ cheaper, but cannot describe the dynamic response to unit forces precisely when not many modes are used



The Hurty-Craig-Bampton Method

Hurty, W.C.: Dynamic analysis of structural systems using component modes. AIAA journal **3**(4), 678–685 (1965)

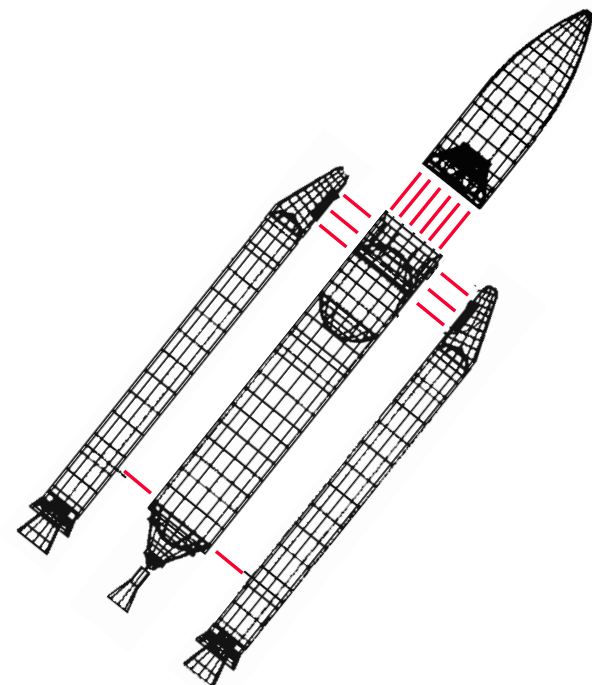
Bampton, M.C.C., Craig, J.R.R.: Coupling of substructures for dynamic analyses. AIAA Journal **6**(7), 1313–1319 (1968)

Dynamics of one substructure

$$\mathbf{M}^{(s)} \ddot{\mathbf{u}}^{(s)} + \mathbf{K}^{(s)} \mathbf{u}^{(s)} = \mathbf{f}^{(s)}$$

Partitioning in internal and boundary Dofs :

$$\begin{bmatrix} \mathbf{M}_{ii}^{(s)} & \mathbf{M}_{ib}^{(s)} \\ \mathbf{M}_{bi}^{(s)} & \mathbf{M}_{bb}^{(s)} \end{bmatrix} \begin{Bmatrix} \ddot{\mathbf{u}}_i^{(s)} \\ \ddot{\mathbf{u}}_b^{(s)} \end{Bmatrix} + \begin{bmatrix} \mathbf{K}_{ii}^{(s)} & \mathbf{K}_{ib}^{(s)} \\ \mathbf{K}_{bi}^{(s)} & \mathbf{K}_{bb}^{(s)} \end{bmatrix} \begin{Bmatrix} \mathbf{u}_i^{(s)} \\ \mathbf{u}_b^{(s)} \end{Bmatrix} = \begin{Bmatrix} \mathbf{0} \\ \mathbf{f}_b^{(s)} \end{Bmatrix}$$

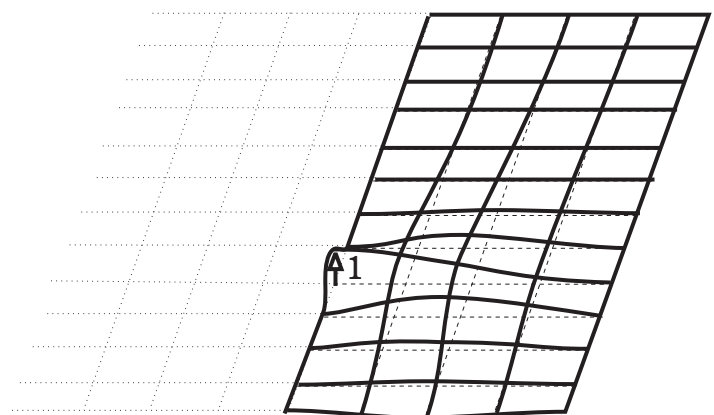


Representation modes (component modes) ?

First idea : static modes (Guyan-Irons) related to interface boundary Dofs

$$\begin{bmatrix} \mathbf{M}_{ii}^{(s)} & \mathbf{M}_{ib}^{(s)} \\ \mathbf{M}_{bi}^{(s)} & \mathbf{M}_{bb}^{(s)} \end{bmatrix} \begin{Bmatrix} \ddot{\mathbf{u}}_i^{(s)} \\ \ddot{\mathbf{u}}_b^{(s)} \end{Bmatrix} + \begin{bmatrix} \mathbf{K}_{ii}^{(s)} & \mathbf{K}_{ib}^{(s)} \\ \mathbf{K}_{bi}^{(s)} & \mathbf{K}_{bb}^{(s)} \end{bmatrix} \begin{Bmatrix} \mathbf{u}_i^{(s)} \\ \mathbf{u}_b^{(s)} \end{Bmatrix} = \begin{Bmatrix} \mathbf{0} \\ \mathbf{f}_b^{(s)} \end{Bmatrix}$$

$$\boldsymbol{\Psi}^{(s)} = \begin{bmatrix} -\mathbf{K}_{ii}^{(s)-1} \mathbf{K}_{ib}^{(s)} \\ \mathbf{I} \end{bmatrix}$$



Static mode

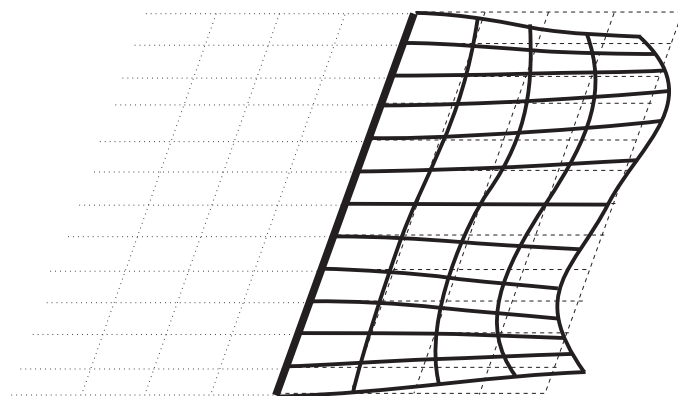
Representation modes (component modes) ?

Improve static representation with fixed interface modes:

$$\begin{bmatrix} \mathbf{M}_{ii}^{(s)} & \mathbf{M}_{ib}^{(s)} \\ \mathbf{M}_{bi}^{(s)} & \mathbf{M}_{bb}^{(s)} \end{bmatrix} \begin{Bmatrix} \ddot{\mathbf{u}}_i^{(s)} \\ \ddot{\mathbf{u}}_b^{(s)} \end{Bmatrix} + \begin{bmatrix} \mathbf{K}_{ii}^{(s)} & \mathbf{K}_{ib}^{(s)} \\ \mathbf{K}_{bi}^{(s)} & \mathbf{K}_{bb}^{(s)} \end{bmatrix} \begin{Bmatrix} \mathbf{u}_i^{(s)} \\ \mathbf{u}_b^{(s)} \end{Bmatrix} = \begin{Bmatrix} \mathbf{0} \\ \mathbf{f}_b^{(s)} \end{Bmatrix}$$

\$M_{ii}^{(s)}\ddot{u}_i^{(s)} + K_{ii}^{(s)}u_i^{(s)} = -M_{ii}^{(s)}\ddot{u}_b^{(s)} - K_{ib}^{(s)}u_b^{(s)}
\$u_i^{(s)} = -K_{ii}^{(s)-1}K_{ib}^{(s)}u_b^{(s)} + u_{i,dyn}^{(s)}

best represented by vibration modes of **fixed** interface

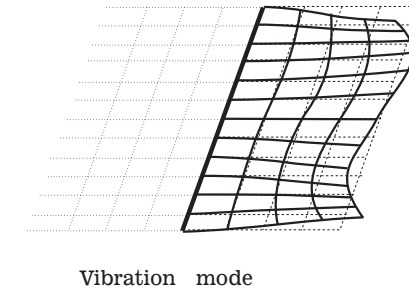


Vibration mode

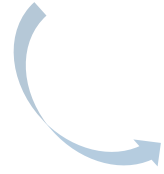
$$\mathbf{u}_i^{(s)} = -\mathbf{K}_{ii}^{(s)-1} \mathbf{K}_{ib}^{(s)} \mathbf{u}_b^{(s)} + \mathbf{u}_{i,dyn}^{(s)}$$

best represented by vibration modes of fixed interface

$$\left(\mathbf{K}_{ii}^{(s)} - \omega_r^2 \mathbf{M}_{ii}^{(s)} \right) \left\{ \phi_i^{(s)} \right\}_r = 0$$



keeping only m modes

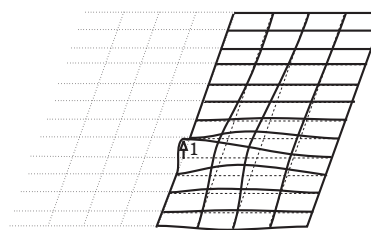


$$\boldsymbol{\Phi}^{(s)} = \begin{bmatrix} \left\{ \phi_i^{(s)} \right\}_1, \dots, \left\{ \phi_i^{(s)} \right\}_m \\ \mathbf{0} \end{bmatrix} = \begin{bmatrix} \boldsymbol{\Phi}_i^{(s)} \\ \mathbf{0} \end{bmatrix}.$$

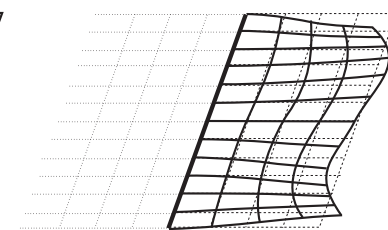


$$\begin{bmatrix} \mathbf{u}_i^{(s)} \\ \mathbf{u}_b^{(s)} \end{bmatrix} \approx \mathbf{T}^{\text{HCB}} \begin{bmatrix} \mathbf{q}_i^{(s)} \\ \mathbf{u}_b^{(s)} \end{bmatrix}$$

$$\mathbf{T}^{(s)\text{HCB}} = \begin{bmatrix} \boldsymbol{\Phi}^{(s)} & \boldsymbol{\Psi}^{(s)} \end{bmatrix}$$



Φ_1



$$\mathbf{T}^{(s)HCB} = \begin{bmatrix} \boldsymbol{\Phi}^{(s)} & \boldsymbol{\Psi}^{(s)} \end{bmatrix}$$

Reduced matrices for a substructure :

$$\mathbf{K}^{(s)HCB} = (\mathbf{T}^{(s)HCB})^T \mathbf{K}^{(s)} \mathbf{T}^{(s)HCB}$$



$$\mathbf{M}^{(s)HCB} = (\mathbf{T}^{(s)HCB})^T \mathbf{M}^{(s)} \mathbf{T}^{(s)HCB}$$

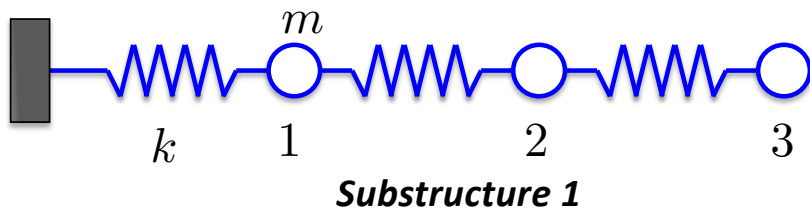


$$\boxed{\mathbf{K}^{(s)HCB} = \begin{bmatrix} \boldsymbol{\Omega}_m^{(s)2} & \mathbf{0} \\ \mathbf{0} & \tilde{\mathbf{K}}_{bb}^{(s)} \end{bmatrix} \quad \text{and} \quad \mathbf{M}^{(s)HBC} = \begin{bmatrix} \mathbf{I} & \tilde{\mathbf{M}}_{ib}^{(s)} \\ \tilde{\mathbf{M}}_{bi}^{(s)} & \tilde{\mathbf{M}}_{bb}^{(s)} \end{bmatrix}}$$

where

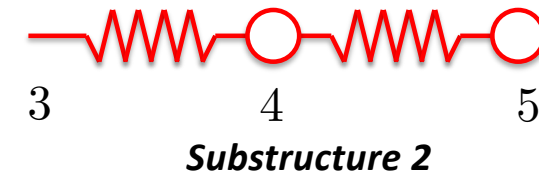
$$\begin{aligned} \tilde{\mathbf{K}}_{bb}^{(s)} &= \mathbf{K}_{bb}^{(s)} - \mathbf{K}_{bi}^{(s)} \mathbf{K}_{bb}^{(s)-1} \mathbf{K}_{bi}^{(s)} \\ \tilde{\mathbf{M}}_{bb}^{(s)} &= \mathbf{M}_{bb}^{(s)} - \mathbf{M}_{bi}^{(s)} \mathbf{K}_{ii}^{(s)-1} \mathbf{K}_{ib}^{(s)} - \mathbf{K}_{bi}^{(s)} \mathbf{K}_{ii}^{(s)-1} \mathbf{M}_{ib}^{(s)} + \mathbf{K}_{bi}^{(s)} \mathbf{K}_{ii}^{(s)-1} \mathbf{M}_{ii}^{(s)} \mathbf{K}_{ii}^{(s)-1} \mathbf{K}_{ib}^{(s)} \\ \tilde{\mathbf{M}}_{ib}^{(s)} &= \boldsymbol{\Phi}^{(s)T} \left(\mathbf{M}_{ib}^{(s)} - \mathbf{M}_{ii}^{(s)} \mathbf{K}_{ii}^{(s)-1} \mathbf{K}_{ib}^{(s)} \right) = \tilde{\mathbf{M}}_{bi}^T \end{aligned}$$

Let us consider the previous example:



$$\mathbf{M}^{(1)} = \left[\begin{array}{c|cc} 1 & 0 & 0 \\ \hline 0 & 1 & 0 \\ 0 & 0 & 1 \end{array} \right]$$

$$\mathbf{K}^{(1)} = \left[\begin{array}{c|cc} 1 & -1 & 0 \\ \hline -1 & 2 & -1 \\ 0 & -1 & 2 \end{array} \right]$$



$$\mathbf{M}^{(2)} = \left[\begin{array}{c|cc} 0 & 0 & 0 \\ \hline 0 & 1 & 0 \\ 0 & 0 & 0.5 \end{array} \right]$$

$$\mathbf{K}^{(2)} = \left[\begin{array}{c|cc} 1 & -1 & 0 \\ \hline -1 & 2 & -1 \\ 0 & -1 & 1 \end{array} \right]$$

N.B.: the mass at node 3 has already been included in substructure (1)



For the first substructure, the internal modes (fixing dof 3) and the Schur complement are, respectively:

$$\Phi^{(1)} = \begin{bmatrix} 0.7071 & -0.7071 \\ 0.7071 & 0.7071 \end{bmatrix} \quad \mathbf{S}^{(1)} = \begin{bmatrix} 0.6667 \\ 0.3333 \end{bmatrix}$$

And the reduction matrix becomes:

$$\mathbf{R}^{(1)} = \begin{bmatrix} 1.0000 & 0 & 0 \\ 0.6667 & 0.7071 & -0.7071 \\ 0.3333 & 0.7071 & 0.7071 \end{bmatrix}$$

To give reduced mass and stiffness matrices:

$$\tilde{\mathbf{K}}^{(1)} = \left[\begin{array}{c|cc} 0.3333 & 0 & 0 \\ \hline 0 & 1 & 0 \\ 0 & 0 & 3 \end{array} \right] \quad \tilde{\mathbf{M}}^{(1)} = \left[\begin{array}{c|cc} 1.5556 & 0.7071 & -0.2357 \\ \hline 0.7071 & 1 & 0 \\ -0.2357 & 0 & 1 \end{array} \right]$$



For the second substructure, the internal modes (fixing dof 3) and the Schur complement are, respectively:

$$\Phi^{(2)} = \begin{bmatrix} 0.7071 & -0.7071 \\ 1 & 1 \end{bmatrix} \quad \mathbf{S}^{(2)} = \begin{bmatrix} 1 \\ 1 \end{bmatrix}$$

And the reduction matrix becomes:

$$\mathbf{R}^{(2)} = \begin{bmatrix} 1 & 0 & 0 \\ 1 & 0.7071 & -0.7071 \\ 1 & 1 & 1 \end{bmatrix}$$

To give reduced mass and stiffness matrices:

$$\tilde{\mathbf{K}}^{(2)} = \left[\begin{array}{c|cc} 0 & 0 & 0 \\ \hline 0 & 0.5858 & 0 \\ 0 & 0 & 3.4142 \end{array} \right] \quad \tilde{\mathbf{M}}^{(2)} = \left[\begin{array}{c|cc} 1.5000 & 1.2071 & -0.2071 \\ \hline 1.2071 & 1 & 0 \\ -0.2071 & 0 & 1 \end{array} \right]$$

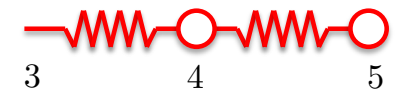
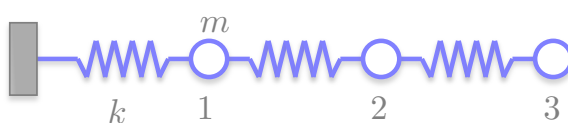
Check yourself

pingo.coactum.de
Code 756413



Is it correct that the reduced Mass matrix for the second substructure has a mass associated to the interface dof ?

$$\tilde{\mathbf{M}}^{(2)} = \left[\begin{array}{c|cc} 1.5000 & 1.2071 & -0.2071 \\ \hline 1.2071 & 1 & 0 \\ -0.2071 & 0 & 1 \end{array} \right]$$



- a. yes sure, why not ...
- b. comes from bad conditioning in the transformation matrix
- c. no, this is an error in the exercise



	<i>Exact</i>	<i>Guyan (static)</i>	<i>Craig Bampton (1 mode)</i>	<i>Craig Bampton (2 modes)</i>
Mode 1	0.3129	0.3303	0.3129	0.3129
Mode 2	0.9080	-	0.9080	0.9080
Mode 3	1.4142	-	1.4883	1.4142
Mode 4	1.7820	-	-	1.7821
Mode 5	1.9754	-	-	1.9753

Other reduction techniques for Substructures

- Free interface modes
- Loaded interface modes in the reduction basis
- Modal Truncation augmentation and Moment Matching
- Balanced truncation
- Mixed methods (Herting, mixed CB)
- Iterative basis improvement

The idea of Impulse-Based Substructuring

- Analysis to predict impact response already during initial design
- Full 3D models difficult to build and analysis too slow
- COTS often combined with specific components.

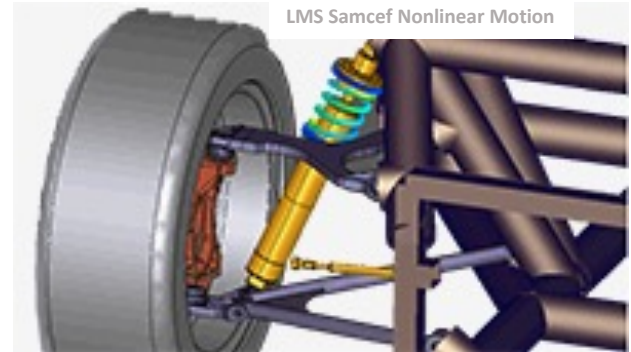
→ substructuring approaches useful ...

... but the frequency domain is not the best
to analyze the problem



- For numerical simulation (numerical components) CMS-type of reduction techniques lose the contribution of higher frequencies, so not appropriate.
- In experimental substructuring (measured components), the FRFs do not contain the necessary information of accurate shock response

→ Write substructuring procedures **directly in time**



Basics of impulse convolution (Duhamel)

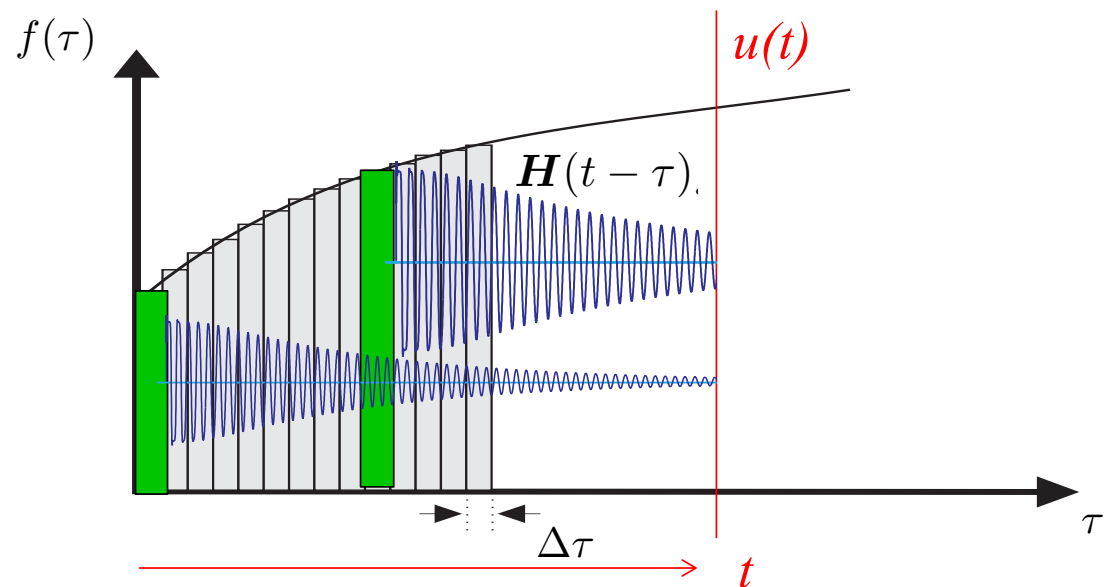
Time response of a **single structure** as convolution of impulse responses

$$\mathbf{u}(t) = \int_0^t \mathbf{H}(t - \tau) \mathbf{f}(\tau) d\tau$$

All impulses before t

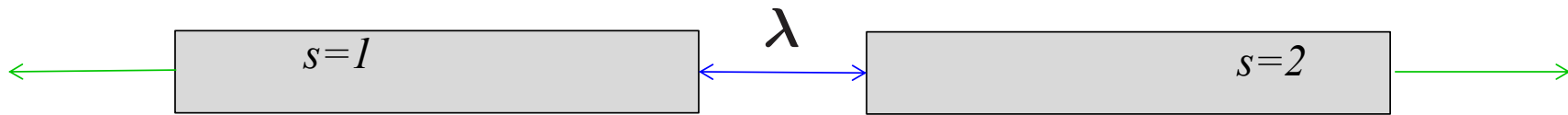
Impulse Response Function (IRF)

Numerically computed
or
Measured (impact hammer)



Time response of assemblies with impulse responses

Enforcing ***compatibility*** at every time t



For every time t , the interface force must be determined to satisfy compatibility

$$\left\{ \begin{array}{l} \mathbf{u}^{(s)}(t) = \int_0^t \mathbf{H}^{(s)}(t - \tau) \left(\mathbf{f}^{(s)}(\tau) + \mathbf{B}^{(s)T} \boldsymbol{\lambda}(\tau) \right) d\tau \\ \sum_{s=1}^{N_s} \mathbf{B}^{(s)} \mathbf{u}^{(s)}(t) = \mathbf{0} \end{array} \right.$$

signed Boolean → compatibility condition

Time discretized assembly by impulse response



$$\left\{ \begin{array}{l} \boldsymbol{u}_n^{(s)} = \boldsymbol{H}_n^{(s)} \left(\boldsymbol{f}_0^{(s)} \frac{dt}{2} + \boldsymbol{B}^{(s)T} \boldsymbol{\lambda}_0 \right) + \sum_{i=1}^{n-1} \boldsymbol{H}_{n-i}^{(s)} \left(\boldsymbol{f}_i^{(s)} dt + \boldsymbol{B}^{(s)T} \boldsymbol{\lambda}_i \right) \\ \sum_{s=1}^{N^s} \boldsymbol{B}^{(s)} \boldsymbol{u}_n^{(s)} = \boldsymbol{0} \end{array} \right.$$

λ dt now renamed λ impulses in the interface

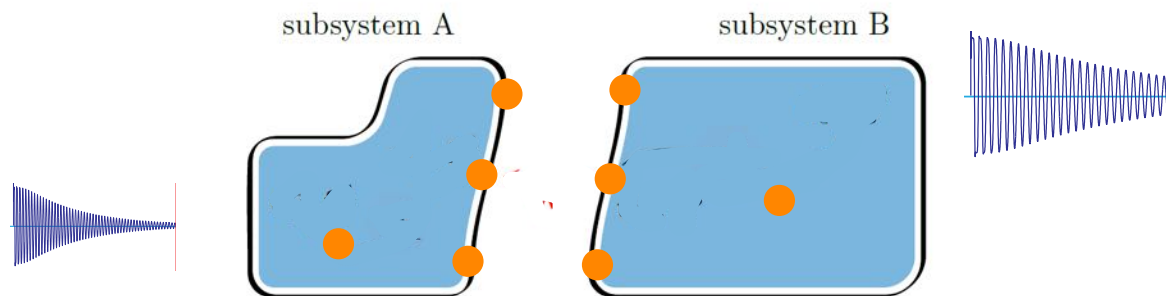
If the Impulse Response $\boldsymbol{H}_n^{(s)}$ is measured for each substructure:

- each substructure represented by IRF on interface: “substructure in time” → **Impulse Based Substructuring (IBS)**
- theoretically equivalent to FBS with Inverse FFT (IFFT), but
- does not need any FFT and is thus not affected by FFT artifacts (windowing, filters ...)

Note: properly writing the discretized form for displacement/velocities/acceleration is important [Rixen, van der Valk. An impulse based substructuring approach for impact analysis and load case simulations. Journal of Sound and Vibration, 332:7174–7190, 2013]

So what is the procedure?

1. Obtain the Impulse Response Functions (IRFs) of the components

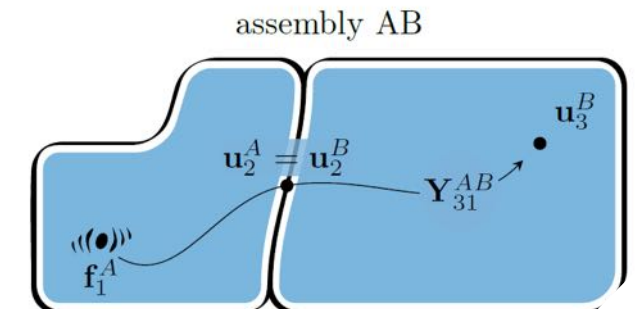


Between all interface/internal dofs!

By impact measurements or simulation

2. Compute the time response by time-stepping :

$$\begin{cases} \mathbf{u}_n^{(s)} = \mathbf{H}_n^{(s)} \left(\mathbf{f}_0^{(s)} \frac{dt}{2} + \mathbf{B}^{(s)T} \boldsymbol{\lambda}_0 \right) + \sum_{i=1}^{n-1} \mathbf{H}_{n-i}^{(s)} \left(\mathbf{f}_i^{(s)} dt + \mathbf{B}^{(s)T} \boldsymbol{\lambda}_i \right) \\ \sum_{s=1}^{N^s} \mathbf{B}^{(s)} \mathbf{u}_n^{(s)} = \mathbf{0} \end{cases}$$



How to solve the coupled problem at each time-step t_n ?

$$\begin{cases} \mathbf{u}_n^{(s)} = \mathbf{H}_n^{(s)} \left(\mathbf{f}_0^{(s)} \frac{dt}{2} + \mathbf{B}^{(s)T} \boldsymbol{\lambda}_0 \right) + \sum_{i=1}^{n-1} \mathbf{H}_{n-i}^{(s)} \left(\mathbf{f}_i^{(s)} dt + \mathbf{B}^{(s)T} \boldsymbol{\lambda}_i \right) \\ \sum_{s=1}^{N^s} \mathbf{B}^{(s)} \mathbf{u}_n^{(s)} = \mathbf{0} \end{cases}$$

- Build predictor for t_n in each substructure

$$\tilde{\mathbf{u}}_n^{(s)} = \mathbf{H}_n^{(s)} \left(\mathbf{f}_0^{(s)} \frac{dt}{2} + \mathbf{B}^{(s)T} \boldsymbol{\lambda}_0 \right) + \sum_{i=1}^{n-2} \mathbf{H}_{n-i}^{(s)} \left(\mathbf{f}_i^{(s)} dt + \mathbf{B}^{(s)T} \boldsymbol{\lambda}_i \right) + \mathbf{H}_1^{(s)} \mathbf{f}_{n-1}^{(s)} dt$$

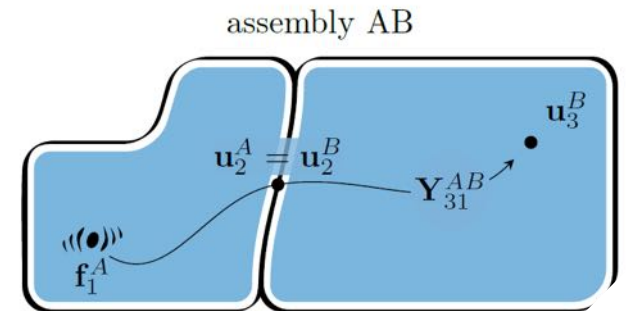
- Compute interface force for compatibility at t_n :

solve the dual interface problem

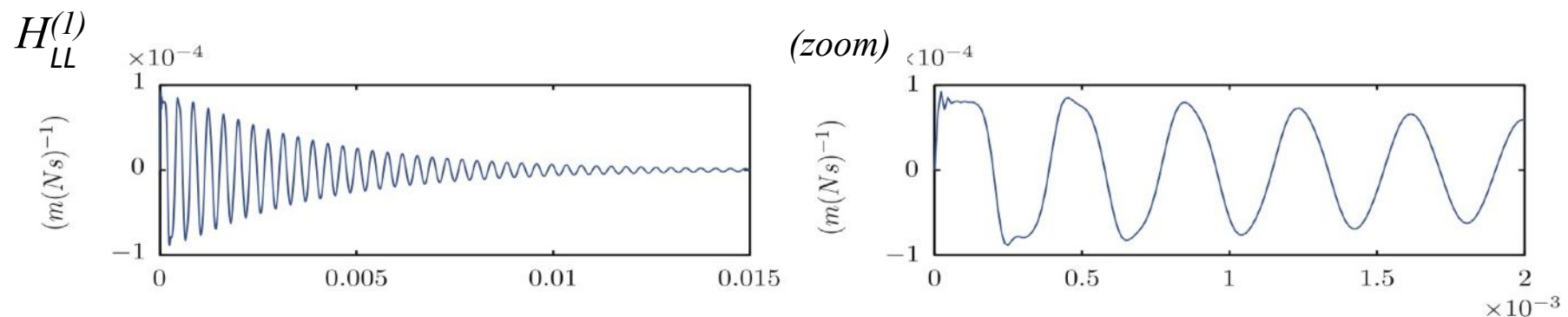
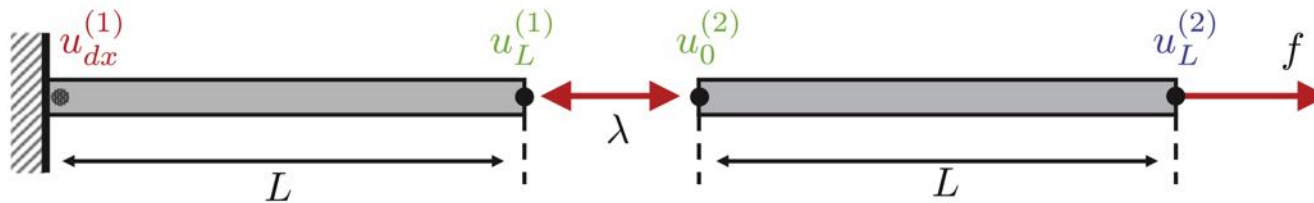
$$\left(\sum_{s=1}^{N^s} \mathbf{B}^{(s)} \mathbf{H}_1^{(s)} \mathbf{B}^{(s)T} \right) \boldsymbol{\lambda}_{n-1} = - \sum_{s=1}^{N^s} \mathbf{B}^{(s)} \tilde{\mathbf{u}}_n^{(s)}$$

- Update

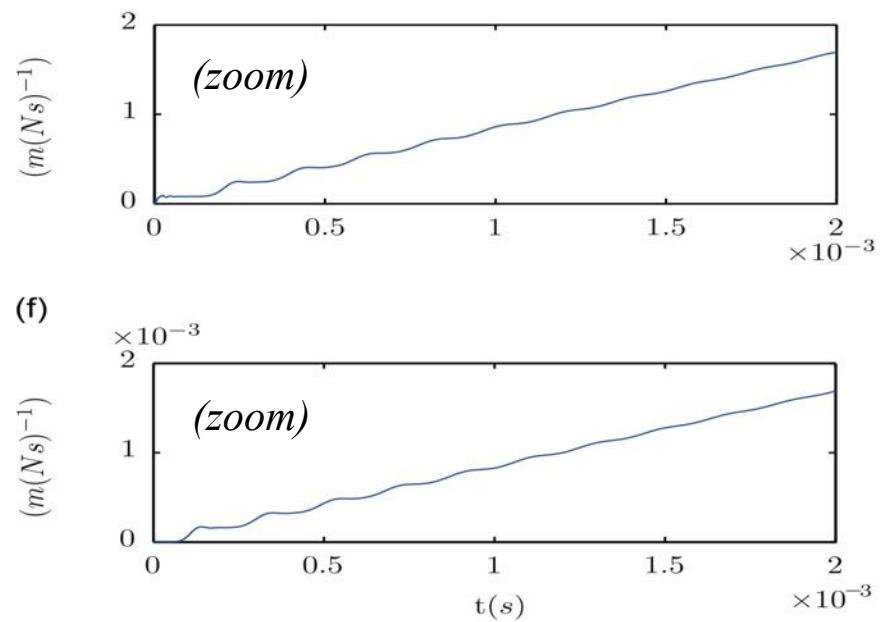
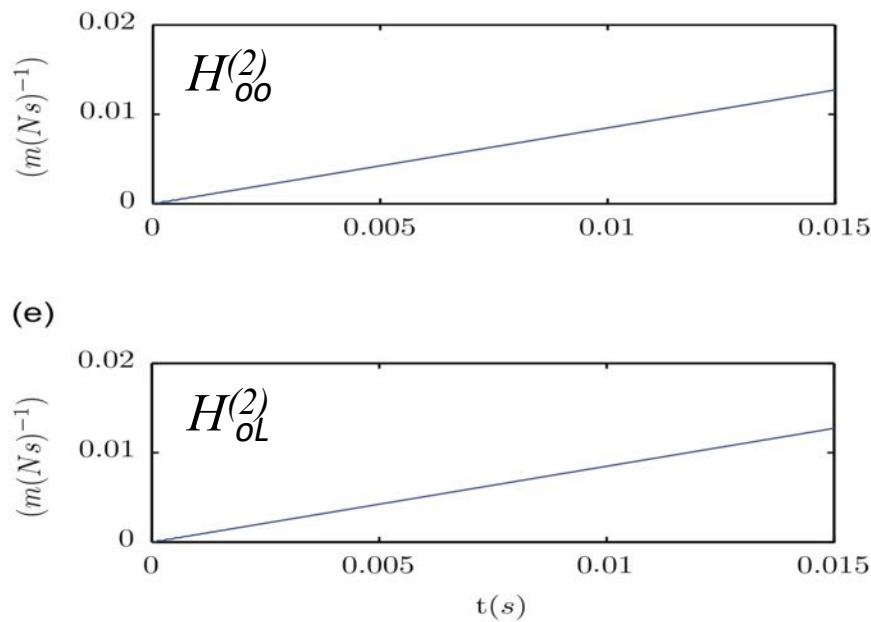
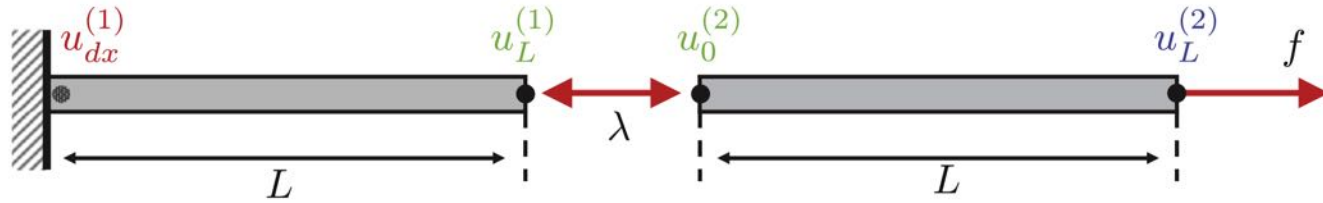
$$\mathbf{u}_n^{(s)} = \tilde{\mathbf{u}}_n^{(s)} + \mathbf{H}_1^{(s)} \mathbf{B}^{(s)T} \boldsymbol{\lambda}_{n-1}$$

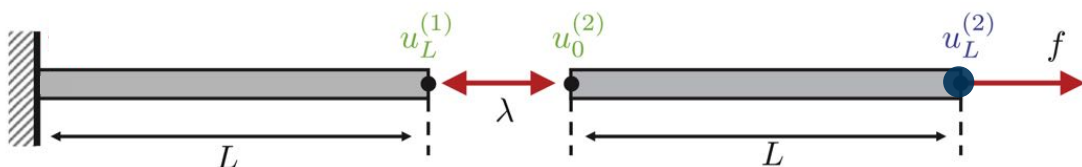


A simple numerical example

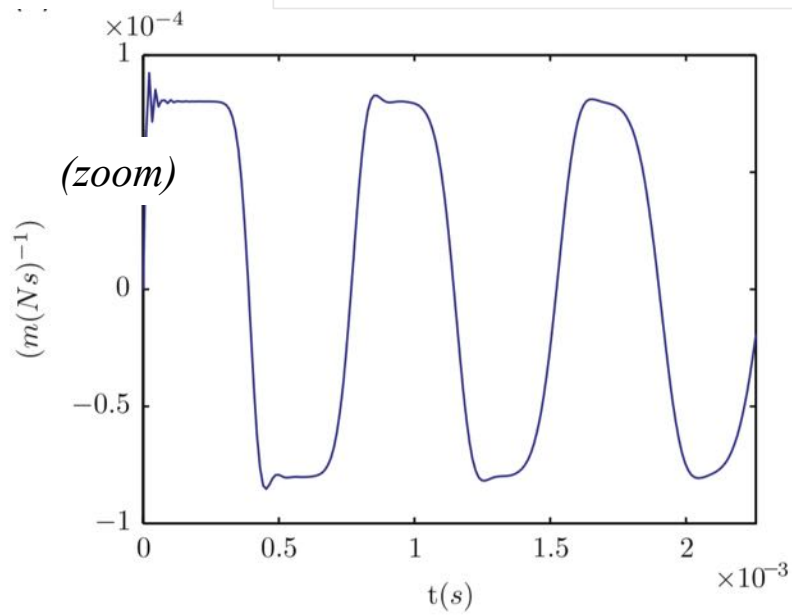
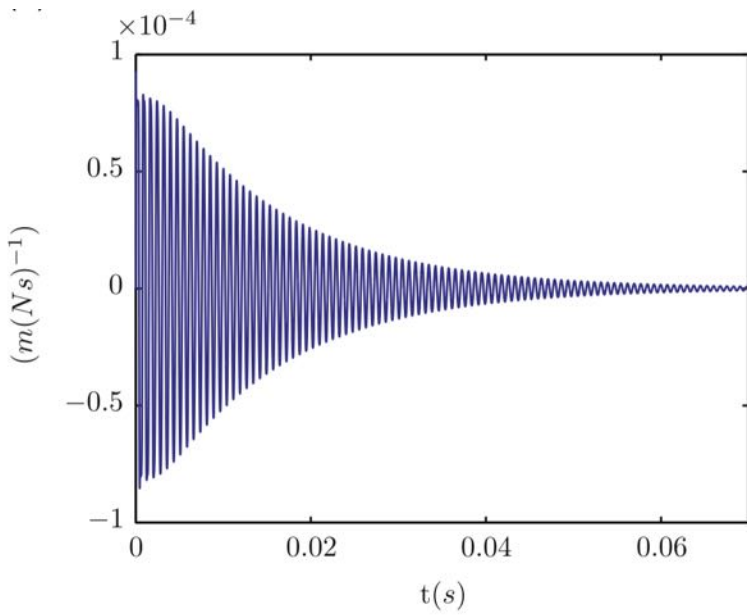


Obtained by time integration of a FE model (see part 2)

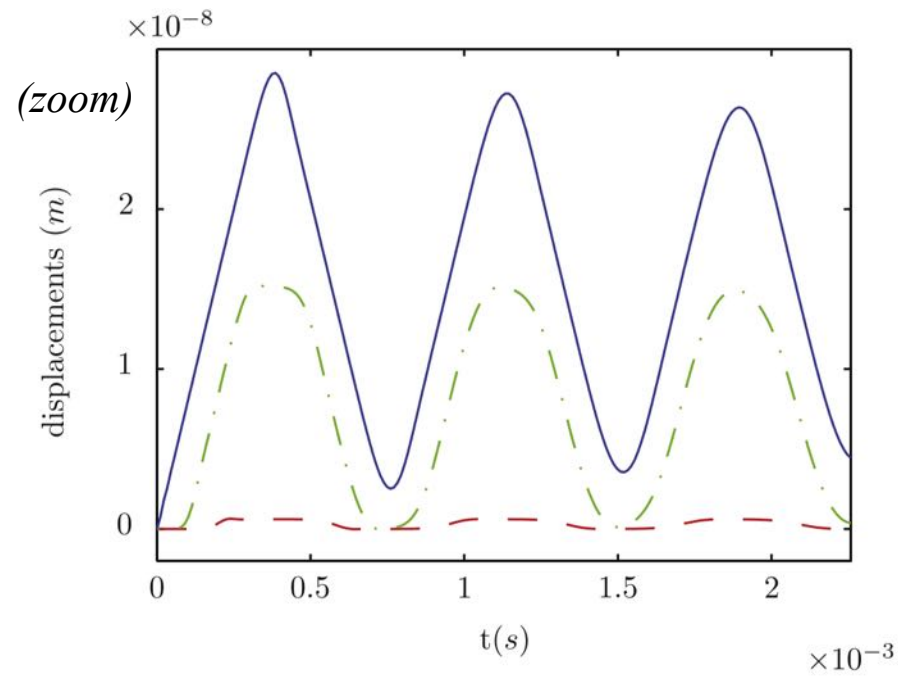
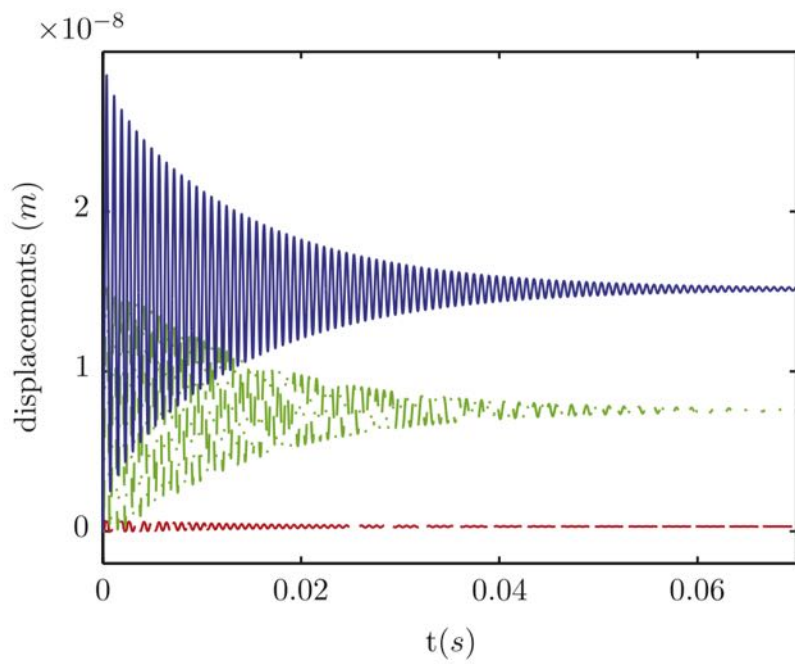
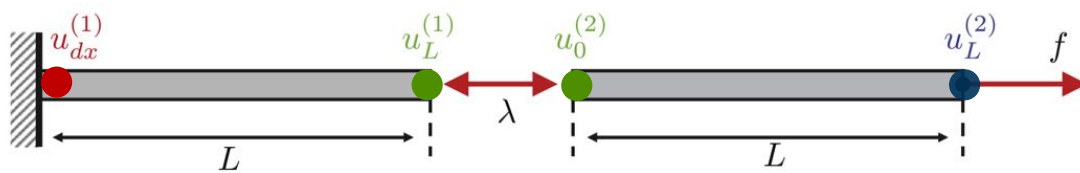




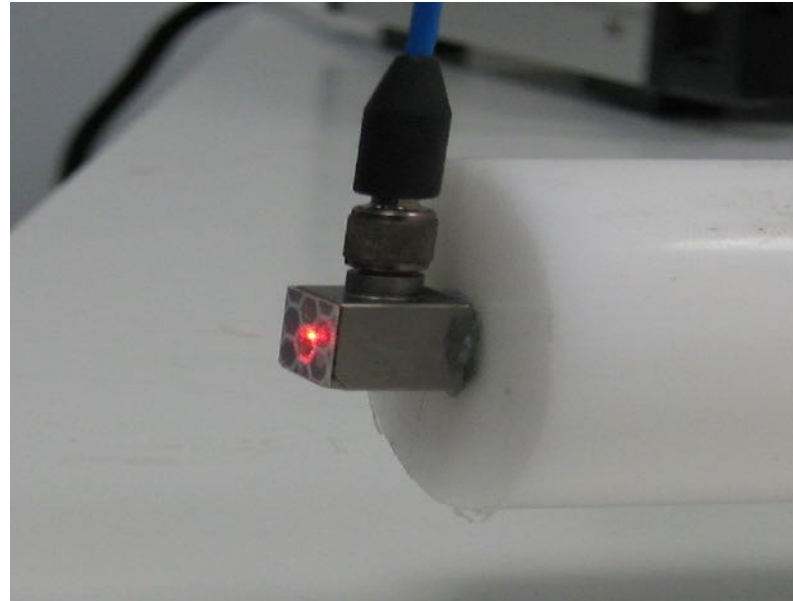
$$\begin{cases} \mathbf{u}_n^{(s)} = \mathbf{H}_n^{(s)} \left(\mathbf{f}_0^{(s)} \frac{dt}{2} + \mathbf{B}^{(s)T} \boldsymbol{\lambda}_0 \right) + \sum_{i=1}^{n-1} \mathbf{H}_{n-i}^{(s)} \left(\mathbf{f}_i^{(s)} dt + \mathbf{B}^{(s)T} \boldsymbol{\lambda}_i \right) \\ \sum_{s=1}^{N^s} \mathbf{B}^{(s)} \mathbf{u}_n^{(s)} = 0 \end{cases}$$



$$\begin{aligned} \mathbf{B}^{(1)} &= [0 \ \dots \ 0 \ -1] \\ \mathbf{B}^{(2)} &= [1 \ \dots \ 0 \ 0] \end{aligned}$$

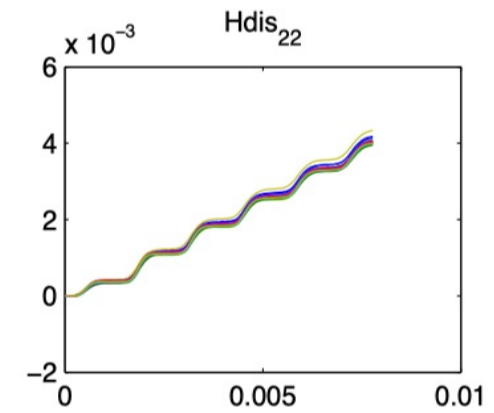
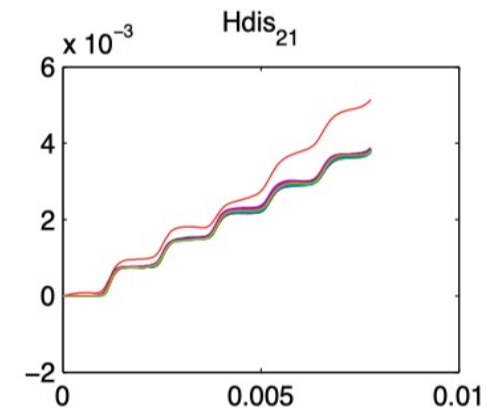
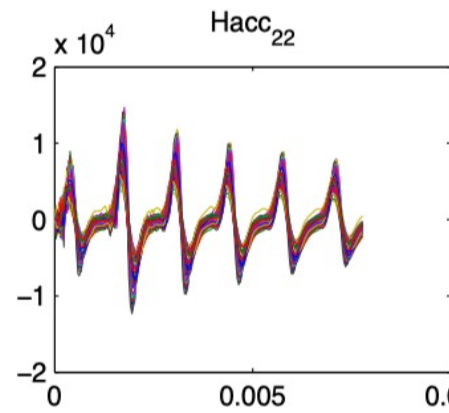
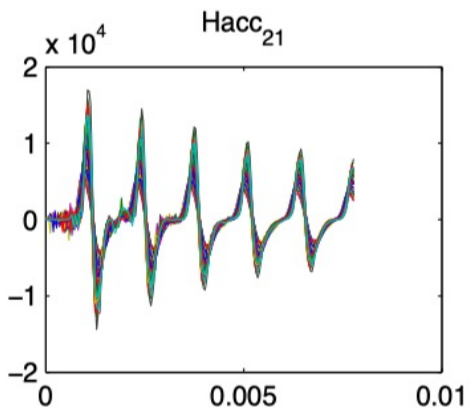
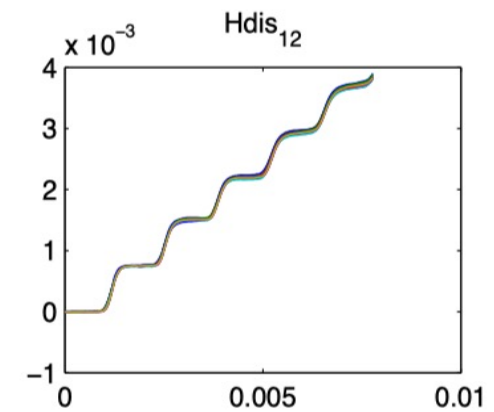
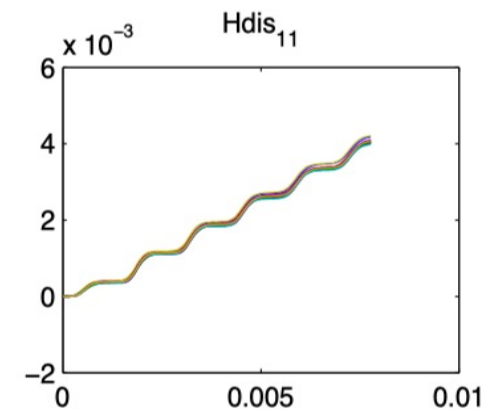
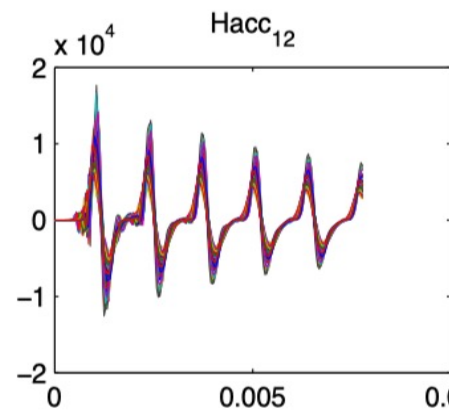
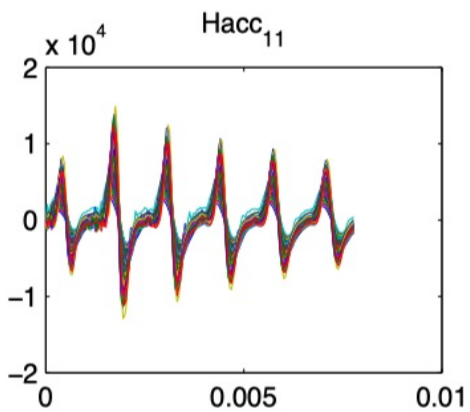


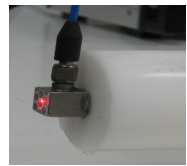
A simple experimental example



A bar made of POM (polyacetal, a thermoplastic material)

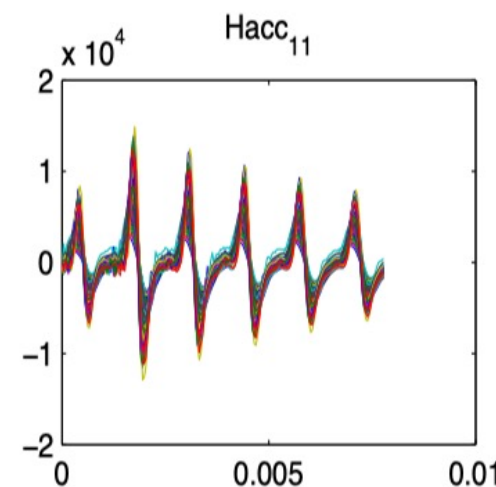
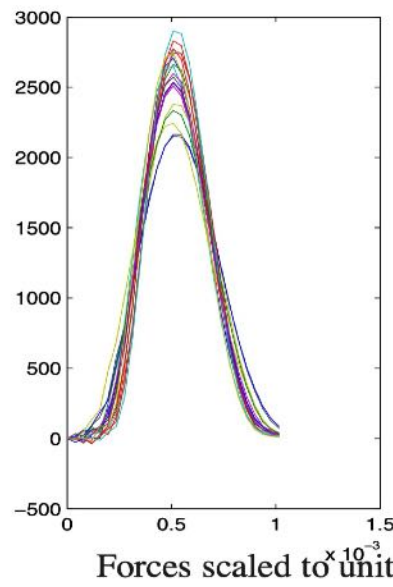
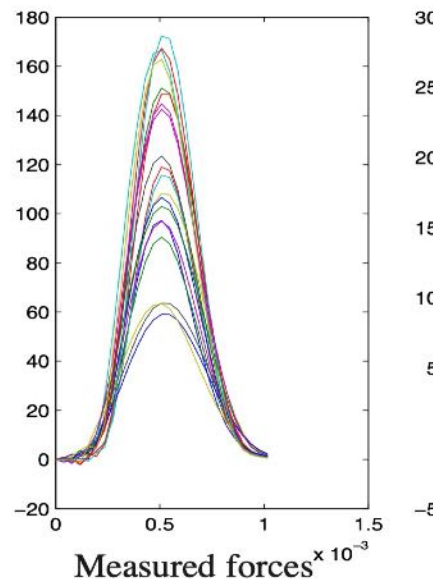
- Excitation by an impulse hammer
- Impulse response measured a laser vibrometer accelerometer
(sampling at 25.6 kHz, no windowing, 20 measurements)





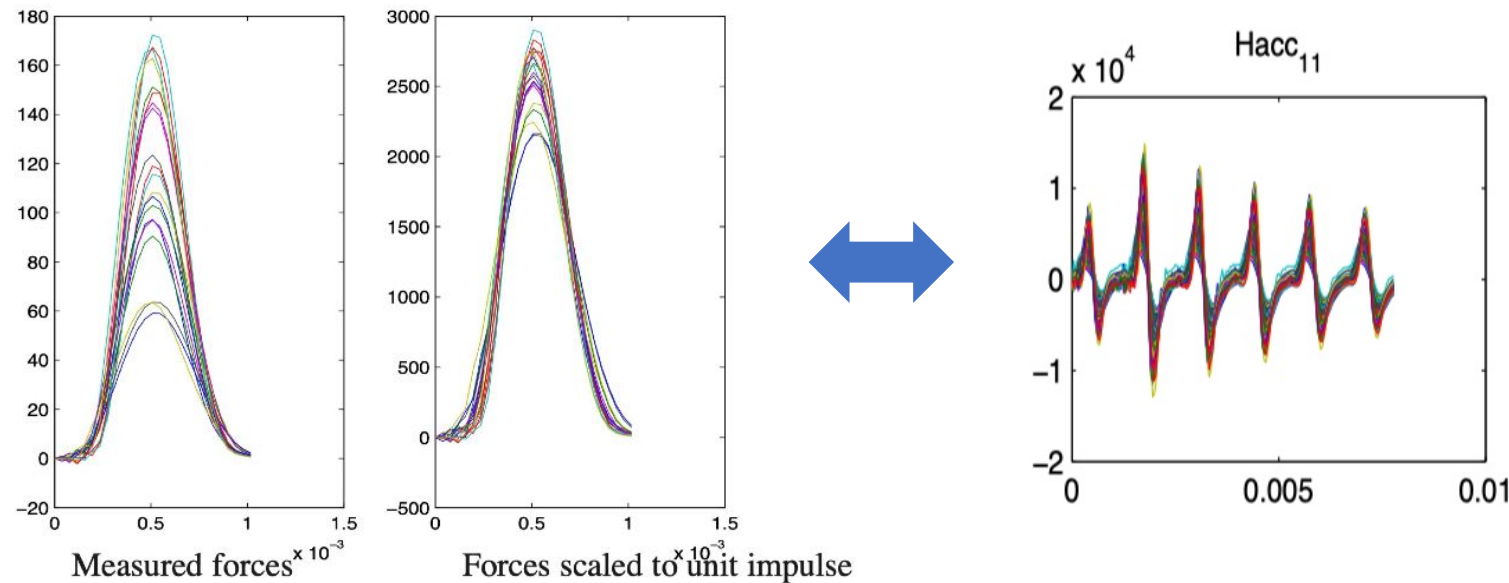
Remark:

- The different measured IRFs are scaled by the impulse of the force (numerical integration of applied force over time)
- Slightly different shape of the impulse for each hit (we did not have an automatic hammer in the past), but impact duration very constant (about 1 ms)



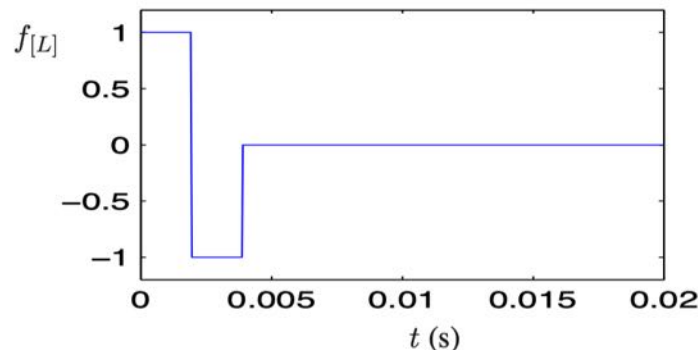
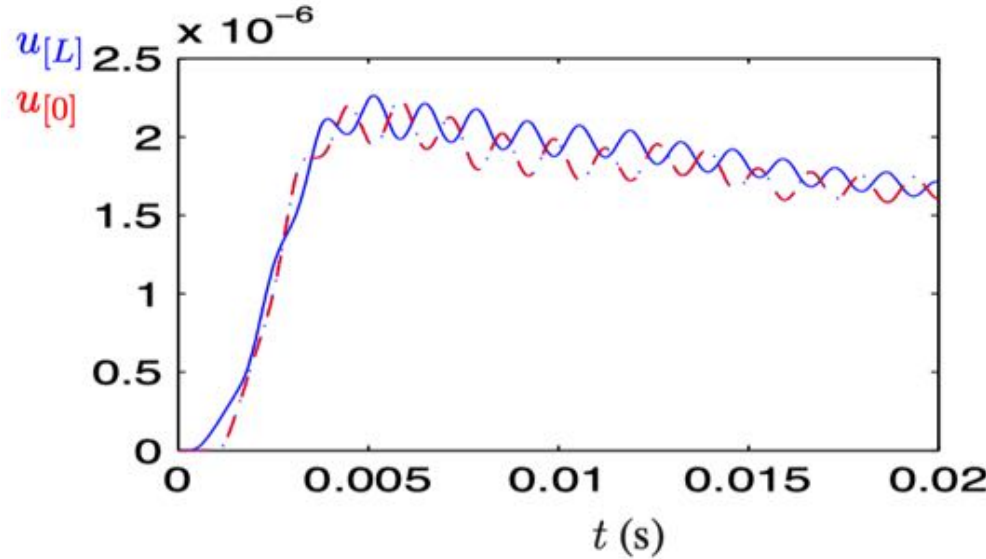
Remark (continued):

- not true IRFs, since impact of hammer not perfect! → problem ?
- Traveling time for a wave over the bar is about 0.75 ms so really not an impulse in that respect
- But maybe ok if the change of the applied force in the true application is not changing too fast



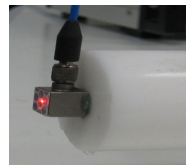


Compute the response to a double step by discrete convolution using the measured IRFs



$$\mathbf{u}(t) = \int_0^t \mathbf{H}(t-\tau) \mathbf{f}(\tau) d\tau$$

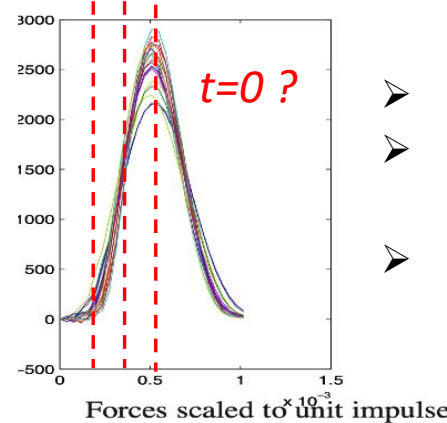
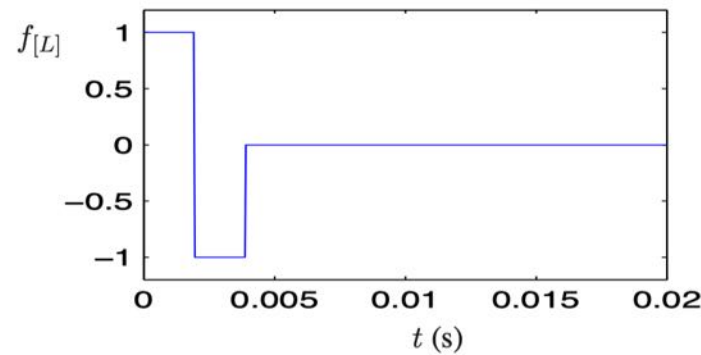
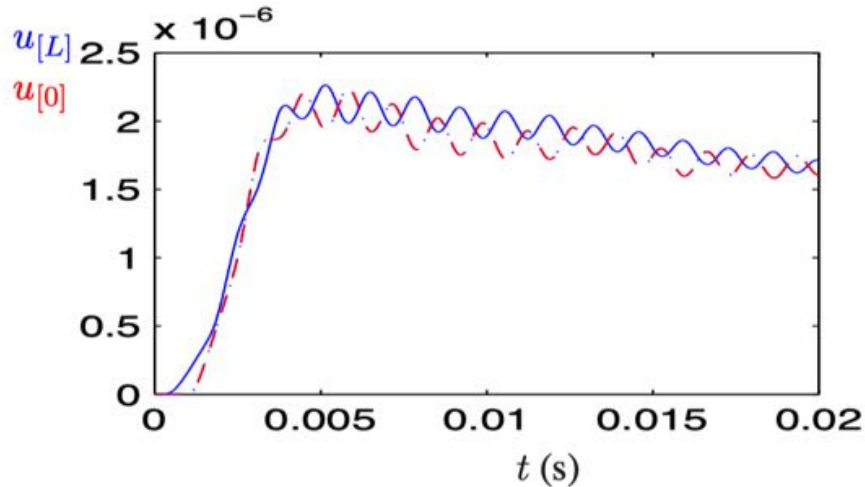
Seems to work, but tricky ...



Compute the response to a double step by discrete convolution using the measured IRFs

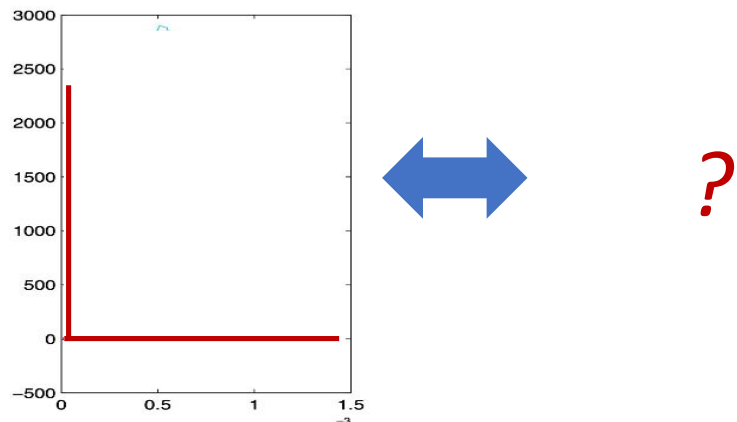
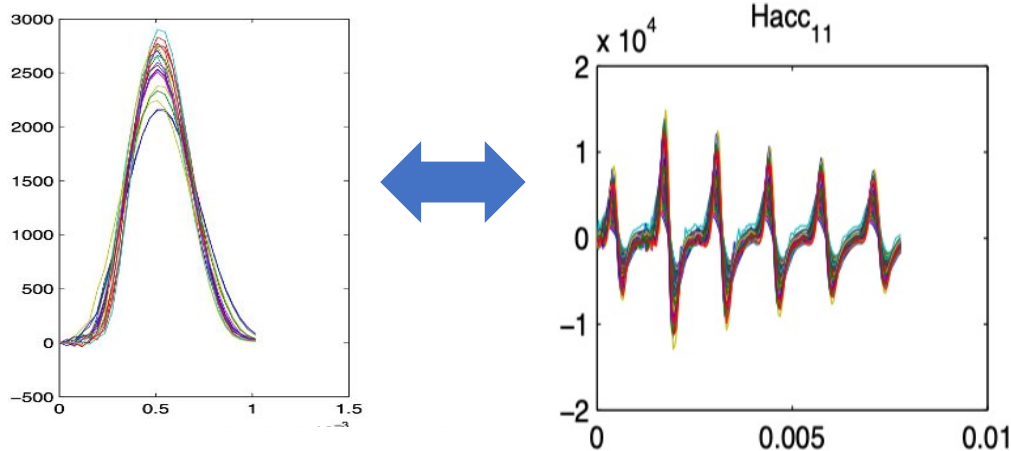


$$u(t) = \int_0^t H(t-\tau) f(\tau) d\tau$$



- One has to decide when $t=0$ in the IRF ..
- The choice of $t=0$ can make the solution of the convolution stable or unstable
- since not perfect impulse, the solution of the convolution is smoothed

Would be good to have clean and “true” IRF



Several ideas proposed in the past:

- Inverting the convolution computation
- Fitting an FE model of the bar with test
- Computing FRFs with FFT, then IFFT
- Inverting the convolution in a least square sense
- Decomposing the applied force in non-perfect impulses

→ Still needs research to see what is really working!

Improving the measured impulse response

$$\begin{aligned} u_n &= \sum_{i=1}^{n-1} y_{n-i+1} f_i \Delta t \\ &= \sum_{i=1}^{n-1} f_{n-i+1} y_i \Delta t \end{aligned}$$



$$\underbrace{\begin{bmatrix} u_1 \\ u_2 \\ \vdots \\ u_N \end{bmatrix}}_{N \times 1} = \underbrace{\begin{bmatrix} f_1 & 0 & \cdots & 0 \\ f_2 & f_1 & \ddots & \vdots \\ \vdots & f_2 & \ddots & 0 \\ f_M & \vdots & \ddots & f_1 \\ 0 & f_M & \vdots & f_2 \\ \vdots & \ddots & \ddots & \vdots \\ 0 & \cdots & 0 & f_M \end{bmatrix}}_{N \times Q} \underbrace{\begin{bmatrix} y_1 \\ y_2 \\ \vdots \\ y_Q \end{bmatrix}}_{Q \times 1} \quad \Delta t = \mathbf{Fy} \Delta t$$

Note: here we follow the notations of the original papers: the discrete impulse response h_n is now denoted y_n

Van Der Seijs, M., Van Der Valk, P., Van Der Horst, T., and Rixen, D. "Towards Dynamic Substructuring Using Measured Impulse Response Functions". Proceedings of the IMAC-XXXII (2014).

Zobel, Oliver. "Experimental Impulse Based Substructuring: A Time-Domain Solution for Modular Structural Dynamics.," MSc thesis, TU Munich (2023).

$$\underbrace{\begin{bmatrix} u_1 \\ u_2 \\ \vdots \\ u_N \end{bmatrix}}_{N \times 1} = \underbrace{\begin{bmatrix} f_1 & 0 & \cdots & 0 \\ f_2 & f_1 & \ddots & \vdots \\ \vdots & f_2 & \ddots & 0 \\ f_M & \vdots & \ddots & f_1 \\ 0 & f_M & \vdots & f_2 \\ \vdots & \ddots & \ddots & \vdots \\ 0 & \cdots & 0 & f_M \end{bmatrix}}_{N \times Q} \Delta t = \mathbf{F} \mathbf{y} \Delta t \xrightarrow{\text{Least square}} \mathbf{y} = \frac{1}{\Delta t} \underbrace{(\mathbf{F}^T \mathbf{F})^{-1}}_{\text{auto-correlation}} \mathbf{F}^T \mathbf{u}$$

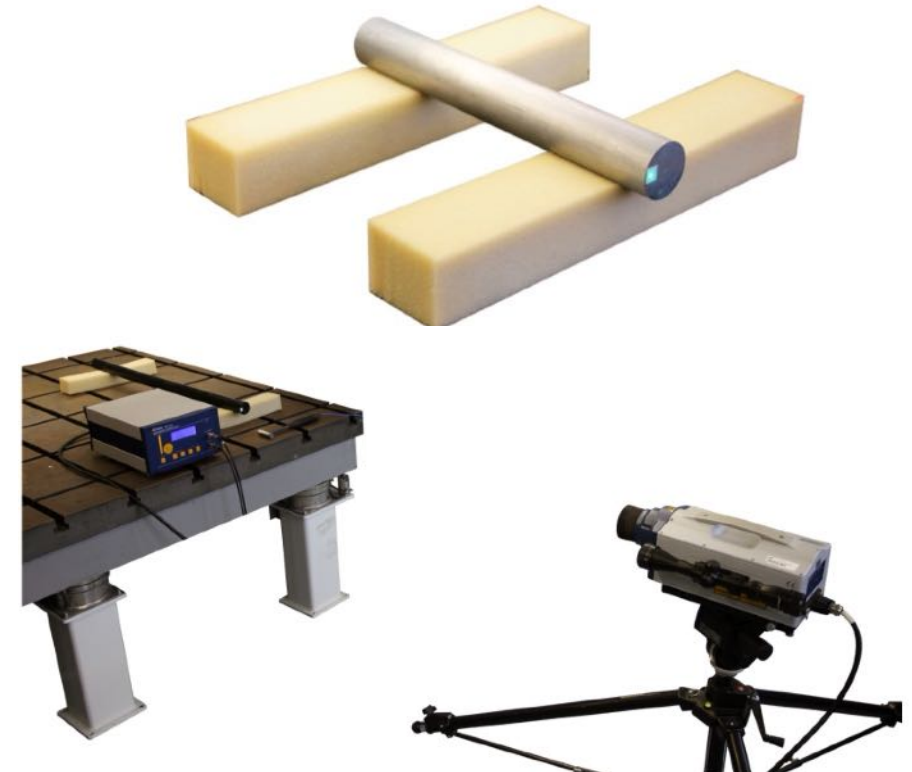
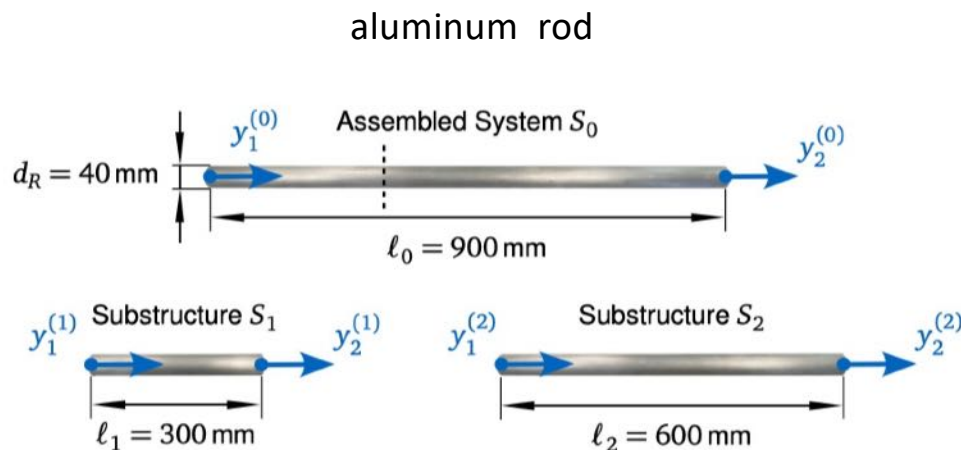
- can also be written for several impacts (averaging) [1]
- Can be combined with down-sampling (with a low-pass filter) in order to improve the robustness of the method [2,3]. This can be compared to a truncation of the FRF to remove high frequencies

[1] Van Der Seijs, M., Van Der Valk, P., Van Der Horst, T., and Rixen, D. "Towards Dynamic Substructuring Using Measured Impulse Response Functions". Proceedings of the IMAC-XXXII (2014).

[2] Zobel, Oliver. "Experimental Impulse Based Substructuring: A Time-Domain Solution for Modular Structural Dynamics.", MSc thesis, TU Munich (2023).

[3] Oliver Maximilian Zobel, Francesco Trainotti, Daniel J. Rixen , Enabling Experimental Impulse-Based Substructuring through Time Domain Deconvolution and Downsampling, Preprint, arXiv:2404.14802

A more complex experimental example



3 test objects with different length were used

$F_{\text{sampling}} = 102.4 \text{ kHz}$

measurement duration of approximately 1.2 s.

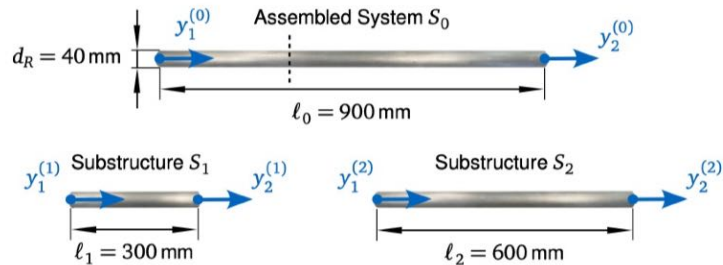
Hammer excitation

Laser measurements (Displacements and velocities)

Accelerometers

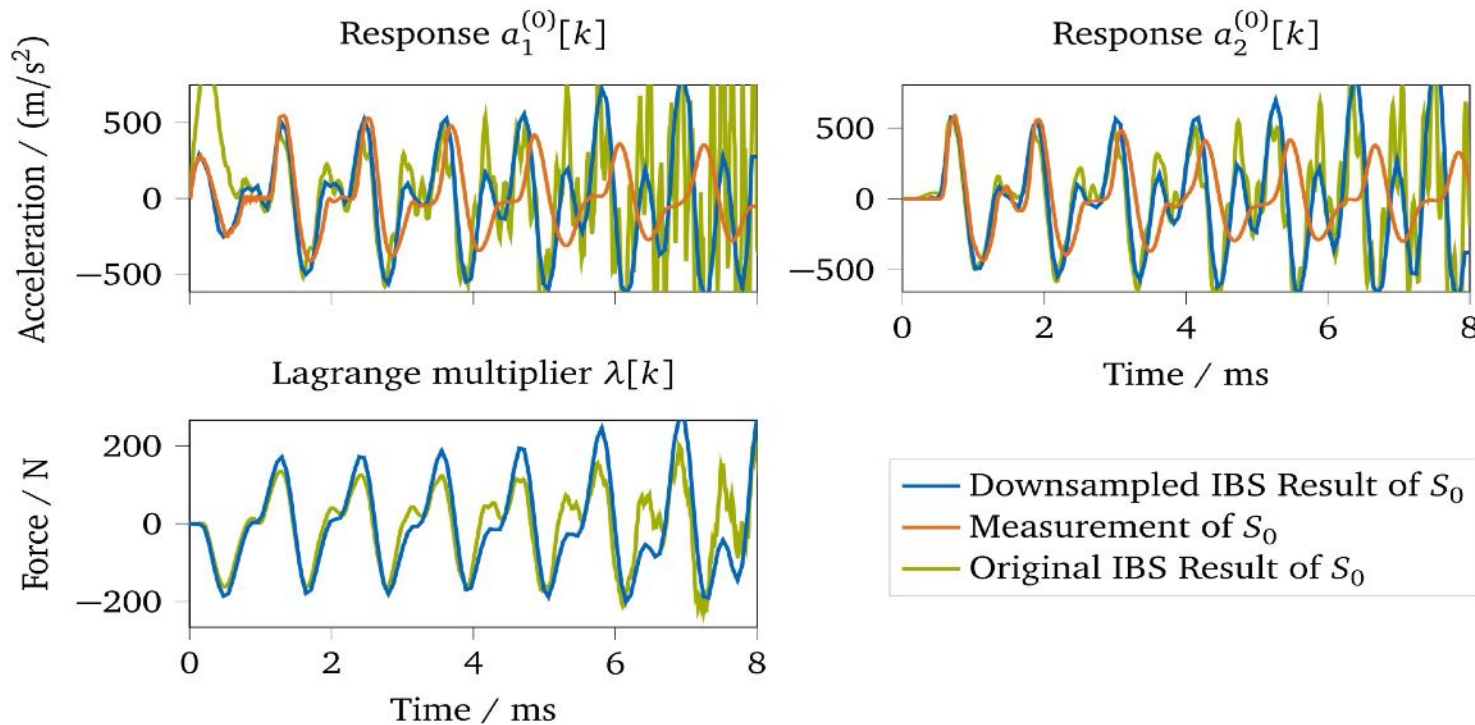
[Zobel, Oliver. "Experimental Impulse Based Substructuring: A Time-Domain Solution for Modular Structural Dynamics.", MSc thesis, TU Munich (2023).]

Oliver Maximilian Zobel, Francesco Trainotti, Daniel J. Rixen , Enabling Experimental Impulse-Based Substructuring through Time Domain Deconvolution and Downsampling, Preprint, arXiv:2404.14802



Pretty good results obtained with low pass filter + down sampling.

Quality of the results still depend on tuning properly all the analysis parameters (down-sampling, type of hammer tip ...)



Was also tried on POM bars. More difficult

Conclusion:

The methods still need to be further improved but, like FBS, it might involve in a very effective analysis and design tool

References



- D. Rixen, T. Godeby, and E. Pagnacco. Dual assembly of substructures and the fbs method: Application to the dynamic testing of a guitar. In *International Conference on Noise and Vibration Engineering, ISMA, Leuven, Belgium, September 18-20 2006*. KUL.
- D. de Klerk, D. J. Rixen, and S. N. Voormeeren. General framework for dynamic substructuring: History, review and classification of techniques. *AIAA Journal*, 46(5):1169–1181, 2008.
- D. J. Rixen. How measurement inaccuracies induce spurious peaks in frequency based substructuring. In *IMAC-XXVII: International Modal Analysis Conference, Orlando, FL, Bethel, CT, February 2008*. Society for Experimental Mechanics.
- D. de Klerk. *Dynamic Response Characterization of Complex Systems through Operational Identification and Dynamic Substructuring: An application to gear noise propagation in the automotive industry*. PhD thesis, Delft University of Technology, Delft, The Netherlands, March 2009.
- M. van der Seijs. *Experimental Dynamic Substructuring, Analysis and Design Strategies for Vehicle Development*. PhD thesis, Delft University of Technology, Delft, The Netherlands, June 2016.
- M. Häußler. *Modular sound & vibration engineering by substructuring - Listening to machines during virtual design*. PhD thesis, Technical University Munich - Department of Mechanical Engineering, April 2021.
- M. S. Allen, D. Rixen, M. van der Seijs, P. Tiso, T. Abrahamsson, and R. L. Mayes. *Substructuring in Engineering Dynamics*, volume 594 of *CISM International Centre for Mechanical Sciences*. Springer, 2020.
- A. Moorhouse, A. Elliott, and T. Evans. In situ measurement of the blocked force of structure-borne sound sources. *Journal of Sound and Vibration*, 325(4–5):679 – 685, 2009.
- A. El Mahmoudi, F. Trainotti, K. Park, and D. J. Rixen. In-situ source characterization for nvh analysis of the engine-transmission unit. In *IMAC-XXXVII: International Modal Analysis Conference, Houston, AR, Bethel, CT, February 2020*. Society for Experimental Mechanics.

Clear Criteria for a High Quality

Together with the publication of research articles in Diamond Open Access, the journal's editorial board is fully committed to ensuring the highest quality of its publications.

The **format** (length) of each paper **is free**, but we require a **supporting document** of maximum 2 pages to be submitted together with the paper. This document has a predefined format and **should answer a list of questions** related to the pertinence, novelty, performance and applicability/usefulness of the presented methods/work.

The supporting document is used as a pre-filter for further peer-reviewing. **Prior to submission, authors are encouraged to discuss the content of their paper** with the associate editor specialist in the field in order to make sure that the paper fits the scope and expectations of the journal.



[link](#)

Masterclasses in

JSD - Folder Print.indd 1-3

Journal of Structural Dynamics

A Diamond Open Access journal
for high-quality papers in the field
of Structural Dynamics



Journal of
Structural
Dynamics

27/05/24 21:29

